Evaluation of a novel mitochondria-targeted anti-oxidant therapy for ischaemia-reperfusion injury in renal transplantation

Mazin O. Hamed

Dissertation submitted for the degree of

Doctor of Philosophy

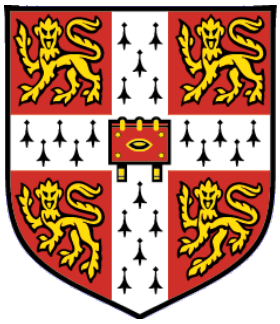

Wolfson College, Cambridge, UK

September 2017

Abstract

Ischaemia-reperfusion (IR) injury makes a major contribution to graft damage during kidney transplantation and increases the risks of primary non-function, delayed graft function and rejection. Oxidative damage to mitochondria is a key early event in IR injury. The aim of this project was to examine the safety and efficacy of the mitochondria-targeted antioxidant MitoQ in reducing pig and human kidney IR injury using an *ex vivo* normothermic perfusion (EVNP) system. Over a range of 500 nM to 250 μM using a 150 pig kidneys and 80 declined deceased human kidneys, MitoQ was successfully taken up by pig and human kidneys in a concentration-dependent manner, resulting in stable tissue concentrations over 24 hours of cold storage followed by 6 hours of EVNP. The uptake of MitoQ was increased approximately 2-fold when MitoQ was administered to warm (rather than cold) kidneys and when kidneys were preserved using hypothermic machine perfusion (rather than cold static storage). 50 μM MitoQ, administered to pig kidneys at the end of warm ischaemia, significantly increased renal blood and urine output flow at the end of 6 h EVNP compared to the control group. Creatinine clearance was numerically higher in the 50 μM MitoQ group compared to the control group but the difference did not reach statistical significance. To test the safety and efficacy of MitoQ in human kidney IRI, pairs of declined deceased human kidneys were used, with one kidney in each pair used as control. The total urine output, creatinine clearance and percentage fall of serum creatinine were numerically higher in the 50 μM MitoQ group compared to the control group, although the differences did not reach statistical significance during 3 h of EVNP. There was a significant difference in the renal blood flow between the 50 μM MitoQ group and the control group at the end of the first hour of EVNP. The renal blood flow remained relatively stable during the first hour of EVNP in the 50 μM MitoQ group compared to a significant decrease in renal blood flow in the control group. There was no effect on fractional excretion of sodium or oxidative injury markers (protein carbonyl formation, lipid peroxidation) in pig or human kidneys, which is consistent with previous studies that demonstrated the requirement of >24 hour after reperfusion for manifestation of changes in these parameters. In this thesis, I was able to successfully demonstrate the safety and potential efficacy of MitoQ in ameliorating renal IRI using pig kidneys. While more declined deceased human kidneys need to be analysed to fully explore the potential efficacy of MitoQ in ameliorating renal IRI, this study provides important data that will help inform future studies and ultimately a clinical trial for assessing the efficacy of the mitochondria-targeted antioxidant MitoQ in human kidney transplantation. My findings suggest that MitoQ has the potential to increase the use of marginal kidneys and to improve graft and patient outcomes.

Acknowledgments

I wish to thank my supervisor Dr. Kourosh Saeb-Parsy (Department of Surgery, University of Cambridge), who was more than generous with his expertise, support and precious time. I really appreciate his countless hours of guiding, supporting, encouraging and most of all believing in me through the whole process.

To Dr. Mike Murphy from The Mitochondrial Biology, thank you for your wisdom, advice and mentorship. I am so grateful for your endless support and valuable effort to ensure the success of this work.

I would like to acknowledge and thank Dr. Angela Logan, Dr. Edward Chouchani and Tracy Prime from The Mitochondrial Biology Unit for their unconditional support, help and advice.

I would also like to express my gratitude to Professor Michael Nicholson and Dr. Sarah Hosgood from the University of Cambridge, Department of Surgery for their invaluable help with the EVNP work.

Special thanks to Dr. Adam Barlow from the University of Cambridge, Department of Surgery for the encouragement, advice and suggestions of the work.

I would like to thank Professor J Andrew Bradley, Professor Christopher Watson, Dr. Eleanor Bolton and Dr. Gavin Pettigrew from the University of Cambridge, Department of Surgery for their valuable insights and comments.

I would like to also thank Dr. Sathia Thiru from the University of Cambridge, Department of Histopathology who performed the histopathological assessment of pig kidneys samples for markers of ischaemia and reperfusion injury.

Deepest thanks to all my colleagues and researchers from the University of Cambridge, Department of Surgery and The Mitochondrial Biology Unit, who offered support and help.

I would like to thank my loving parents, who have always loved me unconditionally, supported and encouraged me to peruse my dreams. Very special thanks to my wife Nadia, who has supported me throughout the process, and for her endless love, which gave me the strength to make this thesis real.

Declaration

This thesis is a presentation of my original research work. Wherever contributions of others are involved, every effort is made to indicate this clearly, with due reference to the literature, and acknowledgement of collaborative research and discussions.

Abbreviations

ACN	acetonitrile
AKI	acute kidney injury
ANOVA	analysis of variance
AP site	apurinic/apyrimidinic site
ATN	acute tubular necrosis
ATP	adenosine triphosphate
BCA	bicinchoninic acid
BHA	butylated hydroxyanisole
BIS-TRIS	Bis(2-hydroxyethyl)amino-tris(hydroxymethyl)methane
BSA	bovine serum albumin
CI	cold ischaemia
CIT	cold ischaemic time
Complex I	NADH: ubiquinone oxidoreductase
Complex II	succinate: ubiquinone oxidoreductase
Complex III	ubiquinone: cytochrome c oxidoreductase
Complex IV	cytochrome c oxidase
Complex V	ATP synthase
CoQ	coenzyme Q
CoQH	coenzyme Q (reduced)
CPDA-1	citrate phosphate dextrose-adenine
Cr	creatinine
CrCl	creatinine clearance
CSS	cold static storage
DBD	donor after brain stem death
DCD	donor after circulatory death
DecylTPP	decyltriphenylphosphonium bromide
DGF	delayed graft function
DNP	dinitrophenylhydrazine
dsDNA	double-stranded DNA
ECD	expanded criteria donors
ECG	electrocardiography
EGL	early graft loss
ELISA	enzyme-linked immunosorbent assay
EOS	electronic offering system
ESI	electrospray ionization
ESRF	end stage renal failure
ETC	electron transport chain
EVNP	*ex vivo* normothermic perfusion
FA	formic acid
FE_{Na}	fractional excretion of sodium
FMN	flavin mononucleotide
HCV	hepatitis C virus
HEPES	4-(2-hydroxyethyl)-1-piperazineethanesulfonic acid
HMP	hypothermic machine perfusion
IM	intra-muscular
IRI	ischaemic reperfusion injury
IS	internal standard

IsoP	isoprostane
IV	intra-vascular
IVC	inferior vena cava
KPS-1®	kidney perfusion solution
LC	liquid chromatography
LD	living donors
LC-MS/MS	liquid chromatography tandem mass spectrometry
MAP	mean arterial pressure
MitoQ	$MitoQ_{10}$mesylate; ([10- (4,5-dimethoxy-2-methyl-3,6-dioxo-1,4-cyclohexadien - 1-yl) decyl] triphenylphosphonium
MitoTMB	10-(3,4,5-trimethoxybenzyloxy) decyltriphenylphosphonium decyltriphenylphosphonium bromide
MPTP	mitochondrial permeability transition pore
MRC	Medical Research Council
MRM	multiple reaction monitoring
MS	moles hydroxyethyl groups per moles anhydroglucose units
MS-010	mitoquinone mesylate β –cyclodextrin complex
mtDNA	mitochondria DNA
NAD^+	nicotinamide adenine dinucleotide (oxidised)
NADH	nicotinamide adenine dinucleotide (reduced)
NADPH	nicotinamide adenine dinucleotide phosphate (reduced)
NGAL	neutrophil gelatinase-associated lipocalin
NOXs	NADPH oxidases
NTP	nucleoside triphosphate
PBS	phosphate buffered saline
Pcr	plasma creatinine
PCR	polymerase chain reaction
PD	parkinson's disease
PNF	primary non-function
P_{Na+}	plasma sodium
PP	post-perfusion
PVC	polyvinyl chloride
RBF	renal blood flow
RET	reverse electron transport
ROS	reactive oxygen species
r*Tth* DNA	recombinant Thermus thermophiles DNA
QqQ-MS/MS	quadrupole mass spectrometry
SD	standard deviation
SOD	superoxide dismutases
TMB	3,3',5,5'-tetramethylbenzidine
TPMP	methyl triphenylphosphonium bromide
TPP	triphenylphosphonium
Ucr	urinary creatinine
U_{Na+}	urinary sodium
Uv	urinary volume
UW	University of Wisconsin preservation salutation
WI	warm ishaemia
WIT	warm ischaemic time

Figures

Tables

Table of Contents

Chapter 1

Introduction

1.1 General introduction

Kidney transplantation is the optimal treatment for selected patients with end-stage renal failure (ESRF) and is associated with improved quality of life, longer patient survival and reduced costs compared to remaining on dialysis (1, 2). The relative shortage of organs over the last 10 years has necessitated the increasing use of kidneys from donation after circulatory death (DCD), in whom brainstem death criteria are not met (3).

The use of kidneys from DCD donors has been shown to be associated with worse short-term graft outcomes; the rate of delayed graft function (DGF) after DCD transplantation can exceed 70% (1). There are various definitions of DGF recorded in literature; the most widely used definition is the requirement of at least one dialysis session during the first week after transplantation (4). DGF is a major cause of morbidity after kidney transplantation that necessitates dialysis, prolonged hospitalisation and results in increased healthcare costs (5). In addition, the use of kidneys from DCD donors has been shown to increase the risk of early graft loss (EGL) and associate with significant risks of recipient morbidity and mortality (6). EGL is a catastrophic outcome both for the recipient and the transplant and necessitates permanent renal replacement therapy in the form of dialysis or re-transplantation. Although previous studies have demonstrated that long-term outcomes are similar between DCD and donation after brain stem death (DBD) kidney recipients (7, 8), DCD transplantation presents challenge above and beyond DBD transplantation.

Ischaemia-reperfusion injury (IRI) is inevitably associated with organ transplantation. IRI occurs when a tissue is exposed to ischemia for a period of time before reperfusion. Upon reperfusion there is a burst of mitochondrial oxidative damage that initiates a chain of events leading to IRI. As ischemia is inevitable during organ storage, IRI occurs when the organ is reperfused in the recipient. Furthermore, many marginal organs are currently not transplanted because it is believed that factors such as age or pathology make the organs unlikely to recover from transplant IRI and retain function for years in the recipient. Moreover, an increasingly greater proportion of organs are now retrieved from DCD donors, where the organs are exposed to a period of warm ischaemia before perfusion with cold preservation solution. This additional period of warm ischaemia, in contrast with DBD donation when normoxaemic organs can be perfused with cold preservation solution, significantly increases the IRI subsequently endured by the organs and doubles the likelihood of delayed graft function after kidney transplantation (7). Therefore, preventing IRI could improve function and outcomes of transplanted organs and increase the pool of organs available for transplantation.

Mitochondria play a central role in the pathogenesis of IRI through the production of reactive oxygen species (ROS) (9). ROS production contributes to mitochondrial damage in organ transplantation and a range of other pathologies. Mitochondria are therefore promising therapeutic targets for ameliorating

IRI, and a number of mitochondria-targeted antioxidants have been developed by our laboratory at the MRC Mitochondrial Biology Unit. MitoQ is the lead and the best–characterised mitochondria-targeted antioxidant (10).

The overall aim of my project is to test the safety and efficacy of MitoQ as a therapeutic candidate for amelioration of IRI in clinical transplantation, using pig and human models of kidney IRI.

1.2 Kidney donor types

Kidneys used for transplantation can be donated by living donors (LD), or retrieved from deceased donation after brainstem death (DBD) or after circulatory death (DCD).

1.2.1 Living donors

Kidneys from living donors have the best short and long term graft outcomes (11). Thorough investigations and tests are normally performed to exclude underlying disease in the donors and to ensure optimal conditions, including elective surgery which is associated with short cold ischaemic time (CIT).

1.2.2 Donation after brainstem death (DBD) donors

In DBD donation, organ procurement can start after declaration of brainstem death based on specific criteria (12). It is therefore possible to maintain the condition of organs before and during organ procurement by commencing surgery on a ventilated donor, so that organs remain perfused with warm oxygenated blood until perfused with cold preservation solution *in situ*. However, DBD kidneys are exposed to longer CIT compared to LD kidneys due to transportation of DBD kidneys from the donor hospital to the recipient hospital. In addition, the widespread physiological changes that occur during brainstem death and ongoing generalized inflammatory and hormonal changes adversely affect DBD kidneys function and susceptibility to rejection (13, 14).

1.2.3 Donation after circulatory death (DCD) donors

DCD donors are diagnosed with terminal irreversible pathology in whom treatment has been deemed to be futile, but do not meet the criteria for brainstem death. In DCD donation, cardiorespiratory support is withdrawn and death is declared after circulatory arrest, which can take a variable time from minutes to several hours (average 85 min)(15).

The use of kidneys from DCD donors has been shown to be associated with worse short-term graft outcomes (7, 8). The rate of DGF post DCD donor transplantation can exceed 70% (1). In addition, the

incidence of primary non-function (PNF) and early graft loss are greater in DCD donation, leading to increased risk of recipient mortality (6).

The inferior short-term outcomes in DCD kidney transplantation can be partially explained by the marked IRI associated with the process of DCD organ procurement. In DCD donors, there is an inevitable agonal phase while waiting for circulatory arrest, followed by primary warm ischaemia (defined as the time from asystole until cold perfusion is commenced) (average 15 min) (7). Preliminary results in animal models suggest that DCD kidneys are more vulnerable to IRI (16).

1.2.4 Expanded criteria donors (ECD)

The increasing demand for kidney transplantation has led to expansion of the donation pool through utilization of marginal or expanded criteria donors (ECD); defined as any deceased donor (DCD or DBD) over the age of 60 years, or a deceased donor over the age of 50 years with two of the following: a history of high blood pressure, a creatinine greater than or equal to 1.5 mg/dL (133 µmol/L), or death from a cerebrovascular accident. The use of kidneys from ECD donors has been shown to be associated with worse long-term graft outcomes in some studies (7, 8).

1.3 Preservation methods

There are two established methods of kidney preservation before transplantation: cold static storage (CSS) and hypothermic machine perfusion (HMP). In both methods, a sterile preservation solution is used at 4 °C to maintain organ viability, reduce cellular metabolism and counteract the deleterious effect of cold ischaemia.

CSS is the most widespread method of kidney preservation where the kidney is kept on ice until transplantation. Several different preservation solutions are used to preserve kidneys during cold static storage, the two most common are Soltran® (Baxter Healthcare) and University of Wisconsin (UW) Viaspan® (Bristol Myers Squibb).

Hypothermic machine perfusion provides a sealed, sterile environment where a preservation solution (such as Kidney Perfusion Solution: KPS-1®) is pumped gently through the renal artery in a closed circuit. Previous studies suggested that hypothermic machine perfusion may reduce delayed graft function when compared with cold static storage (17).

1.4 Ischaemia reperfusion injury (IRI)

Ischaemia and reperfusion are characterized by an initial restriction of blood supply to an organ followed by the subsequent restoration of perfusion and synchronous reoxygenation. IRI occurs in a variety of clinical settings, including reperfusion after single-organ ischaemia (e.g., acute coronary

syndrome, acute kidney injury and cerebrovascular accident), or reperfusion after temporary interruption of blood supply during major surgery (e.g., cardiopulmonary bypass in cardiac surgery or solid organ transplantation) (18). A complex multifactorial pathological process contributes to the deleterious effects of IRI, leading ultimately to cellular dysfunction and death.

1.4.1 IRI in kidney transplantation

There are two distinct phases of kidney injury during transplantation: the ischaemic phase that occurs at different stages throughout the process of donation, procurement and organ storage; and the reperfusion stage that usually happens after kidney transplantation through re-introduction of oxygen and nutrients. Kidneys are exposed to different durations and types of ischaemia (warm and cold) that contribute to the hypoxia-reoxygenation insult at reperfusion.

There are multiple pathophysiological mechanisms that contribute to IRI. The fate of the transplanted organ depends on the ability of cellular repair and regeneration to overcome the structural damage to the renal parenchyma (e.g. loss of brush border and cell polarity in tubule cells) and cellular death (apoptosis, autophagy and necrosis) induced by IRI.

Acute kidney injury (AKI) is the clinical manifestation of kidney IRI. AKI is characterized by a rapid (hours to days) decrease in renal excretory function, with accumulation of nitrogenous metabolic end-products (urea and creatinine) and decreased urine output. Ischaemia-induced AKI in transplantation can be transient (DGF) or permanent (PNF). In addition, ischaemic-induced AKI may contribute to acute and chronic graft rejection (19).

1.4.2 Mitochondria

Mitochondria are double membrane bound organelles. They have an outer membrane and an inner membrane that enclose two compartments, the mitochondrial matrix and the intermembrane space. They are highly dynamic organelles known as the powerhouses of the cell. They provide ATP by the process of oxidative phosphorylation through the electron transport chain (ETC) and the enzyme ATP synthase, located in the inner mitochondrial membrane. In addition, mitochondria play a key role in other cellular processes such as calcium homeostasis, cell signaling, differentiation, cell apoptosis and inflammation (20).

1.4.3 Role of mitochondria in IRI

Mitochondria play a central role in the pathogenesis of IRI (9). During ischaemia, oxygen deprivation results in rapid depletion of intracellular ATP, with inactivation of mitochondrial oxidative phosphorylation, accumulation of lactate and a drop in intracellular pH secondary to anaerobic metabolism. In addition, lack of oxygen leads to disruption of energy-dependent distribution of Ca^{2+},

failure of ATPase pumps, leakage of phospholipases and proteases, and ultimately cell death (21, 22). With re-introduction of oxygen at reperfusion, the damaged mitochondrial ETC increases reactive oxygen species (ROS) generation (23-25), damaging cellular lipids, proteins and DNA (23, 26). This disrupts mitochondrial ATP supply and in conjunction with the accumulation of calcium within mitochondria during ischaemia, leads to the induction of the mitochondrial permeability transition pore (MPTP) (a large conductance channel in the mitochondrial inner membrane), necrotic and apoptotic pathways (27, 28).

1.4.4 Reactive oxygen species

Reactive oxygen species (ROS) are highly reactive oxygen molecules featuring unpaired electrons in their outer orbit (free radicals). They are unstable, short-lived molecules that react readily with proteins, lipids and DNA, causing damage to them. The complete reduction of oxygen during the process of oxidative phosphorylation produces water (Figure 1.1). However, partial reduction produces ROS including superoxide ($O_2^{\bullet -}$), hydrogen peroxide (H_2O_2) and the hydroxyl radical ($OH^{\bullet}$).

Three major sources of ROS *in vivo* IR have been suggested. These are mitochondria, the plasma membrane nicotinamide adenine dinucleotide phosphate (NADPH) oxidases and the xanthine oxidases. The relative contribution of each source to the total level of ROS at reperfusion *in vivo*, oxidative damage and cellular injury is not clearly understood.

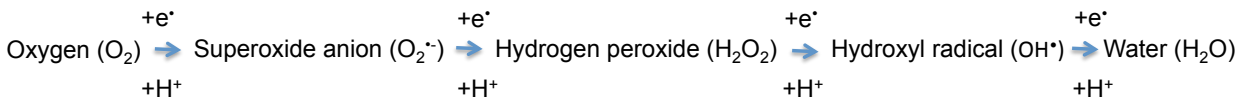

Figure 1.1. Production of ROS through the process of oxidative phosphorylation.

1.4.4.1 Mitochondrial ROS

During oxidative phosphorylation, electrons are transferred from electron donors (e.g. nicotinamide adenine dinucleotide (NADH), coenzyme Q (CoQH)) to electron receptors in redox reactions. The electrons are passed down a series of respiratory chain complexes (I-IV) through electron carriers, ultimately reducing the final electron receptor 'oxygen' to water. Mitochondria constantly generate ROS as a by-product of oxidative phosphorylation. Superoxide radical ($O_2^{\bullet -}$) is the predominant proximal intracellular ROS (29). It is produced by reduction of an oxygen molecule (receiving an electron) by an electron donor (e.g. NADH, $CoQH_2$). Superoxide dismutase (SOD) takes two molecules of superoxide, strips the extra electron off one, and places it on the other. One superoxide molecule therefore forms normal oxygen through loss of an electron, while one molecule with two extra electrons rapidly picks up two hydrogen ions to form hydrogen peroxide (H_2O_2). $O_2^{\bullet -}$ can also react with NO to generate peroxynitrite ($ONOO^-$). In the presence of transition metals, especially Fe^{2+}, H_2O_2 can go on to generate the highly reactive hydroxyl radical $OH^{\bullet}$ (30) (Figure 1.2), which is believed to contribute significantly to ROS damage within cells (30). Hydroxyl radical is further catalyzed to H_2O by glutathione peroxidase.

The generation of $O_2^{\bullet -}$ within the mitochondria matrix depends on the availability of potential electron donors (determined by $NADH/NAD^+$ and $CoQH_2$/CoQ ratios), the protonmotive force, the local oxygen concentration and the rate of interaction between O_2 and the potential electron donors (31).

Respiratory complex I is the entry point for NADH (electron donor) into the respiratory chain. Flavin mononucleotide (FMN) is the co-factor that accepts electrons from NADH and transmits them to the CoQ reduction site. CoQ then acts as an electron carrier to pass electrons on to complex III and IV. The transport of electrons generates a protonmotive force by pumping protons across the mitochondrial inner membrane which is then utilized to generate ATP at complex V by ATP synthase. This pathway is well protected from oxidative damage, however the two sites that are thought to be involved in the production of ROS are complex I and CoQ binding site (complex III). There is growing evidence that complex I is the major source of ROS production within mitochondria *in vivo* through both forward and reverse electron transfer modes (31).

During IRI, mitochondrial superoxide may form at complex I through the forward electron transfer mode as a result of high $NADH/NAD^+$ ratio. This occurs due to the lack of downstream electron demand resulting from low ATP synthesis during cold preservation of organs, in addition to cytochrome c loss and respiratory chain damage (31). The other mode of ROS production is through reverse electron transport (RET), also through complex I, during reperfusion. During ischaemia there is reversal of succinate dehydrogenase and accumulation of succinate. Upon reperfusion the accumulated succinate is rapidly oxidized and a high protonmotive force leads to reverse electron transport at complex I which generates a burst of superoxide (31).

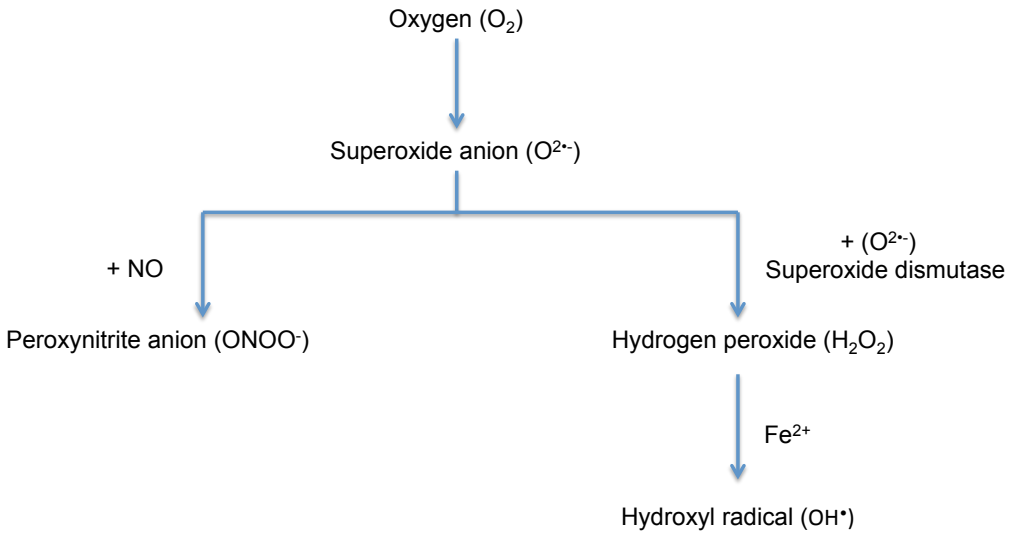

Figure 1.2. Mitochondrial ROS formation**.**

1.4.4.2 NADPH oxidases

The NADPH (nicotinamide adenine dinucleotide phosphate) oxidases (NOXs) are membrane-bound enzyme complexes (32). They are a family of trans-membrane enzymes found in almost all cells, in addition to the membranes of phagosomes used by neutrophils to engulf microorganisms. The biological function of NOXs is to produce ROS. NOXs generate superoxide by transferring electrons from NADPH inside the cell, across the membrane, and reduce oxygen to produce superoxide and other downstream ROS (32). The phagocyte NADPH oxidase was the first identified example of a system that generates ROS not as a byproduct, but rather as the primary function of the enzyme. The discovery of other members of the NOX family of NADPH oxidases demonstrated that enzymes with the primary function of ROS generation are not limited to phagocytes. One of the main physiological functions of NOX family enzymes is host defense (32). NADPH oxidase is responsible for the respiratory burst, characterized by the rapid release of superoxide and other downstream ROS from immune cells such as neutrophils and monocytes targeted at ingested or extracellular microbes. The high concentration of NOX in leucocytes suggests that it is likely to be an important source of ROS, however, the exact contribution of NOX family of ROS to IRI is not fully understood. In the context of kidney transplantation, there are experimental studies in which normothermic blood perfusion was used in pig and human kidney models (33, 34) demonstrating that depletion of leukocytes prior to perfusion reduces the IRI. Leukocytes are a source of ROS production and this, therefore, may partially explain the protective effect of leukocyte depletion.

1.4.4.3 Xanthine oxidase

Xanthine oxidase plays an important role in purine degradation, catalyzing the oxidation of hypoxanthine to xanthine, and further oxidation of xanthine to uric acid. Xanthine oxidase activity is believed to be a source of ROS during IRI. In the process of oxidation of xanthine to uric acid through the use of oxygen as electron acceptor, xanthine oxidase produces superoxide and hydrogen peroxide.

In this context, allopurinol, a xanthine oxidase inhibitor, has been in clinical use for over 20 years in the organ preservation solution UW. However, several previous studies have demonstrated that preservation solutions with allopurinol have no additional protective effect on short-term or long-term kidney transplant outcomes compared with those preserved in solutions without allopurinol (35).

1.5 MitoQ as a mitochondria-targeted anti-oxidant

Mitochondrial oxidative damage plays a key role in IRI. Therefore, the selective inhibition of mitochondrial oxidative damage is a promising therapeutic strategy to ameliorate IRI in kidney transplantation. Ideally, mitochondria-targeted antioxidants should be stable small molecules with *adequate* and selective uptake into the mitochondria of target organs, where they block oxidative

damage and can then be recycled back to the active antioxidant form (36). In this context, a number of mitochondria-targeted antioxidants have been developed by our laboratory at the MRC Mitochondrial Biology Unit, the lead molecule of which is MitoQ (10).

1.5.1 Mechanism of action

The MitoQ molecule comprises a lipophilic triphenylphosphonium (TPP) cation covalently linked to an antioxidant ubiquinone moiety by a 10-carbon alkyl chain (Figure 1.3). The lipophilic TPP cation passes rapidly through the plasma membrane, driven by the plasma membrane potential. This is followed by the extensive accumulation of these molecules within cell-mitochondria, driven by the large mitochondrial membrane potential (10). The ability of the lipophilic TPP cation to move through phospholipid bilayers enables its accumulation in the mitochondrial matrix simply in response to the large negative mitochondrial membrane potential and does not require any specific transport mechanism (37). The lipophilic TPP cations are accumulated into the mitochondria driven by the plasma membrane potential (~30-60 mV, negative inside), and the mitochondrial membrane potential (~140-160 mV, negative inside), where they accumulate several hundredfolds within the mitochondrial matrix relative to the extracellular environment (Figure 1.3). This is consistent with the Nernst equation, which indicates that under normal physiological conditions the uptake of lipophilic cations increases 10-fold for every 61.5mV of membrane potential. MitoQ is largely adsorbed to the inner membrane of mitochondria and the linker chain (10-carbon alkyl) enables the active antioxidant component (ubiquinol) to penetrate deep into the membrane core and prevent lipid peroxidation (38). In acting as an antioxidant the ubiquinol form of MitoQ is oxidized to ubiquinone. Complex II then rapidly reduces ubiquinone back to the active antioxidant form (ubiquinol) (39). This combination of efficient selective uptake and recycling makes MitoQ many hundredfolds more potent at preventing mitochondrial oxidative damage than untargeted antioxidants (38).

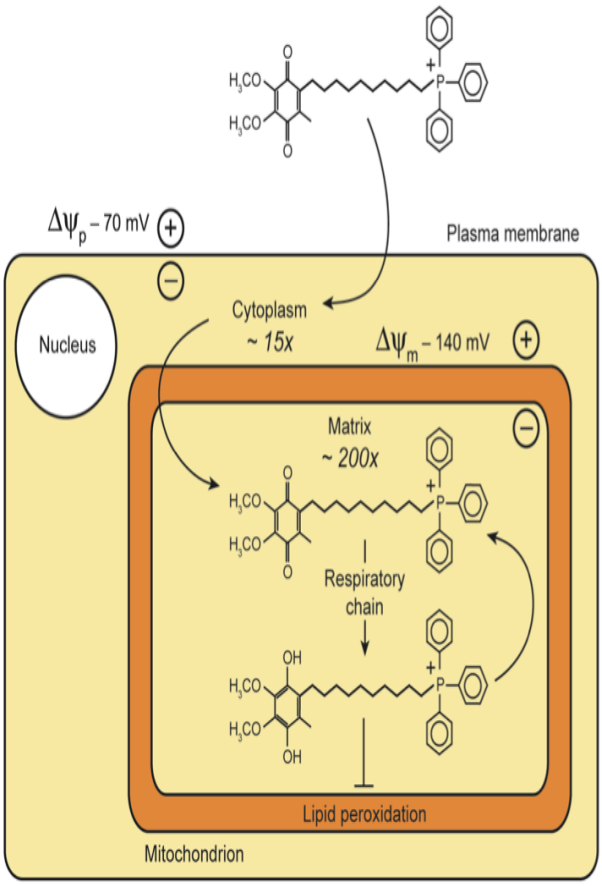

Figure 1.3. The selective uptake of the mitochondria-targeted antioxidant MitoQ. Figure taken from Anna J. Dare et al. 2015 (40).

1.5.2 Safety and uptake

In order to be used clinically as a mitochondria-targeted antioxidant, it is necessary to establish that MitoQ can be delivered safely to organs, and that it accumulates within mitochondria at sufficient concentrations to block oxidative damage. MitoQ has shown to be delivered safely intravenously (i.v.) in mice (~20 mg MitoQ/kg), with toxicity only observed at ~27 mg MitoQ/kg (41). To measure long-term oral toxicity, mice were administered 500 µM (~55-80 mg MitoQ/day/kg) in their drinking water for up to 28 weeks, with no evidence of toxicity (42). In these experiments MitoQ did not change physical activity, O_2 consumption, food consumption, lean mass, glucose or insulin level, or bone mineral density of the mice, but there was a decrease in the percentage of body fat and liver and plasma triglyceride content. This suggests that MitoQ may decrease adiposity with a slight shift to increased lipid utilization (42). However, together these data suggest that the long-term oral administration of MitoQ is safe in mice.

Pharmacokinetics of MitoQ have been investigated using radiolabelled [^{3}H] MitoQ. MitoQ was delivered and rapidly cleared from the plasma. A substantial amount of MitoQ rapidly accumulated in the brain, heart, liver, skeletal muscle and kidney tissue following intravenous injection into mice (41, 43). Orally administered [^{3}H] MitoQ was also taken up into plasma and accumulated in the heart, brain, liver, kidney and muscle. To investigate MitoQ tissue uptake, a liquid chromatography tandem mass spectrometry (LC-MS/MS) assay was developed to assess MitoQ content relative to a deuterated internal standard (IS), d3–MitoQ by multiple reaction monitoring (42). In mice fed 500 µM MitoQ drinking water for 4–6 months, the steady-state level of MitoQ was ~113 pmol MitoQ/g in the heart, ~20 pmol MitoQ/g in the liver, and ~2 pmol/g in the brain (44, 45). Therefore, both bolus i.v. and long-term oral administration of MitoQ leads to substantial uptake of MitoQ within liver and heart, with significantly less uptake in the brain.

MitoQ has also been used in two Phase II clinical trials in humans and been shown to be safe and well tolerated long term (46, 47). In addition, other studies demonstrated that MitoQ was excreted in the urine and bile unchanged and also with sulfation and glucuronidation of the quinol ring, with no indication of other metabolites (48).

1.5.3 Use of MitoQ in IRI

The first report of a laboratory study of the therapeutic effect of MitoQ in IRI used a cardiac IRI model (44). In this study, 500 µM MitoQ was administered to rats in their drinking water for 2 week and the hearts were then isolated and exposed to IRI in a Langendorff perfusion system. MitoQ was shown to be protective against heart dysfunction, tissue damage and mitochondrial dysfunction (44). A similar study also showed that MitoQ was protective against cardiac IRI (49). In addition, our group previously demonstrated the therapeutic efficacy of MitoQ in ameliorating IRI in two animal models. First, MitoQ

was administered intravenously at 4.4 mg/kg MitoQ (corresponding to 20 mg/kg of MS-010 which contains 22.2% MitoQ mesylate by weight) 15 min prior to inducing 45 min of bilateral renal ischaemia followed up by 24 h reperfusion. In this model, MitoQ significantly protected against renal dysfunction (creatinine rise) and oxidative damage (protein carbonyls formation and mitochondrial DNA damage) at 24 h post reperfusion (40). The second model was a syngeneic mouse model of heterotopic cardiac transplantation. This model demonstrated that direct administration of 50 μM of MitoQ to the heart during 4 h of cold preservation decreased oxidative damage at 24 h post-transplantation (50).

1.5.4 Phase II clinical trials

Based on evidence that oxidative stress and mitochondrial damage contribute to liver dysfunction in patients with chronic hepatitis C virus (HCV) infection, MitoQ was administered to patients with HCV infection who were unresponsive to the conventional treatments. (46). MitoQ administration decreased plasma alanine transaminase and aspartate aminotransferase levels in this double-blind trial. There was no beneficial effect of MitoQ on viral load, suggesting that MitoQ may help protect liver cells, but does not inhibit virus replication within the liver. In a study of patients with Parkinson's disease (PD) (47), it was demonstrated that 40 mg or 80 mg of daily MitoQ administered for a year was safe, with only dose-dependent nausea and vomiting reported. The study did not demonstrate therapeutic efficacy of MitoQ in slowing the progression of untreated PD as measured by the Unified Parkinson Disease Rating Scale clinical scores. This lack of efficacy may be explained by the fact that at the time of diagnose approximately 50% of dopaminergic neurons are already lost and it may not be possible to rescue sufficient dopaminergic neurons with an anti-oxidant to improve clinical outcomes.

1.5.5 *Ex vivo* normothermic perfusion

Ex vivo normothermic perfusion (EVNP) has been established as a valid model for investigating IRI (34, 51). The EVNP circuit is based on paediatric cardiopulmonary bypass technology, produced by Medtronic Inc, and adapted for the perfusion of pig and human kidneys. The EVNP circuit has been used as a platform to administer therapeutic interventions in experimental pig models of renal IRI (52, 53). In addition, it has been used in clinical practice for preservation of human kidneys prior to transplantation (54, 55), and as a tool to assess the viability of declined deceased human kidneys for implantation (56, 57). Our group has reported recently the successful transplantation of a pair of deceased human kidneys that were declined for transplantation due to inadequate *in situ* perfusion but subsequently transplanted after perfusion and assessment using EVNP (58).

1.6 Aims and objectives

The overall aim of this thesis is to provide experimental data to support the safety and efficacy of MitoQ as a therapeutic agent for use in clinical renal transplantation. It is anticipated this will ultimately enable design of randomised controlled trials investigating the potential benefit of MitoQ in the prevention of IRI that inevitably occurs in kidney transplantation.

The similarity between pigs and humans in renal anatomy, metabolic demands and sensitivity to ischaemia makes the pig an excellent model to investigate IRI. In this context, this thesis will aim to:

1. Identify the optimal delivery method and time scale for administration of MitoQ using pig kidneys
2. Investigate MitoQ uptake into the pig kidney tissue following cold preservation using static cold storage and hypothermic machine perfusion
3. Evaluate the efficacy of MitoQ in ameliorating IRI using ex vivo normothermic perfusion
4. Conduct critical pre-clinical studies using declined human kidneys to optimise the dose and delivery of MitoQ, with the specific goal of generating sufficient data to support commencement of a human clinical trial

Chapter 2

Materials and methods

2.1 Materials and preparations

2.1.1 Mitochondria-targeted antioxidant

MitoQ ([10- (4,5-dimethoxy-2-methyl-3,6-dioxo-1,4-cyclohexadien-1-yl) decyl] triphenylphosphonium methanesulfonate) was used complexed with β -cyclodextrin supplied by Antipodean Pharmaceuticals Inc and dissolved in organ preservation solution (Soltran® , Baxter Healthcare) for *ex vivo* use during organ preservation.

2.1.2 Control compounds

A number of control compounds were used instead of MitoQ and dissolved in organ preservation solution (Soltran®, Baxter Healthcare) for *ex vivo* use during organ preservation:

Methyl triphenylphosphonium bromide

β – cyclodextrin complex of methyl triphenylphosphonium bromide (TPMP) was synthesized as previously described (59).

Decyltriphenylphosphonium bromide

β – cyclodextrin complex of decyltriphenylphosphonium (DecylTPP) bromide was synthesized as previously described (59).

10-(3,4,5-trimethoxybenzyloxy) decyltriphenylphosphonium bromide

β – cyclodextrin complex of 10-(3,4,5-trimethoxybenzyloxy) decyltriphenylphosphonium bromide (MitoTMB) was prepared by Tom Bright from MItoTMB synthesised by Prof David Larsen, Department of Chemistry, University of Otago, Dunedin, New Zealand.

2.1.3 Dosing and preparation of MitoQ

MitoQ is supplied by the manufacturer as a solid preparation called MS-010, which contains 22.2% MitoQ mesylate by weight. MitoQ mesylate is complexed to cyclodextrin. MS-010 was stored at -20 °C, and the preservation solution (Soltran®, Baxter Healthcare) which contains MitoQ was made up fresh no more than 3 days in advance of each experiment and stored at 4 °C.

2.2 Preservation solutions and methods

2.2.1 Hyperosmolar citrate (Soltran®)

Soltran® solution was used to perfuse pig and declined deceased human kidneys (*in situ* perfusion, back table perfusion), and to preserve pig and declined deceased human kidneys during cold static storage. The solution is a sterile aqueous solution and has approximate osmolality of 486 mOsmol/kg and pH of 7.1 at room temperature. Soltran® solution was supplied by Baxter Health and has the following composition:

Constituents	Amount	Concentration
Sodium	8.2 g/l	84 mmol/l
Mannitol	33.8 g/l	n/a
Potassium	8.6 g/l	80 mmol/l
Citrate	n/a	54 mmol/l
Magnesium	1 g/l	41 mmol/l
Glucose	n/a	194 mmol/l
Sulfate	n/a	41 mmol/l
Sterile water for injection	To 1000 mL volume	n/a

2.2.2 University of Wisconsin (Viaspan®)

University of Wisconsin (Viaspan®) solution was used for *in situ* perfusion of pig and human kidneys and to preserve deceased human kidneys in cold static storage. The solution is clear yellow and has approximate osmolality of 320 mOsmol/kg and pH of 7.4 at room temperature. University of Wisconsin (Viaspan®) solution was supplied by Bristol Myers Squibb Pharmaceutical Limited and has the following composition:

Constituents	Amount	Concentration
Poly (0-2-hydroxyethyl) starch 0.40-0.50 MS[1] (Pentafraction*)	50.0 g/l	n/a
Lactobionic Acid (as Lactone)	35.83 g/l	105 mmol/l
Sodium Hydroxide 40%	3.679 g/l	27 mmol/l
Adenosine	1.34 g/l	5 mmol/l
Allopurinol	0.136 g/l	1 mmol/l
Potassium Dihydrogen Phosphate	3.4 g/l	25 mmol/l
Magnesium Sulphate x $7H_2O$	1.23 g/l	5 mmol/l
Raffinose x $5H_2O$	17.83 g/l	30 mmol/l
Glutathione	0.922 g/l	3 mmol/l
Potassium Hydroxide	14.5 g/l	100 mmol/l

[1]MS= moles hydroxyethyl groups per moles anhydroglucose units.

2.2.3 Kidney Perfusion Solution (KPS-1®)

KPS-1® was only used for hypothermic machine perfusion. The solution is clear and has approximate osmolality of 300 mOsM/kg and a pH of approximately 7.4 at room temperature. KPS-1® was supplied by Organ Recovery System and has the following composition:

Constituents	Amount	Concentration
Calcium chloride (dehydrate)	0.068 g/l	0.5 mmol/l
Sodium hydroxide	9.7 g/l	n/a
HEPES (free acid)	2.3 g/l	10 mmol/l
Potassium phosphate (monobasic)	3.4 g/l	25 mmol/l
Mannitol	5.4 g/l	30 mmol/l
Glucose	1.8 g/l	10 mmol/l
Sodium gluconate	17.45 g/l	80 mmol/l
Magnesium gluconate	1.13 g/l	5 mmol/l
Ribose	0.75 g/l	5 mmol/l
Hydroxyethyl starch	50 g/l	n/a
Glutathione	0.93 g/l	3 mmol/l
Adenine	0.68 g/l	5 mmol/l

2.2.4 LifePort kidney transporter (Organ Recovery Systems)

The LifePort kidney transporter (Organ Recovery Systems) is a portable hypothermic machine perfusion system (Figure 2.1). Unlike conventional cold static storage (i.e. a simple cool box), the LifePort provides a closed circuit, with a continuous perfusion of KPS-1® solution through the renal artery. The LifePort consists of a sterile disposable perfusion circuit and a portable insulated perfusion transporter. The sterile disposable perfusion circuit is a closed system with an in-line filter and pressure sensor, SealRing™, sterile drape and disposable cannula to connect the kidney (through the renal artery) to the perfusion circuit. The portable insulated perfusion transporter includes an ice container, lithium ion batteries, AC cable and data cable (Organ Recovery System). While the kidney is being perfused, the LifePort software records data on temperature, flow rate, vascular resistance and pressure every 10 seconds.

Figure 2.1. LifePort kidney transporter (Organ Recovery Systems).

2.3 Pig models

Three models were used to retrieve pig kidneys: uncontrolled, controlled *in situ* perfusion and controlled back table perfusion.

2.3.1 Uncontrolled model

In order to obtain pilot data on the uptake of MitoQ to inform further experiments, initial experiments were performed using kidneys from pigs sacrificed for meat under conditions dictated by agricultural regulations.

Large female (Landrace) pigs (weighing 40 - 50 kg, aged 3 - 4 months) were sacrificed by electrocution followed by carotid exsanguination at a licensed local abattoir (C A Leech – Royston). The kidneys were retrieved *en bloc* after 10 - 20 min of *in situ* warm ischaemia (WI) to simulate the clinical scenario of donation after circulatory death.

2.3.2 Controlled model

Large female (Landrace) pigs (weighing 40 - 50 kg, aged 3 - 4 months) were supplied by Huntington Life Sciences, Huntingdon, UK. These experiments were performed according to Home Office regulations and using Huntingdon Life Sciences project license. Pigs were fasted for 16 - 17 h before surgery, to ensure that the stomach is empty to prevent aspiration and to improve access to the kidneys during surgery. Before general anaesthesia, pigs were allowed to acclimatize to conditions in the treatment room. Animals received intramuscular (IM) sedation and narcotic analgesia (ketamine 10 mg/kg, medetomidine 0.02 mg/kg and midazolam 0.1 mg/kg). General anaesthesia was induced by intravenous (i.v.) propofol 4 - 6 mL per 50 kg and then maintained by i.v. infusion of remifentanyl (starting at 0.04 mg/kg/min and titrating up to 0.4 mg/kg/min) and propofol (starting at 10 mg/kg/hr and titrating down to 60-70% of the starting amount). Animals were monitored using an oxygen saturation probe on the tongue, a temperature probe and 3-lead electrocardiography (ECG). Intermittent positive pressure ventilation was performed to maintain oxygenation.

2.3.2.1 *In situ* perfusion

Under aseptic conditions, the abdominal cavity was accessed through a midline incision and both kidneys and the inferior vena cava (IVC) were exposed. Heparin (500 IU/kg) was administered i.v. as a bolus through the marginal ear vein. Dissection was performed to expose the distal aorta. The distal aorta and IVC were cannulated 5 min after systemic heparinisation and the animal was exsanguinated through the aorta and IVC. Blood was collected in a sterile receptacle and transferred into CPDA-1 blood bags and stored at 4 °C for normothermic perfusion. After confirmation of death (asystole on a

continuous ECG display and absence of palpable pulse in the abdominal aorta), the kidneys were exposed to 10 min WIT at body temperature. The kidneys were then perfused *in situ* with 2 L hyperosmolar citrate solution (Soltran®) and 1 L University of Wisconsin solution (UW) at 4 °C through the distal aorta cannula. At the same time as starting the *in situ* perfusion, the thoracic cavity was accessed through the diaphragm and the descending thoracic aorta was clamped. Ice was applied to the abdomen cavity and the kidneys were then retrieved. The mid line incision was closed, and pigs were incinerated as per protocol of Huntington Life Sciences.

2.3.2.2 Back table perfusion

Under aseptic conditions, the abdominal cavity was accessed through a wide midline incision. Dissection was performed to expose the renal pedicles and heparin (500 IU/kg) was administered i.v. as a bolus dose through the marginal ear vein. Renal arteries and veins were ligated with 3-0 Vicryl ties (Ethicon, Johnson & Johnson, Livingstone, UK) and divided on the kidney side, to induce warm ischaemia (right followed by left). The ureter was identified, ligated distally with 3-0 Vicryl ties and divided. The kidneys were mobilised free but left in the abdominal cavity, and only removed after 10 min WIT and subsequently perfused on the back table with 500 mL Soltran® ± MitoQ. To collect blood for normothermic perfusion, the distal abdominal aorta was cannulated and pigs were exsanguinated. 1.5 L of blood was collected in a sterile receptacle, then transferred into CPDA-1 blood bags. The midline incision was closed and pigs were incinerated as per protocol of Huntington Life Sciences.

2.4 Declined deceased human kidneys

Full ethical approval (research ethics committee reference number: 12/EE/0202) was obtained to:

- Evaluate the safety and efficacy of MitoQ in ameliorating IRI using deceased human kidneys that have been retrieved and subsequently declined for transplantation from centres across the UK
- Allow the use of ABO compatible donated human blood for the use in EVNP

Informed consent was obtained by Specialist Nurses in Organ Donation (SNODs) prior to organ retrieval from the donor's family for research on declined deceased kidneys. Deceased human kidneys were declined for a variety of reasons including the presence of significant donor vascular disease (evidence on gross macroscopic examination) such as severe aortic atherosclerosis, poor perfusion, malignancy (renal or extra-renal), poor pre-implantation kidney biopsy indicating chronic disease and predicting graft failure, damage during retrieval or significant past medical history. Declined kidneys were received in our transplant centre and assessed for use in this study. Although all kidneys were declined for transplantation, they were deemed to be suitable to investigate the safety and efficacy of MitoQ on the EVNP circuit. Declined deceased human kidneys with more than two renal arteries were excluded due to technical difficulties in placing the kidney on the EVNP circuit or occlusion in the renal artery. In

addition, declined deceased human kidneys were excluded if the expected CIT was more than 24 h at the time of placing the kidney on the EVNP circuit (mimicking clinical practice).

The following donor related data were collected were obtained from NHS Blood and Transplant electronic offering system (EOS): age, gender, donor type, cause of decline, time of cardiac arrest, time of perfusion, warm and cold ischaemia times and co morbidities).

Declined deceased human kidneys were labelled as type of donor and treatment group (DBD vs. DCD, control vs. treatment) and in numerical order. This numerical order was correlated to patient identifiable information held in a password-protected Excel Database in the Department of Surgery, University of Cambridge.

2.5 Treatment of pig and declined deceased human kidneys

2.5.1 Treatment during cold ischaemia

Pig and declined deceased human kidneys were placed in a kidney dish filled with ice and Soltran® solution. The kidneys were flushed with 500 mL Soltran® ± MitoQ at 4 °C using a Tibbs cannula (Bolton Surgical, Sheffield, UK) placed in the renal artery and secured with a Vicryl tie. The kidneys were then preserved in either cold static storage (CSS) in 500 mL of Soltran® ± MitoQ or placed on the LifePort with 1 L KPS-1® with MitoQ for a maximum of 24 h post retrieval. A maximum of six wedge biopsies of 5 mm x 10 mm (approximately 120 mg tissue wet weight) were obtained traversing the cortex, medulla and inner medulla at different times during the cold ischemic time. A typical biopsy schedule consisted of a biopsy at 'time zero' (before infusion with 500 mL of Soltran® ± MitoQ), after the initial perfusion with 500 mL of Soltran ® ± MitoQ, and every 6 h subsequently (6 h, 12 h, 18 h, 24 h). Wedge biopsies were snap-frozen in liquid nitrogen and stored at -80 °C until analysed.

2.5.2 *Ex vivo* normothermic perfusion

The *Ex vivo* normothermic perfusion (EVNP) apparatus is a modified paediatric cardiopulmonary bypass circuit that supplies a single pig or declined deceased human kidney with oxygenated and heated blood as shown in Figure 2.2. It consists of a paediatric centrifugal pump, flow probe (BP50), pressure transducer, heat exchanger (Grants Instruments, Cambridge, UK) and temperature probe (Acorn, Oakton Instruments, Vernon Hills, IL, USA). Disposable perfusion sets (Medtronic, Watford, UK) were used for each experiment and consisted of a centrifugal pump, venous reservoir, polyvinyl chloride (PVC) tubing and membrane oxygenator (Minimax Plus, Medtronic). In addition to the perfusion system, two Gemini PC-2 infusion pumps (Imed, San Diego, CA, USA) were used to infuse a perfusate solution into the venous reservoir and arterial arm of the EVNP. The disposable perfusion set is connected to a custom-made glass chamber (University of Leicester, UK), where the kidney lies during the re-perfusion.

At the end of the desired period of cold ischaemia, the kidneys were flushed with 80 mL Ringer's lactate solution (Baxter Healthcare, Thetford, UK) and placed on EVNP circuit (at 38° C) in the glass chamber. The renal artery and ureter were cannulated with 12 Fr soft silastic catheters (Pennine, UK). Kidneys were reperfused at a mean arterial pressure of 80-90 mmHg with 250 mL blood collected at time of exsanguination for pig kidneys or with one unit (~ 300 mL) of ABO-compatible donated human packed red blood cells for declined deceased human kidneys, both diluted 1:1 with Ringer's lactate solution (Baxter Healthcare, Thetford, UK). The following were added to the perfusate:

- 6,250 U heparin (CP Pharmaceuticals, Wrexham, UK)
- 5 g mannitol 10% (Sigma-Aldrich)
- 5 mL cefuroxime 750 mg (Stragen, Reigate, UK)
- 12 mL sodium bicarbonate 8.4% (Fresenius Kabi, Cheshire, UK)
- 7 mL/h of glucose 5% (Baxter Healthcare)
- 100 U insulin (Novo Nordisk, Denmark)
- 20 mL/h nutriflex infusion (B Braun, Sheffield, UK)

The perfusate was oxygenated with 95% O_2/5% CO_2 at 0.5 L/min. To measure creatinine clearance as a marker of renal function, creatinine (Sigma-Aldrich, Steinheim, Germany) was added to the perfusate to achieve an initial circulating concentration of 1000 µmol/L. Creatinine was added to the perfusate because no external metabolic source of creatinine exist in the isolated perfused kidney. Urine output was recorded hourly and replaced mL for mL with Ringer's solution (Baxter Healthcare, Thetford, UK).

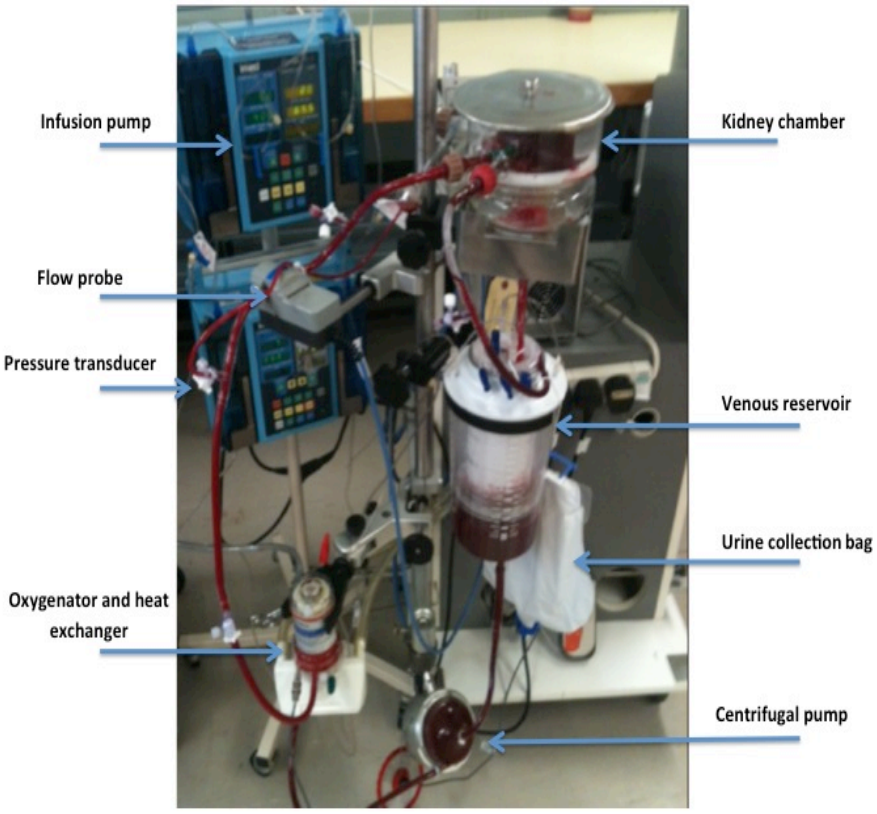

Figure 2.2. *Ex Vivo* Normothermic Perfusion Circuit. The EVNP circuit is based on paediatric cardiopulmonary bypass technology, produced by Medtronic Inc. The renal artery, vein and ureter were cannulated and the kidney was then placed in the kidney chamber. The blood perfusate (autologous for pig kidneys and donated human ABO compatible for declined deceased human kidneys) was then pumped from the venous reservoir via a centrifugal pump into a membrane oxygenator and heat exchanger. Oxygenated and warmed blood entered the arterial circuit and flowed into the kidney via the renal artery cannula. Deoxygenated venous blood then flowed from the renal vein back into the venous reservoir where it was re-circulated. Urine produced by the kidney was collected into a urinary bag attached to the cannulated ureter. Fluids, glucose and insulin were continually infused into the circuit at a set rate (60). Urinary losses were replaced mL for mL with Ringer's lactate solution. The arterial pressure across the circuit was fixed at 85 mmHg, allowing for the kidney to autoregulate its blood flow.

2.6 Assessment of pig and declined deceased human kidneys

To assess organ function in pig and declined deceased human kidneys, pairs of kidneys were placed on the EVNP circuit. Experimental end points included assays of:

- Renal functions: urine output, serum creatinine, creatinine clearance and fractional excretion of sodium
- Perfusion parameters: renal blood flow (RBF)
- Oxidative damage markers: protein carbonyls and lipid peroxidation (isoprostanes)

2.6.1 Renal function

2.6.1.1 Urine output

Urine produced by the kidney was collected into a urinary bag attached to the cannulated ureter. Urine output was recorded hourly during EVNP.

2.6.1.2 Creatinine concentration

Blood and urine samples were collected hourly during EVNP. The urine in the collection bag was well mixed before obtaining the sample. Serum and urinary creatinine levels were measured by the Clinical Biochemistry Department at Addenbrookes Hospital. The assay used to measure creatinine levels in each sample was based on the Jaffe reaction (61) using automated biochemical analyser (Siemens Dimension RxL analyser, Siemens AG, Healthcare Division, Germany).
The change of serum creatinine concentration at the end of EVNP was calculated as a percentage change using the following equation:

Percentage of serum creatinine fall = absolute change in serum creatinine concentration/initial concentration of serum creatinine x 100 (%)

Absolute change in serum creatinine concentration = initial concentration of serum creatinine - serum creatinine concentration at the end of EVNP

2.6.1.3 Creatinine clearance

Creatinine Clearance (CrCl) was calculated hourly during EVNP using the following equation:

$$CrCl = Ucr \times Uv/Pcr$$

Ucr = urinary creatinine (mg/mL) Uv = urinary volume (mL/min)

Pcr = plasma creatinine (mg/mL)

2.6.1.4 Fractional excretion of sodium

High percentage of fractional excretion of sodium (FE_{Na}) is an indicator of acute tubular necrosis (ATN), and has been used as an injury marker for pig and human kidneys in the *ex vivo* perfusion model (62, 63). Fractional excretion of sodium was calculated hourly during EVNP using the following equation:

$$(FE_{Na}) = (U_{Na+} \times P_{Cr}) / (P_{Na+} \times U_{Cr}) \times 100\ (\%)$$

U_{Na+} = urinary sodium (mmol/L) P_{Cr} = plasma creatinine (mg/dL)

P_{Na+} = plasma sodium (mmol/L) U_{Cr} = urinary creatinine (mg/dL)

2.6.2 EVNP parameters

Renal blood flow (RBF), mean arterial pressure (MAP) and temperature were recorded every 15 min for the first hour, then hourly during EVNP.

2.6.3 Markers of oxidative damage

Oxidative damage assays (protein carbonyl formation and lipid peroxidation) were performed on tissue samples taken from pig and declined deceased human kidneys at different times depending on the model used, but all within 30 h from retrieving the kidneys.

2.6.3.1 Protein carbonyl formation

Protein carbonyls are formed through oxidation of proteins by a variety of mechanisms. They are sensitive markers of oxidative injury. Protein carbonyl formation is irreversible, and occurs relatively early compared to other oxidative damage markers (64).

The Bicinchoninic acid (BCA protein) assay was used to measure the protein concentration of tissue homogenates (65). The principle of the BCA protein assay is based on the formation of a Copper (II) (Cu^{2+}) protein complex under alkaline conditions, followed by reduction of the Cu^{2+} to Copper (I) (Cu^{1+}). BCA forms a purple-blue complex with Cu^{1+} in alkaline environments providing a basis to monitor the reduction of alkaline Cu^{2+} by proteins.

Tissue samples (30 mg wet weight) were homogenized in phosphate buffered saline (PBS) supplemented with a protease inhibitor cocktail (Complete, Mini, EDTA-free tabs, Roche) at 4 °C. The collected supernatants were diluted 1:5 in 1% (v/v) Triton X-100. 20 µL of samples, bovine serum albumin (BSA) standards and blanks were then added to a 96-well plate in triplicate. Reagent A solution (pH 11.25) consists of:

- 1% (w/v) BCA
- 2% (w/v) sodium carbonate (Na_2CO_3)

- 0.16% (w/v) sodium tartrate (Na_2-tartrate)
- 0.4% (w/v) sodium hydroxide (NaOH)
- 0.95% (w/v) sodium bicarbonate ($NaHCO_3$)

50 parts reagent A solution was mixed with 1 part reagent B solution (4% (w/v) Copper (II) Sulfate Pentahydrate ($CuSO_4$.5H20) and 200 µL was added to the plate wells. The plate was then incubated at 37 °C for 45 min and absorbance read at 562 nm using an Elx808 Biotek plate reader. A BSA standard curve (range 0 - 500 µg/mL) was constructed using DeltaSoft 3 software (BioMetallics Inc.). The protein concentrations of the samples were quantified relative to the bovine serum albumin (BSA) standard curve.

Total protein carbonyls concentration in kidney tissue was then determined by enzyme-linked immunosorbent assay (ELISA), using the BioCell PC test kit (Biocell Corp, Auckland, New Zealand) according to the manufacturer's instructions.

Samples, standards and controls were incubated with dinitrophenylhydrazine (DNP) which reacts selectively with protein carbonyl groups. These were then adsorbed onto the ELISA plate and non-bound DNP was washed away. The adsorbed protein was then probed with biotinylated anti-DNP biotinantibody, washed and incubated with streptavidin-linked horseradish peroxidase. A chromatin reagent containing H_2O_2 was then added which catalysed the oxidation of 3,3',5,5'-tetramethylbenzidine (TMB). The reaction was followed at 650 nm until the highest standard reached the value recommended by the manufacturer. On average this took ~ 8 min. The reaction was then stopped by the addition of a proprietary acid reagent and the absorbance was measured for each well at 450 nm. A linear standard curve was constructed using samples with known amounts of carbonylated protein (provided). R^2 values >0.95 were always obtained. The carbonyl content of the samples were determined using the regression factors obtained from the standard curve (66).

2.6.3.2 Isoprostanes

8-*iso* prostaglandin $F_{2\alpha}$ is an isoprostane produced by the non-enzymatic peroxidation of arachidonic acid in membrane phospholipids and has been established as an oxidative injury biomarker in oxidative stress and renal IRI (67, 68). 8-*iso* prostaglandin $F_{2\alpha}$ was measured by ultra-high performance liquid chromatography (UHPLC) coupled with a 6460 triple quadrupole mass spectrometry (QqQ-MS/MS) relative to internal standard (40 µL containing 100 nM of 8-iso-PGF2a-d4).

Tissue samples (25 mg) for isoprostane (IsoP) quantification were processed according to Milne *et al.* 2013 protocol (67). The dried lipid extract was resuspended in 1 mL of methanol containing 0.005 % butylated hydroxyanisole (BHA, Sigma-Aldrich, St. Louis, MO, USA) and vortexed. Next, 1 mL aqueous potassium hydroxide (KOH) (15 % w/v) was added and after vortexing, samples were incubated at 37 °C for 20 min. The mixture was then centrifuged at 11000 *g* for 5 min. The supernatant was subjected to

solid phase extraction using a Strata X-AW cartridge, 100 mg/3 mL (Phenomenex, Torrance, CA, USA), as previously described (69). Samples were diluted in 2 mL BIS-TRIS (Bis-(2-hydroxyethyl)-amino-tris(hydroxymethyl)-metha; Sigma-Aldrich, St. Louis, MO, USA) buffer (0.02 M HCl pH = 7) and applied to a cartridge (conditioned and equilibrated with 2 mL of methanol and 2 mL milliQ-water). Each sample was loaded at a flow rate of about 1 drop per 2 seconds. The target compounds were eluted with 1 mL methanol and dried using SpeedVac concentrator (Savant SPD121P, Thermo Scientific, MA, USA). The dry extracts were reconstituted with 200 µL of A/B solvents, 90:10, *v/v* (solvent A, Milli-Q water/acetic acid (99.99:0.01, *v/v*) and solvent B (MeOH/acetic acid). Samples were then sonicated for 10 min and filtered through 0.45 µm filter (Millipore, MA, USA) (70).

The separation of IsoP present in the tissue samples was performed using ultra-high performance liquid chromatography (UHPLC) coupled with a 6460 triple quadrupole mass spectrometry (QqQ-MS/MS) (Agilent Technologies, Waldbronn, Germany). All LC-MS grade solvents were obtained from J.T. Baker (Phillipsburg, NJ, USA). Synthetic 8-*iso* prostaglandin $F_{2\alpha}$ was purchased from Cayman Chemicals (Ann Arbor, MI, USA).

Chromatographic separation was carried out on an ACQUITY UPLC BEH C_{18} column (2.1 x 150 mm, 1.7 µm; Waters). The temperatures of the column ovens were 6 °C (left) and 6 °C (right). The mobile phases employed were solvent A and solvent B. The flow rate was 0.15 mL/min using the linear gradient scheme (t; %B): (0.00; 60), (7.00; 60), (7.01; 73), (10.00; 73), (10.01; 80), (18.00; 100), (19.00; 100), and (19.01; 60). The sample volume injected was 20 µL. The operating conditions for the MS parameters were as follows: gas flow: 8 L/min, nebulizer: 30 psi, capillary voltage: 2750 V, nozzle voltage: 1500 V, gas temperature: 325 °C, sheath gas temperature: 350 °C, and jet stream gas flow: 12 L/min. The MS analysis was applied in the multiple reaction monitoring (MRM) negative Electrospray ionization (ESI) mode. Data acquisition and processing were performed using MassHunter software version B.04.00 (Agilent Technologies) (71).

2.7 Uptake of MitoQ

MitoQ concentration in pig and declined deceased human kidneys was measured by liquid chromatography tandem mass spectrometry (LC-MS/MS) relative to a deuterated internal standard (d_{15}-MitoQ) (42). Tissue biopsies were briefly rinsed in normal saline to remove any MitoQ from the tissue surface and then flash frozen in liquid nitrogen. To extract MitoQ from kidney tissue, the sample (20 or 50 mg wet weight) was thawed to 4 °C and homogenised in a 2 mL Eppendorf tube using a bullet blender (Next Advance Inc, NY) in 500 µL Tris-HCl buffer (50 mM, pH 7.0). The homogenate was then spiked with internal standard (50 pmol d_{15}-MitoQ), vortexed (10 s) and 1.5 mL 95 % acetonitrile (ACN)/ 0.1 % formic acid (FA) added, vortexed again and centrifuged (10 min at 16,000 *g*). The supernatant was transferred to a fresh tube, the pellet re-extracted and the combined supernatants dried under vacuum

(Savant SpeedVac 3-4h). The dried sample was re-suspended in 200 µL 20 % ACN/0.1 % FA, vortexed (5 min), sonicated (Ultra BT Ultrasonic Bath, Ultrawave Ltd) (5 min), centrifuged (10 min at 16,000 *g*) and filtered (0.22 µm PVDF filter, Millex from Millipore) into an autosampler vial (1.5 mL silanised, Chromacol). Samples were then analysed by LC-MS/MS with multiple reaction monitoring (MRM) in positive ion mode using a Xevo TQ-S mass spectrometer and an I-Class Acquity UPLC (both from Waters, UK). This step was performed by Dr. Angela Logan (MRC Mitochondria Biology Unit, UK). Data were then analysed using MassLynx MS software (Waters, UK). For all experiments a standard curve was prepared and run in parallel using tissue spiked with d_{15}-MitoQ and different concentrations of MitoQ.

Histopathology

A wedge biopsy sample 5 mm x 10 mm (around 120 mg tissue wet weight) from cortex, medulla and inner medulla was taken from the pig and declined human kidneys at different times depending on the model used, but all within 24 h of retrieving the kidneys. ~ 20 mg of each collected biopsy was fixed in 10% formaline, sectioned, stained with haematoxylin and eosin. Samples were assessed for markers and degrees of IRI such as microvascular damage by a histopathology consultant. Histopathological assessment was performed blinded to experimental group identity.

2.8 Disposal of kidneys

Pig and declined deceased human kidneys were incinerated after treatment as per protocol of Cambridge University Hospitals NHS Trust. Whole pig blood perfusate or donated ABO compatible blood perfusate used for the *ex vivo* normothermic perfusion were also discarded as per the Trust's guidelines. Universal precautions were taken when handling pig and declined deceased human tissues or blood.

2.9 Statistical analysis

Data are presented as mean ± standard deviation (SD), unless otherwise stated. The difference between a pair of kidneys was analysed using the two-tailed paired t-test. In cases where several conditions were compared, one-way analysis of variance (ANOVA) was used. In all subgroup analysis, p values were adjusted for multiple testing using Bonferroni correction (p value x number of statistical tests performed). Statistical analysis was performed using GraphPad Prism (GraphPad, La Jolla, CA). All tests were performed at the 5% significance level.

2.10 Contribution of others

The pig surgery was carried out initially with the supervision and assistance of:

- Dr. Kourosh Saeb-Parsy (Department of Surgery, Addenbrookes Hospital, Cambridge).

- Professor Michael Nicholson (Department of Surgery, Addenbrookes Hospital, Cambridge).
- Dr. Adam Bradlow (Department of Surgery, Addenbrookes Hospital, Cambridge).

Thereafter, I became independent in retrieving pig kidneys and the surgery was carried out with the assistance of:

- Nikkitas Georgakopoulos (Research Assistance, Department of Surgery, Addenbrookes Hospital, Cambridge).
- Keziah Crick (Perfusionist, Department of Surgery, Addenbrookes Hospital, Cambridge).
- Diogo Fouto (Perfusionist, Department of Surgery, Addenbrookes Hospital, Cambridge).
- Corrina Fear (Perfusionist, Department of Surgery, Addenbrookes Hospital, Cambridge).

The *ex vivo* normothermic perfusion was performed with the assistance of Dr. Sarah Hosgood (Department of Surgery, Addenbrookes Hospital, Cambridge).

I prepared the samples to investigate MitoQ uptake (MitoQ extraction from kidney tissue). The step of quantification of MitoQ by LC-MS was performed by Dr. Angela Logan (MRC Mitochondrial Biology Unit, UK).

I prepared the samples to investigate 8-*iso* prostaglandin $F_{2\alpha}$ as a marker of lipid peroxidation. The steps of quantification of isoprostane, mass-spectrometry and data processing were performed by Dr. Zsuzsanna Ament (MRC Human Nutrition Research, UK).

The original ethical approval for the declined human kidney work was obtained by Miss. Ioanna Panagiotopoulou (Department of Surgery, Addenbrookes Hospital, Cambridge) and the repeat approval was obtained by Nikkitas Georgakopoulos (Research Assistance, Department of Surgery, Addenbrookes Hospital, Cambridge).

The work presented in this thesis was funded by Evelyn Trust. The LifePort kidney transporter used to investigate the uptake of MitoQ during cold preservation was lent by Organ Recovery Systems.

Chapter 3

MitoQ uptake

3.1 Introduction

Since the 1970s organ preservation has relied on hypothermic conditions to minimize ischaemic injury, maintain organ viability, reduce cellular metabolism and to allow an organ to be preserved outside the body from the time of retrieval until transplantation.

The work of Belzer (72) and his colleagues and that of Collins *et al*. (73) established the foundation for two alternative methods of organ preservation during ischaemia; continuous perfusion with cold preservation solution using hypothermic machine preservation (HMP) or initial flushing with cold preservation solution followed by cold static storage (CSS) on ice.

Due to the disparity between organ supply and demand, the use of DCD kidneys has recently increased (74). The use of kidneys from DCD donors is shown to be associated with a higher delayed graft function (DGF) rate than those from DBD donors (1), at least partly due to the unavoidable period of warm ischaemia inherent in the process of DCD organ procurement. Optimizing the preservation of such kidneys has become an increasingly important issue in transplantation. It has been suggested that preservation by HMP of DCD kidneys results in a lower rate of DGF and better graft survival compared with kidneys preserved by CSS (75, 76). However, a well-powered randomized control trial performed in our centre has demonstrated that preservation by HMP of DCD kidneys has no additional protective effect on short-term or long-term kidney transplant outcomes compared with those preserved by CSS (77)

MitoQ uptake into the solid organs has been investigated in small animal models, following different modes of delivery. These studies confirmed that MitoQ uptake is driven by the mitochondrial membrane potential, described by the Nernst equation, whereby cation uptake (TPP moiety in MitoQ) increases 10-fold for every 61.5 mV at 37 °C. However, it remains unclear if the mitochondria are able to maintain a sufficient membrane potential during cold preservation (4 °C) to drive uptake of MitoQ. To address this concern, Tracy Prime (MRC Mitochondrial Biology Unit) showed that there was a significant uptake of MitoQ at 4 °C using isolated rat mitochondria, albeit less than at 37 °C (personal communication). In addition, successful uptake of MitoQ was demonstrated in donor mouse hearts during flushing and cold preservation (50).

MitoQ has been shown to be effective when administered prior to reperfusion in a rat cardiac IRI model, where oral MitoQ before onset of cardiac ischaemia significantly reduced mitochondrial damage after reperfusion (78). Systemic intravenous administration of a bolus of MitoQ, 15 min prior to the onset of ischaemia, has also been shown to significantly reduce oxidative damage following renal IRI in a mouse model (40).

However, MitoQ uptake has not been characterised in large animal models, and specifically with regard to this work, MitoQ uptake by pig kidneys during cold preservation has not been investigated before. As

shown in small animal models, it is essential to administer MitoQ before reperfusion. In principle, MitoQ can be administered at different time points during cold preservation (after retrieval, later during cold storage, or just before reperfusion). This would allow treatment of an isolated organ with MitoQ rather than the whole donor. In addition, pre-mortem interventions in DCD donors are not currently permissible. In clinical practice kidneys are exposed to a variable period of cold ischaemia depending on several factors (e.g. the distance between the donor and recipient hospital). Maintaining a constant safe and therapeutic tissue concentration of MitoQ may be difficult if there is ongoing uptake of MitoQ during cold preservation. Delivery of MitoQ at a later time point during cold preservation (e.g. just before reperfusion) offers another alternative to avoid the variability in CIT, and might lead to more predictable and controlled MitoQ tissue concentrations. However, the optimal time for the administration of MitoQ depends on whether MitoQ is taken up equally by warm (immediate delivery of MitoQ) and cold kidneys (delayed delivery of MitoQ), and also whether it is continuously taken up into the tissue during cold storage.

Finally, MitoQ uptake has not been compared between the two methods of organ preservation (HMP and CSS). It is unclear if the continuous circulation of the preservation fluid in the hypothermic machine perfusion will have an impact on MitoQ tissue concentrations.

In this context, I aimed to characterise MitoQ uptake using:

1. Different pig models (controlled vs. uncontrolled)
2. Different time points during cold preservation (cold vs. warm kidneys)
3. Different modes of organ preservation (CSS vs. HMP)
4. A range of MitoQ concentrations

This was done in order to help determine what concentration, route and duration of delivery of MitoQ are most appropriate for subsequent experiments.

3.2 MitoQ uptake by the kidney using the uncontrolled pig model

3.2.1 MitoQ dose

The dose of MitoQ used in these experiments (5 μM and 50 μM) were based on previous studies which demonstrated 50 μM MitoQ to be safe and effective in reducing IRI using a mouse model of heterotopic cardiac transplantation (79).

3.2.2 Simulation of a DCD model

In order to obtain pilot data on MitoQ to inform further experiments, initial experiments were performed using kidneys from pigs sacrificed for meat under conditions dictated by agricultural regulations. As outlined in chapter 2, large female (Landrace) pigs (weighing 40-50 kg, aged 3-4 months)

were sacrificed by electrocution followed by carotid exsanguination at a licensed local abattoir (C. A. Leech – Royston, Cambridgeshire). The kidneys were retrieved *en bloc* after 10 to 20 min of *in situ* warm ischaemia (WI) to simulate the clinical scenario of donation after circulatory death. Once kidneys were retrieved, they were placed in a kidney dish filled with ice and Soltran® solution on the back table. Kidneys were flushed with 500 mL of Soltran® with MitoQ at 4 °C. The kidneys were then preserved in either cold static storage (CSS) in 500 mL of Soltran® with MitoQ or placed on the LifePort with 1 L of KPS-1® with MitoQ for 24 h post retrieval (Figure 3.1). Wedge biopsies were obtained after the initial perfusion with 500 mL of Soltran® with MitoQ and every 6 h subsequently (6 h, 12 h, 18 h, 24 h). Wedge biopsies were snap-frozen in liquid nitrogen and stored at -80 °C until analysed. LifePort parameters (flow, resistance, pressure and temperature) were recorded throughout the procedure at hourly intervals.

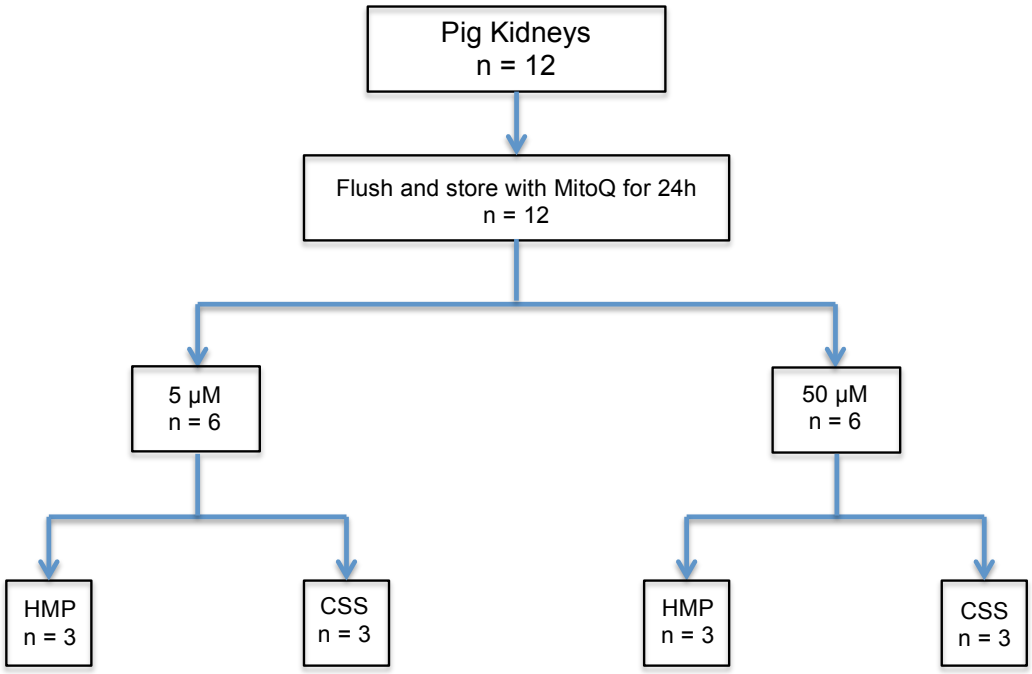

Figure 3.1. Experimental design for MitoQ uptake by the kidneys using the uncontrolled pig model. The kidneys were flushed with and stored in MitoQ at the indicated concentrations and kidney preservation methods.

3.2.3 MitoQ uptake using the uncontrolled pig model

In the uncontrolled pig model, MitoQ uptake by the kidney, investigated using two doses: 5 µM and 50 µM, was higher in HMP group compared to CSS group during 24 h of cold preservation. Most of the MitoQ uptake in the HMP group occurred during the first 6 h post perfusion, with the 5 µM dose having a mean tissue concentration of 1.2 ± 1.3 pmol/mg post perfusion, and 33.2 ± 2.9 pmol/mg at 6 h post perfusion. The trend of the 50 µM dose uptake of the HMP group was similar, with a mean of 17.7 ± 17.9 pmol/mg at post perfusion samples, which increased to 143.6 ± 128.9 pmol/mg at 6 h post perfusion (Figure 3.2a, Figure 3.2b).

Unlike in the HMP group, the majority of MitoQ uptake in the CSS group happened immediately after perfusion, with a mean tissue concentration of 4.7 ± 5.7 pmol/mg and 16.9 ± 16.5 pmol/mg in the post perfusion samples for the 5 µM and the 50 µM doses respectively. Thereafter, MitoQ tissue concentrations were stable during the 24 h CSS preservation (Figure 3.2a, Figure 3.2b).

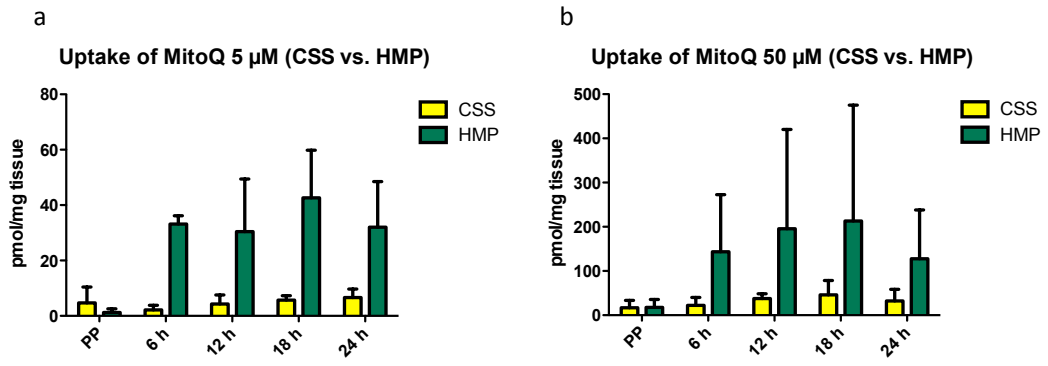

Figure 3.2. MitoQ uptake by the kidneys using the uncontrolled pig model using the indicated methods of kidney preservation (n = 3 per group). (a) The kidneys were flushed with, and stored in 5 µM MitoQ for 24 h. (b) The kidneys were flushed with, and stored in 50 µM MitoQ for 24 h. Biopsy samples were taken immediately post-perfusion on the back table (PP), at 6 h CSS, 12 h CC, 18 h CSS and 24 h CSS.

Data are mean ± SD.

3.2.4 Machine perfusion parameters

Flow significantly improved during the HMP preservation period. A similar trend was observed in both groups (5 µM MitoQ, 50 µM MitoQ) suggesting that this positive effect might solely be secondary to HMP (Figure 3.3a). There was a corresponding reduction in resistance in both groups (Figure 3.3b).

The temperature of the HMP fluid was maintained at a mean of 4°C through the 24 h cold preservation (data not shown). The pressure remained static at 29 ± 1 mmHg during 24 h cold preservation (data not shown).

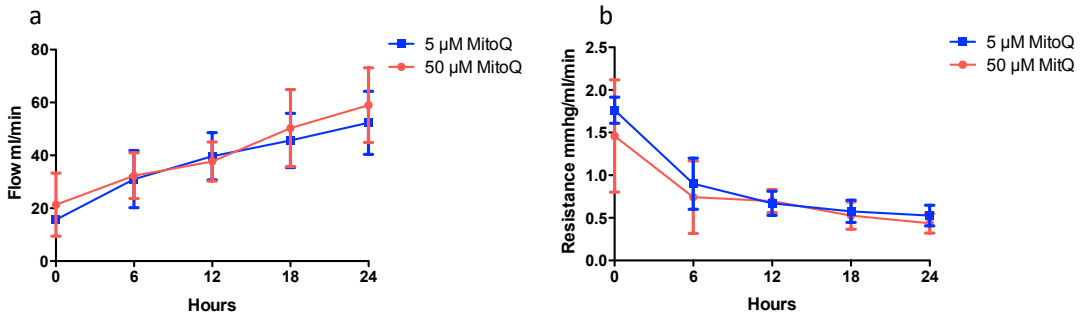

Figure 3.3. HMP parameters in kidneys using the uncontrolled pig model (n = 3 per group). The kidneys were perfused with, and stored in MitoQ at the indicated concentrations for 24 h. (a) HMP flow (b) HMP resistance. Data are mean ± SD.

3.3 MitoQ uptake by the kidney using the controlled pig model

The key aim of using a controlled pig model was to overcome the marked vascular spasm, which was noticed in the uncontrolled pig model, evident by the difficulty in perfusing the kidneys on the back table. Our pilot data indicated that the uncontrolled nature of inducing death, through electrocution and exsanguination, resulted in significant variability between animals and was not appropriate for subsequent experiments.

3.3.1 The controlled DCD pig model

As outlined in chapter 2, large female Landrace pigs (weighing 40 - 50 kg, aged 3 - 4 months) were supplied by Huntingdon Life Sciences, Huntingdon, UK. Pigs were allowed to acclimatize to the treatment room. To relieve the pain and reduce stress, all animals received intra-muscular (IM) sedation and narcotic analgesia (ketamine 10 mg/kg, medetomidine 0.02 mg/kg and midazolam 0.1 mg/kg). General anaesthesia was induced by i.v. propofol 4 - 6 mL per 50 kg and then maintained by i.v. infusion of Remifentanyl (starting at 0.04 mg/kg/min and titrating up to 0.4 mg/kg/min) and propofol (starting at 10 mg/kg/hr and titrating down to 60-70% of the starting amount). The abdominal cavity was accessed through a mid-line incision. Dissection was performed to expose the renal pedicles and heparin (500 IU/kg) was administered i.v. as a bolus through the marginal ear vein. Renal arteries and veins were ligated with 3-0 Vicryl ties and divided on the kidney side to induce warm ischaemia. The kidneys were mobilised free but left in the abdominal cavity, and only removed after 10 min WIT and subsequently perfused on the back table with 500 mL of Soltran® ± MitoQ.

In this experiment, MitoQ was introduced at two time points, either immediately on the back table (at the end of WIT) or after 12 h cold preservation, in order to investigate if there are any differences in MitoQ uptake between warm and cold kidneys. Some kidneys were flushed immediately with 500 mL Soltran® with MitoQ at 4 °C on the back table. The kidneys were then preserved in either cold static storage (CSS) in 500 mL Soltran® with MitoQ or placed on the LifePort with 1 L KPS-1® with MitoQ for 24 h. Other kidneys were flushed with and stored in 500 mL Soltran® only in CSS for 12 h. After this period, the cooled pig kidneys were then flushed with 500 mL Soltran® with MitoQ at 4 °C and stored either with or without MitoQ for another 12 h in CSS. Control kidneys (no MitoQ) were preserved in either CSS in 500 mL of Soltran® only or placed on the LifePort with 1 L of KPS-1® only for 24 h post retrieval (Figure 3.4).

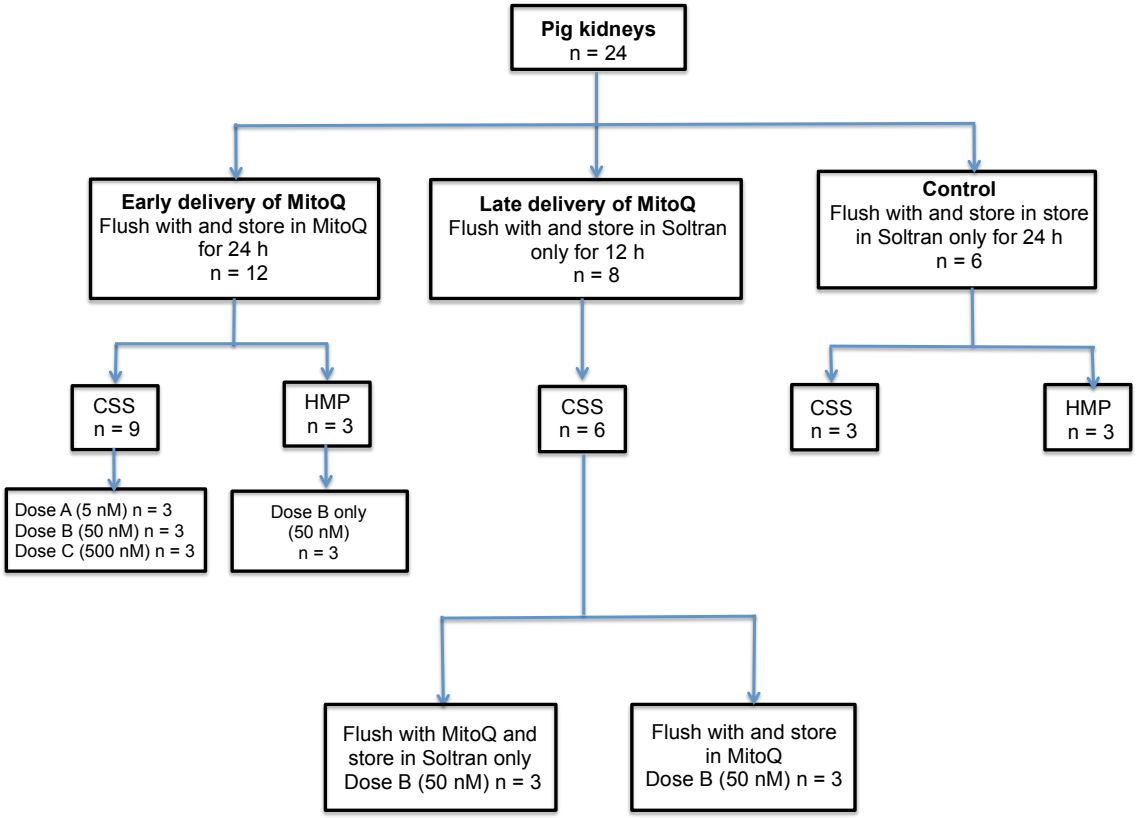

Figure 3.4. Experimental design for MitoQ uptake in the controlled DCD pig model. The kidneys were flushed with, and stored in MitoQ at the indicated concentrations, time points and kidney preservation methods.

3.3.2 MitoQ dose

Based on preliminary MitoQ uptake data obtained from Dr. Anna Dare (MRC Mitochondrial Biology Unit; personal communication) in the uncontrolled DCD pig model, a range of 5 nM - 500 nM MitoQ were used in initial experiments. MitoQ uptake for higher concentrations of MitoQ (5 μM - 250 μM) were also investigated using EVNP, as described in chapter 4.

3.3.3 MitoQ uptake following early delivery

In this model, kidneys were flushed with MitoQ immediately on the back table (after 10 mins of WIT) and stored in MitoQ for 24 h of cold preservation either using CSS or in HMP. Most of the MitoQ uptake in the CSS group occurred immediately after perfusion, with a mean tissue concentration of 6.3 ± 4.8, 0.4 ± 0.1 and 0.1 ± 0.1 pmol/mg at post perfusion samples for the 500, 50 and 5 nM doses, respectively. Thereafter the MitoQ tissue concentrations were static during the 24 h of CSS preservation (Figure 3.5). In comparison with the previous uncontrolled pig model CSS group (Figure 3.2); despite using 100-fold lower concentration of MitoQ (500 nM vs. 50 μM), levels of MitoQ were only 3-fold lower (mean 6.3 vs. 16.9 pmol/mg).

Next, I investigated MitoQ uptake by the kidneys using the controlled pig model during 24 h HMP preservation. I decided to use only one dose of MitoQ (50 nM) in this model and subsequent models (as showed in Figure 3.4), to maximise the utilization of controlled pig kidneys, and to be able to investigate MitoQ uptake at different time points using different modes of organ preservation (CSS, HMP). The uptake of 50 nM MitoQ by the kidneys using the controlled pig model at the end of 24 h cold preservation was numerically higher in the HMP group compared to the CSS group but the difference did not reach statistical significance (50 nM MitoQ HMP 1.5 ± 0.4 vs. 50 nM MitoQ CSS 0.6 ± 0.3 pmol/mg; p = 0.100 unpaired t-test; Figure 3.6). The difference in MitoQ uptake by the kidneys between CSS and HMP in controlled pig model was less prominent compared to the marked difference that was observed in the uncontrolled pig model (Figure 3.2).

Most of the MitoQ uptake by the kidneys in the HMP controlled pig model group occurred by 6 h post perfusion. Using the 50 nM, the mean tissue concentration of 0.3 ± 0.2 pmol/mg at post perfusion samples increased to 1.2 ± 0.6 pmol/ mg at 6 h post perfusion. Thereafter, using 50 nM MitoQ, tissue concentrations were static during the 24 h of HMP preservation (Figure 3.6).

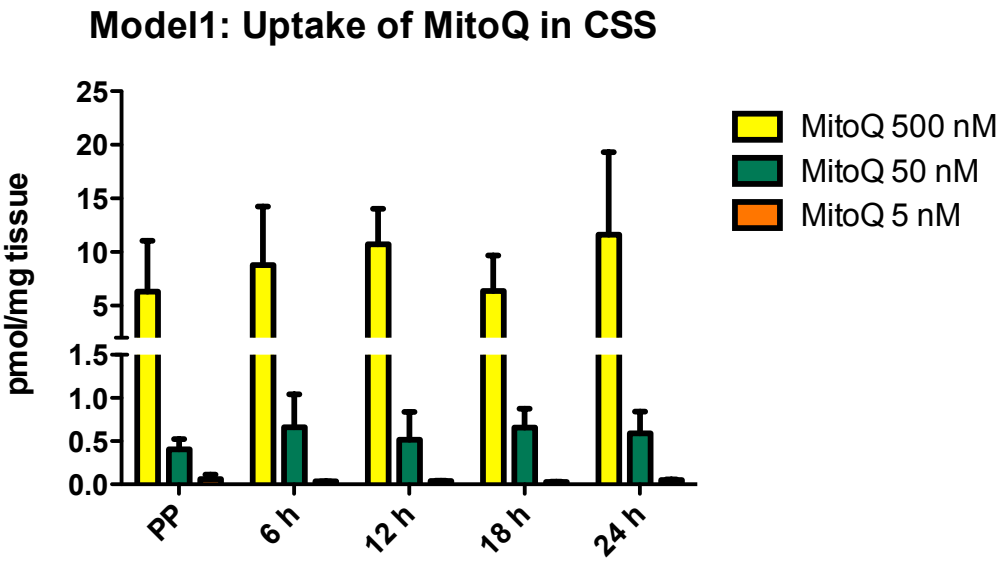

Figure 3.5. MitoQ uptake by the kidneys using the controlled pig model during 24 h of CSS. The kidneys were flushed with, and stored in MitoQ at the indicated concentrations (n = 3 per group). Biopsy samples were taken immediately post-perfusion on the back table (PP), at 6 h CSS, 12 h CC, 18 h CSS and 24 h CSS. Data are mean ± SD.

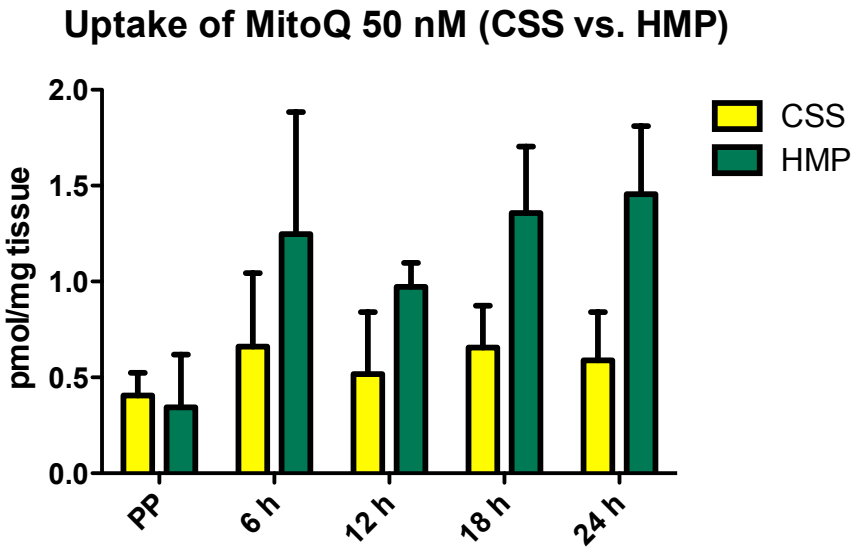

Figure 3.6. MitoQ uptake by the kidneys using the controlled pig model. The kidneys were flushed with and stored in 50 nM MitoQ for 24 h, at the indicated methods of kidney preservation (n = 3 per group). Biopsy samples were taken immediately post-perfusion on the back table (PP), at 6 h CSS, 12 h CC, 18 h CSS and 24 h CSS. Data are mean ± SD.

3.3.4 MitoQ uptake following delivery to cold kidneys

The aim of this experiment was to investigate MitoQ uptake at a different time point (after 12 h of cold preservation), and explore if cooled pig kidneys are able to take up substantial amounts of MitoQ. In addition, I investigated whether flushing cooled pig kidneys with a bolus of MitoQ (without storing thereafter in MitoQ) is sufficient to achieve and maintain a stable tissue concentration, or whether it is necessary to flush and store the kidneys in MitoQ to maintain tissue concentrations.

MitoQ was administered after 12 h cold preservation; the kidneys were initially flushed and preserved in 500 mL Soltran® in CSS for 12 h. Cooled pig kidneys were then flushed with 500 mL Soltran® with MitoQ at 4 °C. Thereafter, the kidneys were preserved by CSS either with or without MitoQ for a further 12 h (Figure 3.7). Cold pig kidneys were able to take up MitoQ successfully after 12 h CSS. Most of the MitoQ uptake happened immediately after perfusion with MitoQ in both groups (stored with or without MitoQ). In addition, there was no further MitoQ uptake during the subsequent 12 h of cold preservation using 50 nM MitoQ, and there was no difference in tissue concentrations between kidneys stored with or without MitoQ (Figure 3.7). However, the uptake of 50 nM MitoQ by cooled kidneys at 12 h cold preservation using the controlled pig model was significantly less than the uptake of 50 nM MitoQ by warm kidneys at the start of cold preservation using controlled pig model (0.2 ± 0.1 vs. 0.4 ± 0.1 pmol/mg; $p = 0.029$ unpaired t-test; Figure 3.7, Figure 3.5).

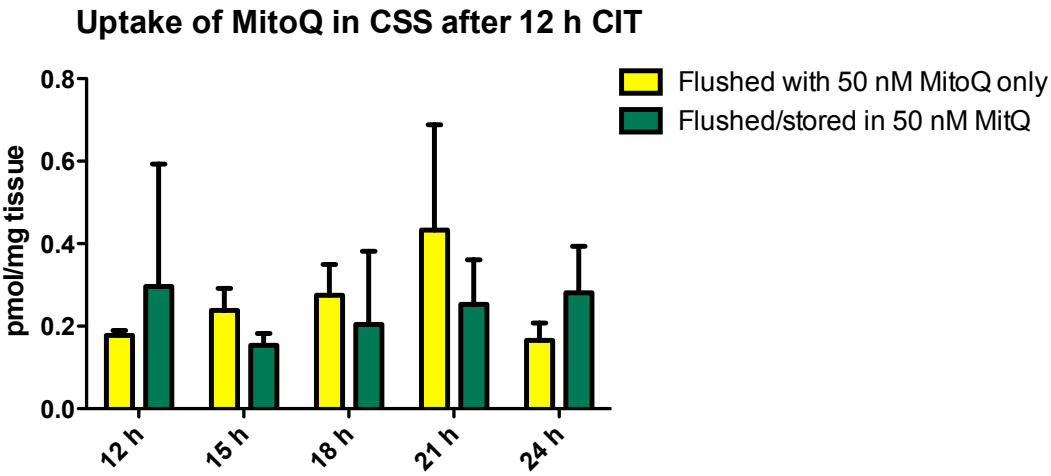

Figure 3.7. MitoQ uptake by kidneys using the controlled pig model. The kidneys were flushed with 50 nM MitoQ after 12 h of CSS. Thereafter, the kidneys were preserved in CSS with or without MitoQ for another 12 h (n = 3 per group). There was no significant difference between the kidneys that were flushed with 50 nM MitoQ only and the kidneys that were flushed and stored in 50 nM MitoQ at 12 h CSS (0.2 ± 0.1 vs. 0.3 ± 0.3 pmol/mg; p = 0.528 unpaired t-test) or at the end of 24 h CSS (0.2 ± 0.1 vs. 0.3 ± 0.1 pmol/mg; p = 0.172 unpaired t-test). Data are mean ± SD.

3.3.5 Hypothermic machine perfusion parameters in the controlled pig model

Throughout the 24 h cold preservation, there was no difference in the flow between the control group (no MitoQ) and the 50 nM MitoQ group. In both groups, there was a minor improvement in the flow during the first 6 h of HMP preservation. Thereafter, the flow remained static during 24 h of HMP preservation. There was a corresponding reduction in resistance in both groups.

The temperature of HMP fluid was maintained in a mean of 4 °C through the 24 h cold preservation (data not shown). The pressure remained static at 29 mmHg during the 24 h cold preservation (data not shown). The kidneys in the controlled pig model had better flow and lower resistance compared to the kidneys in the uncontrolled pig model (Figure 3.8). This might be explained by the cumulative effect of sedation, analgesia and general anaesthesia, in reducing the marked vascular spasm, which was noticed in the uncontrolled pig model.

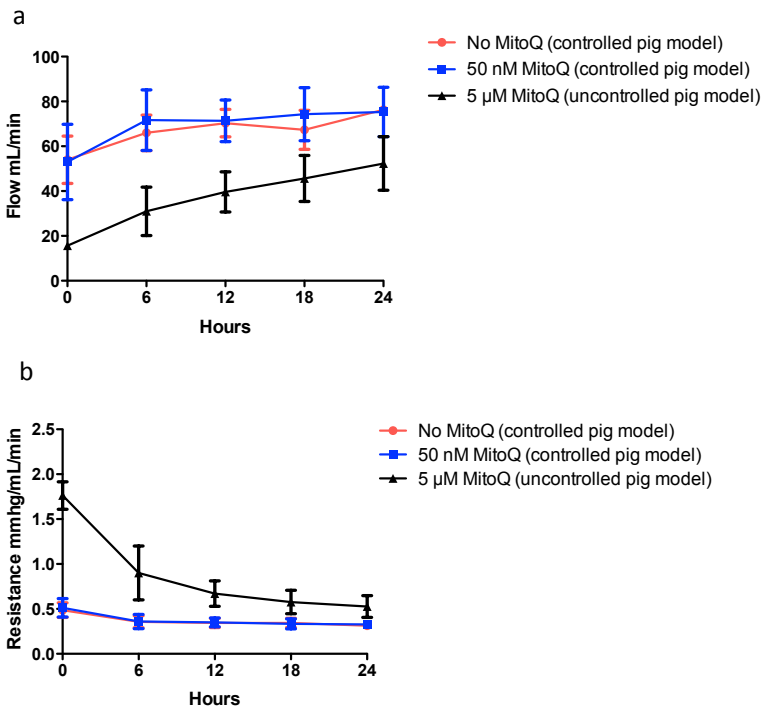

Figure 3.8. HMP parameters in kidneys using two pig models: controlled and uncontrolled. The kidneys were flushed and stored with or without MitoQ (control) at the indicated concentrations for 24 h (n = 3 per group). (a) HMP flow (b) HMP resistance. Data are mean ± SD.

3.4 Discussion

In this chapter I was able to demonstrate that:

1. The controlled pig model is more appropriate than the uncontrolled pig model for subsequent experiments
2. MitoQ is taken up efficiently by pig kidneys
3. Most of the MitoQ uptake occurs rapidly upon flushing with MitoQ
4. There is no difference whether kidneys are stored with or without MitoQ
5. HMP increases MitoQ uptake by approximately 2-fold compared to CSS
6. MitoQ tissue concentrations are stable over time
7. MitoQ uptake by cold kidneys (late delivery of MitoQ) is approximately half of the uptake by warm kidneys (early delivery of MitoQ)

The uncontrolled pig model provided a cost-effective model for pilot experiments to investigate MitoQ uptake by kidneys using two different methods of organ preservation (HMP and CSS). MitoQ uptake by kidneys was higher in the HMP group compared to the CSS group. In addition, HMP appeared to have a bigger impact on MitoQ uptake in the uncontrolled pig model compared to the controlled model. This can be partially explained by the marked vascular spasm in the uncontrolled pig model, which might result in suboptimal delivery of MitoQ to the capillary network using CSS, and HMP was able to partially overcome this. In support of this, most of the MitoQ uptake in the HMP group was during the first 6 h post perfusion, corresponding with the significant improvement in HMP flow and reduction in resistance during the same period. In addition, in the uncontrolled pig model, the process of electrocution and exsanguination resulted in marked vascular spasm in those agitated pigs. This was evident in the great difficulty in flushing the kidneys on the back table, and the initial high resistance for the kidneys placed on the HMP.

The controlled pig model allowed reduction of the marked vascular spasm, which was noticed in the uncontrolled pig model, evident by the high HMP flow and the low resistance for those kidneys stored via HMP. In support of this, the time needed to flush the kidneys on the back table was less. In addition, MitoQ uptake by the kidneys using the controlled pig model was better compared to the uncontrolled pig model. The controlled pig model (but not the uncontrolled model) also had comparable HMP parameters (flow and resistance) to the human kidney HMP parameters in clinical practice (80). In the Patel et al. 2012 study, the mean initial HMP flow was 59 ± 35 mL/min compared to 54 ± 11 mL/min in the controlled pig kidney model and 16 ± 1 mL/min in the uncontrolled pig model. The initial mean resistance in the human kidneys was 0.5 ± 0.3 mm Hg/mL/min compared to 0.5 ± 0.1 mm Hg/mL/min in the controlled pig kidney model and 1.8 ± 0.2 mm Hg/mL/min in the uncontrolled pig model. Taken together, these findings suggest that the controlled pig model was more appropriate than the

uncontrolled pig model for subsequent experiments.

Most of the MitoQ uptake by the kidneys in the controlled pig model CSS group occurred rapidly upon perfusion, and remained stable thereafter. This can be explained by the fact that in the CSS group, after the initial perfusion with MitoQ, there are only two sources to supply CSS kidneys with MitoQ, the static perfusion fluid in the kidney intravascular space and the surrounding perfusion fluid. It is possible that the static perfusion fluid in the limited kidney intravascular space is unlikely to provide a significant source for ongoing MitoQ uptake during CSS. In addition, the renal capsule is composed of dense connective tissue, which would not be expected to permit a significant uptake of the MitoQ from the surrounding perfusion fluid, into the underlying renal parenchyma during cold preservation. In support of this interpretation, there was no difference in MitoQ uptake whether the kidneys were bathed in external preservation solution with or without MitoQ, indicating that there is negligible uptake through the surface of the organ.

The uptake of MitoQ by the kidneys using the controlled pig model during the 24 h cold preservation period was higher in the HMP group compared to the CSS group. Most of the MitoQ uptake in the controlled pig model was completed in the first 6 h post perfusion and remained static thereafter, corresponding to the improvement in the HMP flow and reduction in resistance during the same period. It is unclear if the higher uptake of MitoQ in the HMP group compared to the CSS group was solely due to the ability of the HMP to overcome the vascular spasm and open up new capillary networks, which may be occluded during CSS, or replenish the MitoQ content in the capillary network, or a combination of both.

The difference in MitoQ uptake between HMP and CSS is of a great importance for subsequent experiments. The therapeutic MitoQ dose might need to be adjusted according to the mode of preservation (e.g. lower in the HMP group and higher in the CSS group). However, in the controlled pig model HMP increases MitoQ uptake by only 2-fold compared to CSS, which is likely to remain within the therapeutic window. Furthermore, in clinical practice, kidneys are exposed to a variable period of CIT, and the MitoQ tissue concentrations should ideally remain stable and within the therapeutic window during that period. Thus, the stability of MitoQ tissue concentrations over time observed in the controlled pig model is important, as this will allow MitoQ to be administered at an early time point with little or no risk of toxicity even if the kidney is transplanted up to 24 hours later.

The demonstration that MitoQ can be taken up efficiently after a period of cold preservation provides the option for the administration of MitoQ at a later time point, for example during the process of bench-work preparation of the kidney. Most of the MitoQ uptake by the cold kidneys after a period of cold preservation happened rapidly upon perfusion with MitoQ, and there was no difference whether the kidneys were stored with or without MitoQ. However, the uptake of MitoQ by the cold kidneys was less than (approximately half) the uptake of MitoQ by warm kidneys at the start of the cold preservation

using the controlled pig model. Thus, the therapeutic dose of MitoQ might need to be adjusted according to the time point of MitoQ delivery. Of note, administering MitoQ to warm kidneys on the back table after a period of WIT might mimic administering MitoQ in the *in situ* perfusion of warm human kidneys. However, it is not an accurate reflection of the back table perfusion in clinical practice. In DCD donation, the organs are flushed *in situ* with cold preservation solution and organs are cooled down with wet ice, so when removed from the donor, they are likely to be at a temperature in the range 15 – 20 °C (11).

Having successfully confirmed and characterised MitoQ tissue uptake, I decided to optimise a controlled DCD pig model to start investigating the efficacy of MitoQ in ameliorating IRI.

Chapter 4

Optimisation of the controlled DCD pig model

4.1 Introduction

In chapter 3, I confirmed the uptake of MitoQ in pig kidney tissue during 24 h of cold preservation and characterised the difference in MitoQ uptake at different time points using two different methods of preservation (HMP, CSS). I also demonstrated that MitoQ could be taken up by the kidney after a period of cold preservation. The data also highlighted the advantages of using a controlled pig model, confirming it as the most appropriate model for subsequent experiments.

The ideal large animal model to investigate ischaemic reperfusion injury following kidney transplantation is autologous or allogeneic pig kidney transplantation. However, this is an expensive and technically challenging model and is not suitable for the early phases of the study. I therefore used the *Ex Vivo* Normothermic Perfusion (EVNP) circuit, developed and optimised by Professor Michael Nicholson and Dr Sarah Hosgood.

As outlined in chapter 2, the EVNP circuit is a modified paediatric cardiopulmonary bypass unit adapted for the perfusion of pig and human kidneys, that has been established as a valid model for investigating IRI (34, 51, 55). This technique has proven to be of great value in transplantation research. EVNP removes numerous systemic influences and enables controlled investigation and optimisation of candidate therapeutic agents such as MitoQ. In addition, it provides controlled perfusion conditions, where specific and accurate adjustments can be made to perfusion arterial pressure.

Pig and human kidneys are characterised by a multipapillary and multilobular structure, unlike the unipapillary and unilobular kidneys found in rodent and dogs. In addition, pig and human kidneys share similar vasculature in term of interlobular and segmental arteries supplying the multiple kidney lobes (81). However, there is only one renal artery in pig kidneys unlike human kidneys in which ~27 - 30% possess multiple renal arteries (82).

Anatomical differences have been reported between the right and the left pig kidneys in terms of alignment and position; there is no close proximity between the right kidney and the liver, unlike in other species. In addition, preliminary work by Dr Sarah Hosgood and Dr Anna Dare, using an uncontrolled DCD pig model had raised the possibility that the right pig kidney may function better than the left pig kidney following EVNP, as measured by urine output and renal blood flow (personal communications).

The “ideal” ischaemic injury to examine the efficacy of a potential treatment should be moderate to mimic the clinical situation, where the extent of the injury is severe enough to enable the efficacy of MitoQ to be demonstrated, but not so severe as to result in irrecoverable damage.

In this context, in this chapter I aimed to:

1. Investigate whether there are functional differences between the right and the left pig kidney after EVNP, to eliminate potential bias in subsequent experiments
2. Characterise the relative effect of warm ischaemic time (WIT) and cold ischaemic time (CIT) on kidney function by exposing pig kidneys to variable length of warm and cold ischaemia, to identify the ideal ischaemic injury for subsequent experiments

4.2 Assessment of functional differences between the right and the left pig kidney

4.2.1 Controlled pig model - *In situ* perfusion

I used a controlled pig model to investigate potential functional differences between the right and left pig kidney. In previous experiments by Professor Michael Nicholson and Dr Sarah Hosgood, pig kidney function was severely impaired when the kidneys were exposed to 10 min WIT and 18 h CIT (83). I therefore opted to expose the kidneys to 10 min WIT and 10 h CIT to induce a less severe ischaemic injury, which I anticipated would be sufficient to enable assessment of functional differences between the right and the left kidneys. After exsanguination through the IVC and confirmation of death (asystole on a continuous ECG display, and absence of palpable pulse in the abdominal aorta), the kidneys were exposed to 10 mins of WIT followed by perfusion *in situ* with cold preservation solution. The kidneys were then removed and flushed with cold preservation solution and stored at 4 °C.

There are two EVNP circuits in our laboratory. This allowed pairs of kidneys from the same pig to be exposed to the same CIT (10 h) and assessed in parallel to eliminate a number of potential biological confounders. The kidneys were placed on the normothermic perfusion circuit (at 38 °C) for 3 h at a mean arterial pressure of 80 - 90 mm Hg with 250 mL heparinised blood (collected and stored from the same pig during exsanguination) diluted 1 : 1 with Ringer's lactate solution (Baxter Healthcare, Thetford, UK). The perfusate was oxygenated with 95 % O_2 and 5 % CO_2 at 0.5 L/min. To measure creatinine clearance as a marker of renal function, creatinine (Sigma-Aldrich, Steinheim, Germany) was added to the perfusate to achieve an initial circulating concentration of 1000 µmol/L. Urine produced by the kidney was collected in a urinary bag attached to the cannulated ureter. Fluids, glucose and insulin were continually infused into the circuit at a set rate based on published data from a pig model of liver EVNP (60). Urinary losses were replaced mL for mL with Ringer's lactate solution.

In preliminary experiments, I encountered significant technical difficulties with *in situ* perfusion in the controlled pig model. There was a high variation in the time taken for the pig to undergo circulatory arrest following exsanguination through the IVC (range 5 to 15 min). In addition, the quality of the *in situ* perfusion of the pig kidneys was poor, despite perfusing the abdominal organs *in situ* with 2 L of Soltran® and 1 L of UW®. The patchy *in situ* perfusion of the first pair of pig kidneys was improved after perfusing the kidney with 500 mL of Soltran® on the back table. However, the second kidney did not perfuse *in situ*, likely as a consequence of vascular spasm, and the perfusion improved only moderately on subsequent back table perfusion with 500 mL of Soltran®.

The two pairs of pig kidneys assessed in these preliminary experiments showed signs of poor reperfusion once placed on the EVNP circuit, with both pairs of kidneys developing large areas of patchy and dusky discoloration. In addition, the renal blood flow and the urine output during EVNP were poor

for both pairs of *in situ* perfused pig kidneys (data not shown). Nonetheless, there were no differences in the renal blood flow or total urine output between the right and the left kidney for both pairs of kidneys (data not shown).

4.2.2 Controlled pig model – Back table perfusion

In light of the technical difficulties described above, a modified controlled pig model was adopted, consisting of back table (rather than *in situ*) perfusion of the kidneys. As outlined in chapter 2, after laparotomy and systematic heparinisation, dissection was performed to expose the renal pedicles. Renal arteries and veins were ligated with 3-0 Vicryl ties and divided on the kidney side, to induce warm ischaemia (right followed by left). The kidneys were mobilised free but left in the abdominal cavity, and removed after 10 min WIT and subsequently perfused on the back table with 500 mL of Soltran® only, and preserved in 500 mL Soltran® for 10 h using CSS. The kidneys were then placed on the EVNP circuit for 3 h (Figure 4.1). To expedite exsanguination and maximize the volume of blood collected, pigs were exsanguinated through the aorta instead of the IVC. There were no significant differences between the right (n = 5) and the left (n = 5) kidneys in renal blood flow (Figure 4.2), renal function (Figure 4.3) and oxidative damage markers (Figures 4.4). There was a slight trend towards better renal blood flow in the right kidney group at the end of 3 h EVNP compared to the left kidney group, but the difference was not statistically significant (Figure 4.2).

The total urine output was similar between the right and left kidneys at the end of 3 h EVNP (Figure 4.3a). Creatinine clearance showed no difference between right and left kidneys at the end of 3 h EVNP (Figure 4.3b). In addition, there was no significant difference in the percentage of serum creatinine cleared at the end of 3 h EVNP between right and left kidneys (Figure 4.3c). A high percentage of fractional excretion of sodium is an indicator of acute tubular necrosis (ATN). Fractional excretion of sodium has been used as a sensitive marker for kidney damage in a controlled IRI pig model (62). There was no significant difference in fractional excretion of sodium at the end of 3 h EVNP between the right and left pig kidneys (Figure 4.3d).

Protein carbonyl formation is a marker of oxidative injury (64). Total protein carbonyl concentration in pig kidney tissue was determined by enzyme-linked immunosorbent assay (ELISA). Tissue biopsies for protein carbonyl assessment were taken following back table perfusion with 500 mL Soltran®, after 10 h of CSS, and at 15 min and 3 h after EVNP. There was no significant difference in protein carbonyl content of the left and right kidney groups during 3 h of EVNP (Figure 4.4).

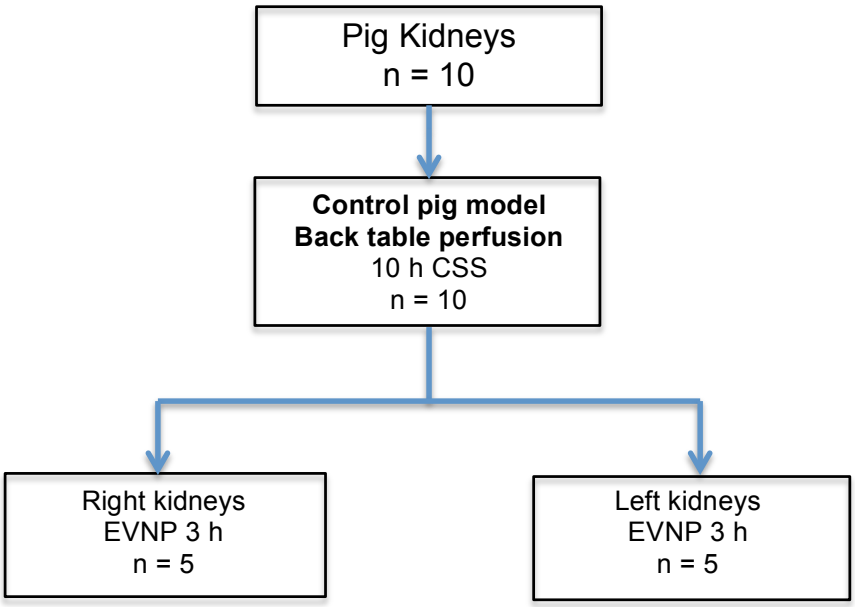

Figure 4.1. Experimental design for assessment of functional differences between right (n = 5) and left (n = 5) pig kidneys during 3 h EVNP. The kidneys were retrieved using a controlled pig model, exposed to 10 min WIT, perfused with Soltran® on the back table and subsequently exposed to 10 h of cold ischaemia using CSS.

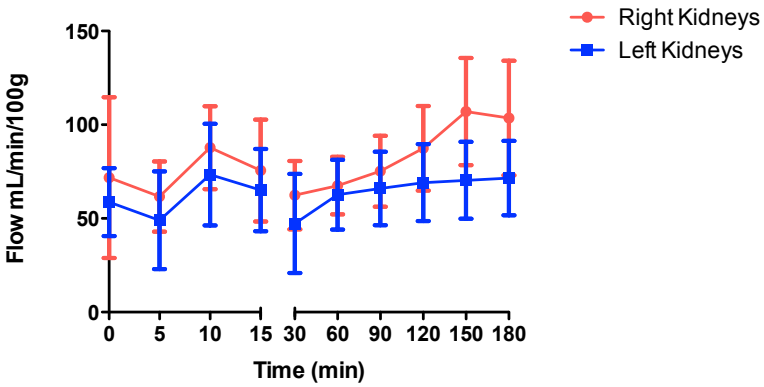

Figure 4.2. Renal blood flow in the right (n = 5) and the left (n = 5) kidneys during 3 h EVNP using a controlled pig model. The kidneys were perfused on the back table with Soltran® only, and exposed to 10 min WIT followed by 10 h CIT. There was no significant difference between right and left kidneys at the end of 3 h EVNP (104 ± 31 vs. 71 ± 20 mL/min/100 g; p = 0.063; paired t-test). Data are mean ± SD.

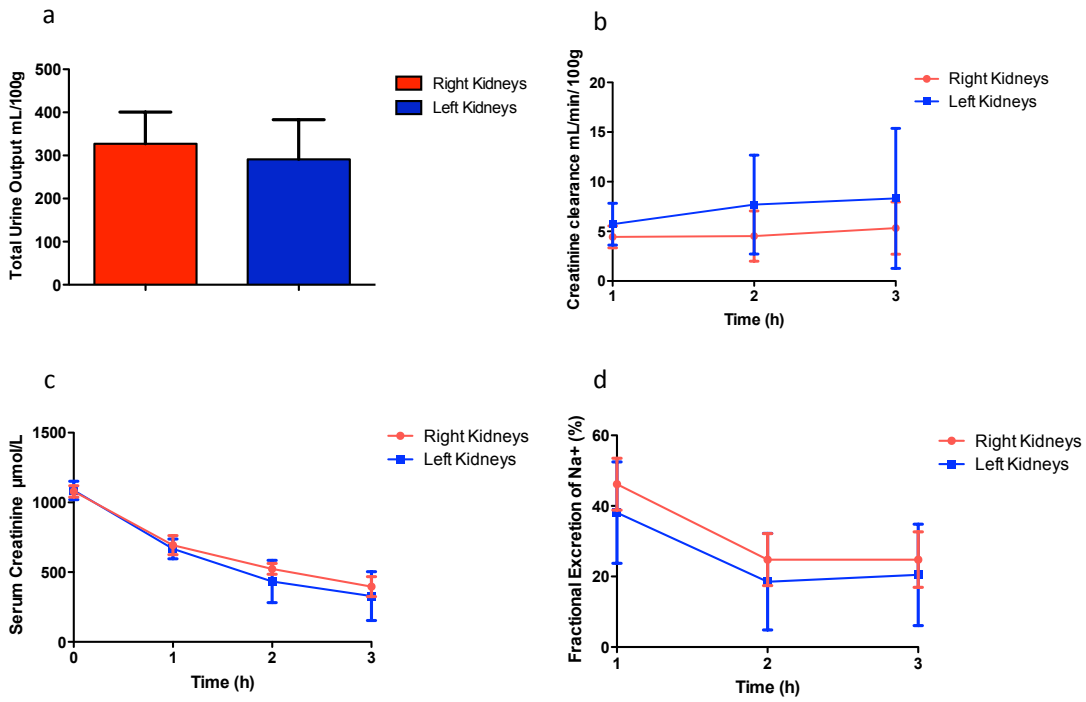

Figure 4.3. Renal function in right (n = 5) and left (n = 5) kidneys during 3 h EVNP. The kidneys were perfused on the back table with Soltran® only, and exposed to 10 min WIT and 10 h CIT. There were no differences between right and left kidneys at the end of 3 h EVNP in (a) total urine output (327 ± 73 vs. 321 ± 84 mL/100g; p = 0.913; paired t-test), (b) creatinine clearance (5.3 ± 2.6 vs. 8.3 ± 7.1 mL/min/100g; p = 0.350; paired t-test), (c) percentage of serum creatinine fall (63.2 ± 6.7 vs. 69.3 ± 17.0; p = 0.428; paired t-test) or (d) fractional excretion of sodium (24.8 ± 7.9 vs. 20.1 ± 14.4 %; p = 0.366; paired t-test). Data are mean ± SD.

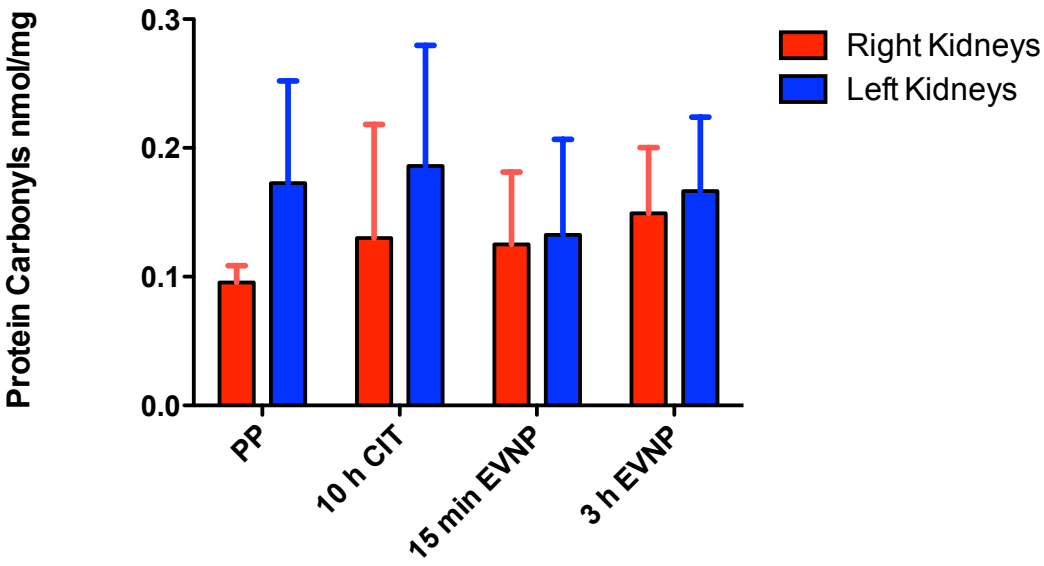

Figure 4.4. Protein carbonyls in right (n = 5) and left (n = 5) pig kidneys. The kidneys were perfused on the back table with Soltran® only, and exposed to 10 min WIT and 10 h CIT. Biopsy samples were taken immediately post-perfusion (PP), 10 h CSS, and at 15 min and 3 h of reperfusion. There was no significant difference in protein carbonyl content in both groups at the end of 3 h EVNP (0.149 ± 0.051 vs. 0.166 ± 0.057 nmol/mg; p = 0.726; paired t-test). Data are mean ± SD.

4.3 The relative effects of WIT and CIT

To determine the optimal level of IRI for subsequent experiments, I compared the function of kidneys exposed to mild, moderate and severe IRI. The minimal WIT required after removal of the kidney to cannulate the renal artery and flush with cold preservation solution was ~ 3.3 min (3.3 ± 1.2 min, n = 6). The minimal cold ischemia time (CIT) to transfer the organ to the laboratory for EVNP was ~ 3 h 10 min (190 ± 39.9 min, n = 6). This was taken as the mildly damaged state and was compared with prolonged warm and cold ischaemia conditions mimicking DCD kidney transplantation. The moderate and severe IR injury groups were chosen so that the duration of WIT and CIT spanned clinically applicable times. The comparison groups were:

- Mild IRI: ~3 min WIT + ~3 h CIT
- Moderate IRI: 10 min WIT + 10 h CIT
- Severe IRI: 10 min WIT + 18 h CIT

Kidneys were thus exposed to different WIT and CIT, and their function was compared after 3 h of EVNP. This investigation showed that the increased WIT and CIT in the moderate and the severe IRI groups significantly increased the level of kidney injury as measured by fractional excretion of sodium compared to the mild IRI group (Figure 4.5). In addition, the moderate and the severe IRI groups demonstrated significant decrease in kidney function as measured by creatinine clearance compared to the mild IRI group (Figure 4.6). However, urine production (Figure 4.7), the renal blood flow (Figure 4.8) and protein carbonyl formation (Figure 4.9) were similar in all three groups during 3 h of EVNP. Therefore I chose to use the moderate IRI model (10 min WIT and 10 h CIT) in all subsequent experiments.

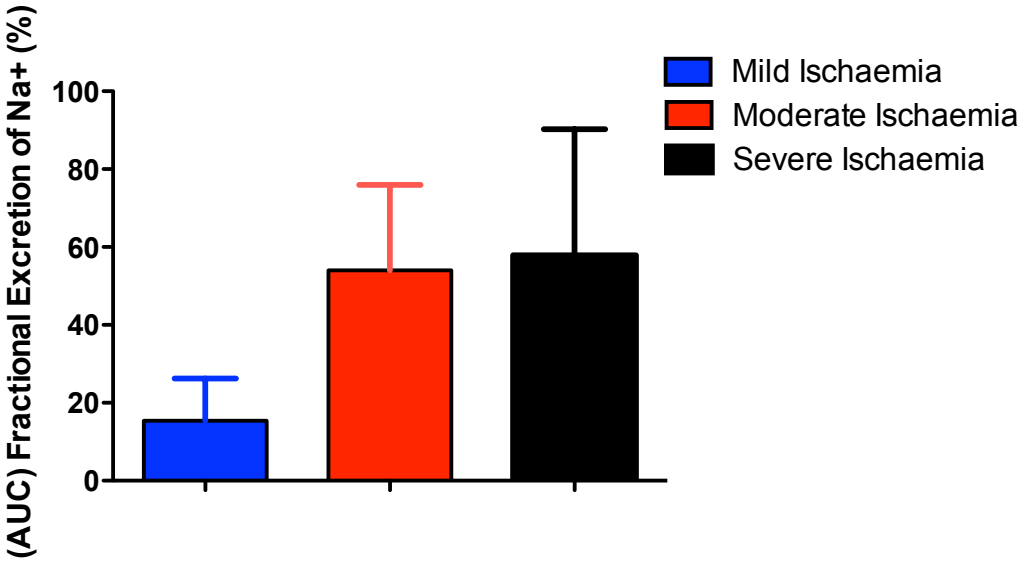

Figure 4.5. Effect of severity of IRI on fractional excretion of Na. Fractional excretion of Na was significantly less in the mild ischaemia group (n = 6) compared to the moderate (n = 6) and the severe ischaemia groups (n = 4) during 3 h of EVNP (15.4 ± 10.9 vs. 54.1 ± 1.9 vs. 57.9 ± 3.3 % area under the curve (AUC); p = 0.006; one-way ANOVA). However, Bonferroni post-hoc testing demonstrated no significant difference in the moderate ischaemia vs. severe ischaemia groups. Data are mean ± SD.

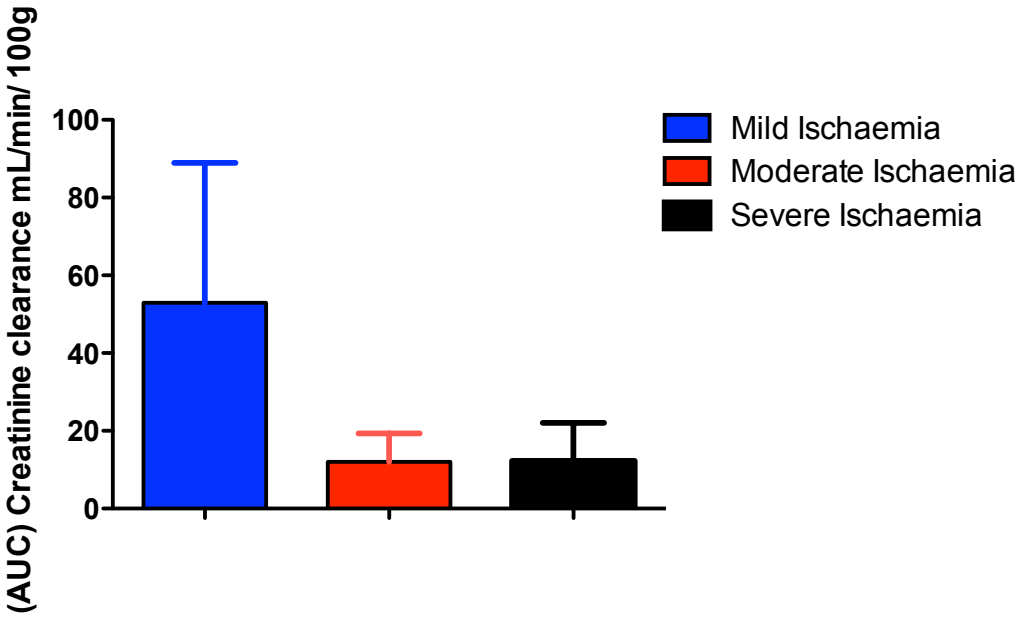

Figure 4.6. Effect of severity of IRI on creatinine clearance. Creatinine clearance was significantly higher in the minimal ischaemia group (n = 6) compared to the moderate (n = 6) and the severe ischaemia groups (n = 4) during 3 h of EVNP (52.9 ± 36.1 vs. 12.1 ± 7.3 vs. 12.3 ± 9.8 mL/min/100g area under the curve (AUC); p = 0.003; one-way ANOVA). Bonferroni post-hoc testing demonstrated no significant difference in the moderate ischaemia vs. the severe ischaemia groups. Data are mean ± SD.

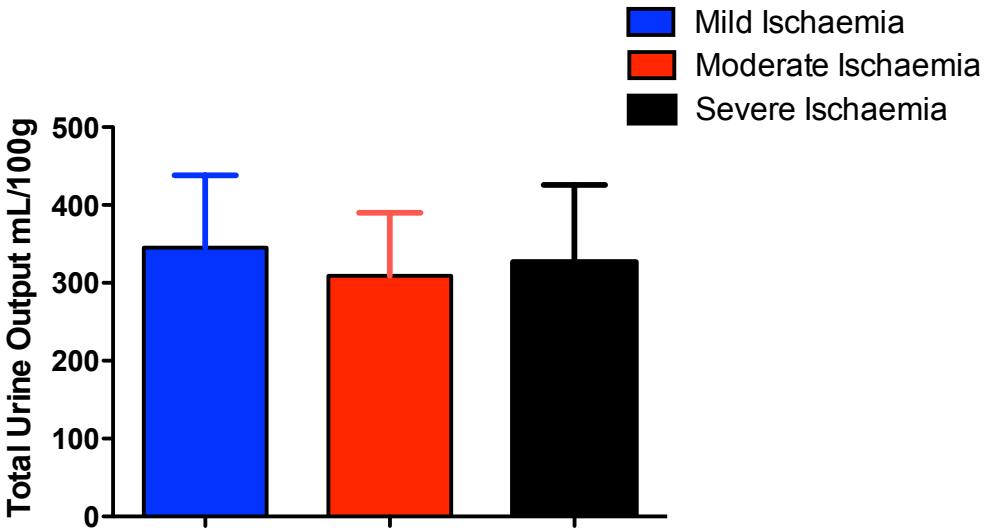

Figure 4.7. Effect of WIT and CIT on total urine output. There was no significant difference in the total urine output between the minimal (n = 6), moderate (n = 6) and severe (n = 4) ischaemia groups during 3 h of EVNP (345 ± 93 vs. 309 ± 81 vs. 327 ± 99 mL/100g; p = 0.732; one-way ANOVA). Data are mean ± SD.

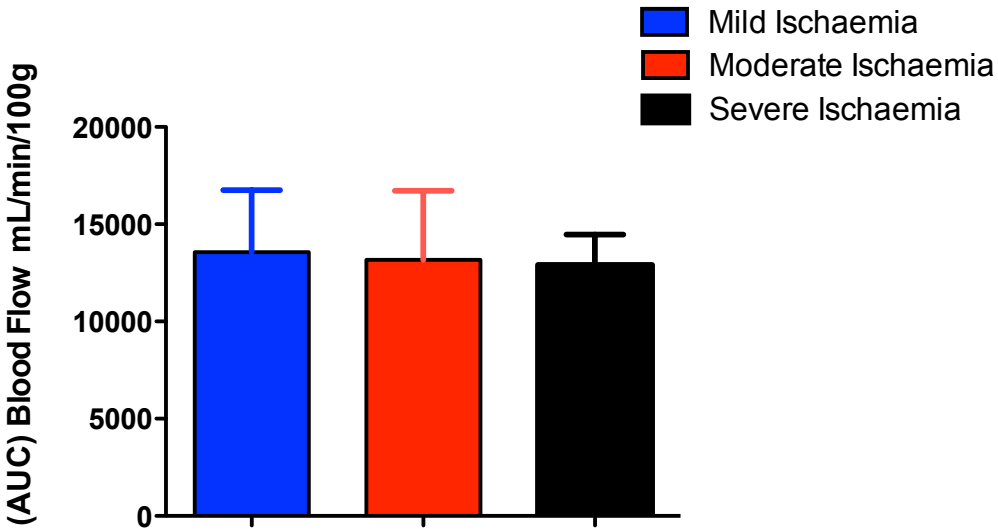

Figure 4.8. Effect of WIT and CIT on renal blood flow. There was no significant difference in the renal blood flow between the minimal (n = 6), moderate (n = 6) and severe (n = 4) ischaemia groups during 3 h of EVNP (AUC mL/min/100g; p = 0.947; one-way ANOVA). Data are mean ± SD.

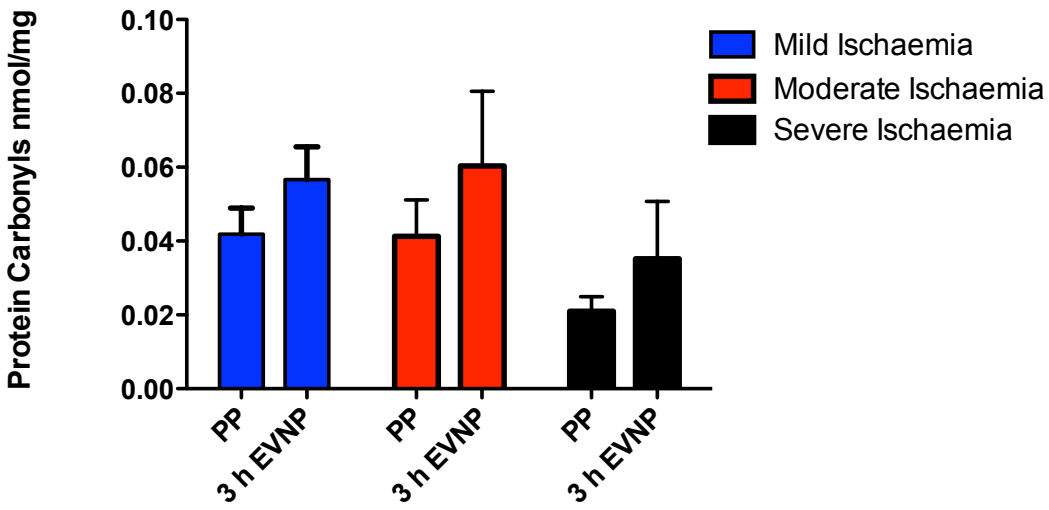

Figure 4.9. Effect of WIT and CIT on protein carbonyl formation. Biopsy samples were taken post perfusion on the back table (PP) and at the end of 3 h of EVNP. There was no significant difference in the oxidative damage to proteins, measured by protein carbonyl formation at the end of 3 h EVNP between the minimal (n = 6), ischaemia (n = 6) and the severe (n = 4) ischaemia groups (0.057 ± 0.009 vs. 0.063 ± 0.020 vs. 0.035 ± 0.012 nmol/mg; p = 0.061; one-way ANOVA). Bonferroni post-hoc testing demonstrated no significant difference in the moderate ischaemia vs. the severe ischaemia groups. Data are mean ± SD.

4.4 Discussion

In this chapter I was able to:

1. Demonstrate that there were no functional or cellular differences between the right and the left pig kidneys
2. Optimise the controlled pig model for subsequent experiments
3. Demonstrate that 10 min of WIT and 10 h of CIT produced moderate IRI, which is appropriate for investigation of efficacy of MitoQ in ameliorating IRI in subsequent experiments

I demonstrated that there were no significant functional differences between the right and the left pig kidneys using a controlled DCD pig model of renal IRI. This eliminates a potential source of bias, which could otherwise compromise the analysis of variables and outcomes in subsequent experiments. I was also able to successfully overcome the complexity and challenges involved in optimising the controlled DCD pig model for subsequent experiments. However, it should be noted that there are a number of differences between my chosen pig model and the standard DCD protocol used in clinical practice. Due to the significant technical problems associated with the *in situ* perfusion in the controlled pig model, I opted to perfuse the kidneys on the back table instead. This allowed for a reproducible and better controlled WIT. Previous experiments have shown pigs to be hyper-coagulable (Dr. Sarah Hosgood; personal communication) and heparin (500 IU/kg) was thus administered i.v. before the onset of warm ischaemia to prevent formation of microthrombi in the renal vasculature. Pre-mortem heparinisation is not part of the DCD protocol in the UK, due to concerns that it may be detrimental to the donor. Of note, pre-mortem administration of heparin is part of the DCD protocol in some part of the United States, (84). The primary purpose of using heparin in DCD donors is to reduce the risk of blood clotting in the donor organs.

Characterisation of the relative effect of WIT and CIT was an important step in the design of my controlled DCD pig model. The data indicate that 10 min of WIT and 10 h of CIT in the moderate IRI group produced a significant functional injury to the kidney, compared to the mild IRI group. However, extending CIT from 10 h to 18 h in the severe IRI group did not lead to significant additional functional or cellular injury. I therefore opted to examine the effect of MitoQ on pig kidneys using 10 min of WIT and 10 h of CIT in subsequent experiments, confident that this represents significant, but not overwhelming, organ damage. Although this controlled DCD pig model does not precisely replicate clinical DCD kidney transplantation, it is an appropriate approximation of the DCD protocol in clinical practice. Importantly, it is a consistent and reproducible model which is ideally suited for examining the efficacy of MitoQ in subsequent experiments.

Having successfully optimised the experimental model, I investigated the efficacy of MitoQ in ameliorating renal IRI using the controlled DCD pig model as described in chapter 5.

Chapter 5

Evaluation of efficacy of MitoQ in ameliorating renal IRI using a controlled DCD pig model

5.1 Introduction

In many previously published uncontrolled pig models of renal IRI the non-anaesthetised animal is sacrificed by an approved method before the organ is removed. However, this approach results in significant variability in the level of injury endured by the kidneys and makes it difficult to predictably model clinical transplantation (85). Having successfully optimised the pig kidney IRI model in chapter 4, the focus of this chapter is to investigate whether functional kidney injury and mitochondrial oxidative damage can be ameliorated by the administration of MitoQ in an experimental DCD model of pig renal IRI.

During a typical kidney transplantation from a DCD donor there is a period of ~ 10 min warm ischaemia during organ retrieval (86), followed by flushing of the organ with cold preservation solution and several hours of storage at ~ 4 ˚C. The kidney is then re-perfused in the recipient, leading to IRI. To model DCD transplantation as closely as possible in pigs, and to minimize the variation between experiments, pairs of kidneys removed from each pig under general anaesthesia were assessed in parallel. As outlined in chapter 4, 10 min of WIT and 10 h of CIT produced sufficient injury to enable the efficacy of MitoQ to be investigated. Both kidneys from each pig were thus exposed to 10 min WIT at body temperature. One 'control' kidney from each pair was then flushed with and stored in cold storage solution (Soltran®) only, while the other kidney from the pair was flushed with and stored in Soltran® + MitoQ at ~ 4 ˚C for 10 h. The kidneys were then placed simultaneously on two *ex vivo* normothermic perfusion (EVNP) circuits and perfused with oxygenated autologous pig blood. EVNP allowed assessment of the safety and efficacy of MitoQ in ameliorating renal IRI by quantifying kidney function such as urine production and creatinine clearance. All pig kidneys were exposed to the same WIT and CIT, thereby minimising biological variation and bias (Figure 5.1). As outlined in chapter 4, there were no significant functional differences between the right and the left pig kidneys. However, there was a slight trend towards better renal blood flow in the right kidney group at the end of 3 h EVNP compared to the left kidney group, but the difference was not statistically significant. In this context I decided to alternate introducing MitoQ treatment between the right and the left pig kidneys in subsequent experiments.

As outlined in chapter 3, I have investigated MitoQ uptake by the kidney over a range of doses from 5 nM to 500 nM MitoQ using the controlled DCD pig model. In this chapter, I decided to start with investigating a higher range of MitoQ concentrations (5 µM - 100 µM) to fully characterise MitoQ uptake by the kidneys during CSS. In addition, MitoQ tissue concentrations during EVNP have not been previously investigated. Understanding the trend of MitoQ concentrations during EVNP may help determine the appropriate dose of MitoQ and the duration of EVNP for subsequent experiments.

Administration of MitoQ prior to the onset of ischaemia has been shown to be protective in ameliorating renal IRI in a small animal model (40). The overall aim of these experiments was to see if

the promising MitoQ small animal data could be extended to a large animal model of DCD renal IRI. This would provide a clear path for clinical translation of the findings by informing the design and conduct of pre-clinical studies using declined human kidneys. The long-term intention is that these data would ultimately support the design of human clinical trials to test the efficacy of MitoQ.

In this context, this chapter will aim to:

1. Further characterise MitoQ uptake and tissue concentrations during CSS and EVNP
2. Evaluate the role of MitoQ in ameliorating renal IRI using the controlled DCD pig model
3. Investigate the therapeutic window for MitoQ using a series of dose-response experiments

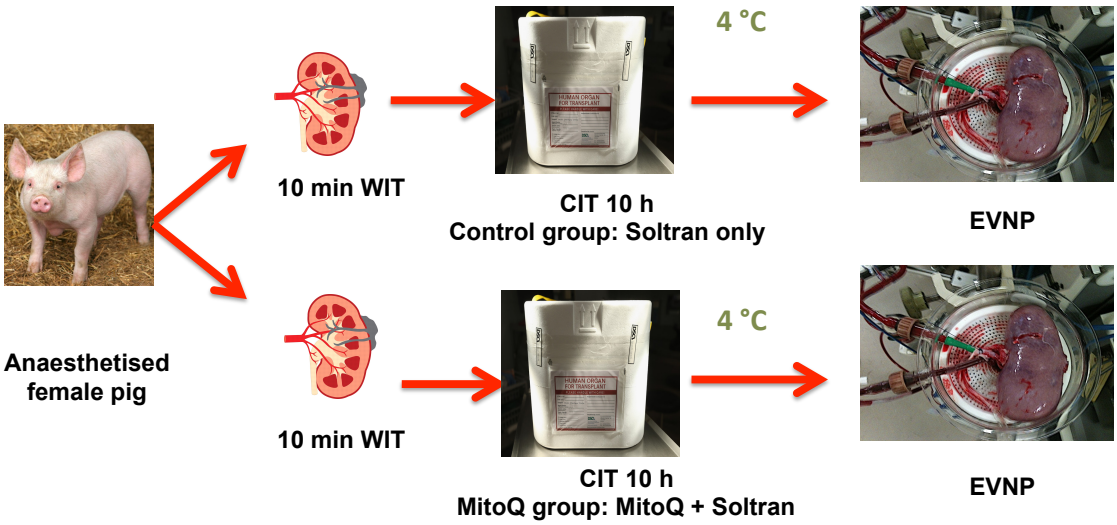

Figure 5.1. Flushing and cold static storage of pairs of pig kidneys with or without MitoQ and subsequent analysis of kidney function by EVNP. Each pair of kidneys is removed from the pig under general anaesthesia, exposed to 10 min of WIT at body temperature, then flushed and stored with cold storage solution (Soltran®) with or without MitoQ at ~ 4 ˚C for 10 h. The kidney is then placed on an EVNP circuit and perfused with normothermic oxygenated autologous blood allowing kidney function to be assessed by measuring urine production, blood flow and creatinine excretion. In addition, cellular injury was assessed by analysis of serial biopsies for a panel of mitochondrial markers of damage.

5.2 MitoQ doses

To assess the uptake and retention of MitoQ within pig kidneys, I flushed the kidneys over 15 - 20 min with 500 mL Soltran® cold preservation solution supplemented with various concentrations of MitoQ (5 µM - 100 µM), with the flushed MitoQ containing Soltran® going to waste. The kidney was then placed in 500 mL of fresh cold Soltran® containing the same concentration of MitoQ and preserved at 4 °C for 10 h. I measured the amount of MitoQ in the kidney by taking biopsies (~ 120 mg wet weight) during CSS and assessed the amount of MitoQ by Liquid Chromatography Mass Spectrometry and Liquid Chromatography – Tandem Mass Spectrometry (LC-MS/MS). To assess the retention of MitoQ in the kidney following reperfusion on the EVNP rig, I also measured the concentration in the kidney tissue biopsies following 30 min, 3 h and 6 h of reperfusion on the EVNP circuit. There was a statistical significant dose-dependent rise in the post perfusion MitoQ tissue concentration in the 5 µM (n = 4), 50 µM (n = 4) and 100 µM (n = 5) MitoQ groups. The majority of MitoQ uptake took place immediately after flushing. Compared to immediate post-perfusion levels, MitoQ tissue concentrations were numerically higher at 6 h of CSS preservation in the 5 µM, 50 µM and 100 µM MitoQ groups, but the differences were not statistically significant. MitoQ tissue concentrations were then stable and did not significantly change during preservation for 10 h in CSS. MitoQ tissue concentrations remained stable during 6 h of EVNP in the 5 µM, 50 µM and 100 µM MitoQ groups (Figure 5.2).

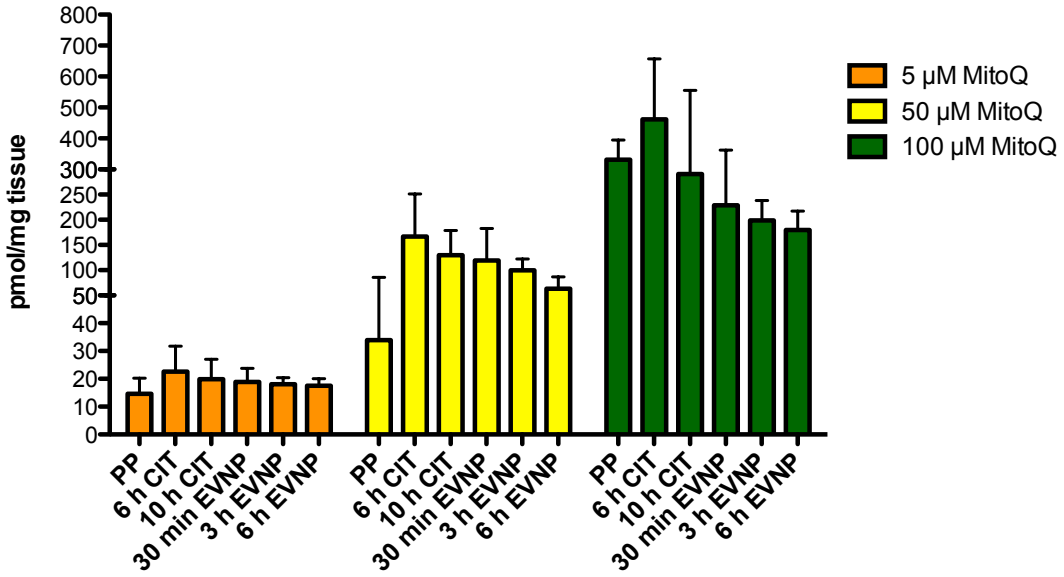

	PP pmol/mg	6 h CIT pmol/mg	10 h CIT pmol/mg	6 h EVNP pmol/mg
5 µM MitoQ (n = 4)	14.6 ± 5.6	22.6 ± 9.2	19.9 ± 7.2	17.5 ± 6.8
50 µM MitoQ (n = 4)	89.9 ± 44.2	166.8 ± 84.4	129.5 ± 49.1	63.1 ± 23.5
100 µM MitoQ (n = 5)	331.5 ± 63.3	461.3 ± 195.5	290.6 ± 264.9	179.8 ± 37.5

Figure 5.2. MitoQ tissue levels in pig kidneys upon cold static storage and during 6 h of EVNP. Pig kidneys were removed after 10 min WIT and then flushed with 500 mL cold Soltran® supplemented with various concentrations of MitoQ as indicated, and then stored in 500 mL cold Soltran® containing the same concentration of MitoQ in CSS. Wedge biopsies of the kidney (~ 120 mg wet weight) were obtained at the indicated times. There was a dose dependent significant difference in post perfusion MitoQ tissue level in the 5 µM (n = 4), 50 µM (n = 4) and 100 µM (n = 5) MitoQ groups ($p = 0.021$; one-way ANOVA). MitoQ tissue concentrations were numerically higher at the end of 6 h of CSS compared to immediate post-perfusion (PP) levels. However, the difference did not reach statistical significance ($p > 0.060$ in all comparisons; paired t-test). Thereafter, MitoQ tissue concentrations were stable and did not significantly change upon preservation for up to 10 h CSS ($p > 0.200$ in all comparisons; paired t-test). Of note, there were no significant changes in MitoQ tissue concentrations at the end of 6 h EVNP compared to the MitoQ tissue concentrations at the end of 10 h CSS ($p > 0.074$ in all comparisons; paired t-test). Data are mean ± SD.

5.3 Effect of 500 nM MitoQ on kidney function and IRI during 3 h of EVNP

I used MitoQ at a concentration of 500 nM to start investigating whether functional kidney injury and mitochondrial oxidative damage could be ameliorated by the administration of MitoQ. This concentration was chosen based on MitoQ uptake data presented in chapter 3. MitoQ concentrations in kidney tissue after perfusion with 500 nM MitoQ (8.7 ± 2.4 pmol/mg) were at the level expected to ameliorate renal IRI, whereas lower tissue concentrations were observed after administration of 50 nM MitoQ and 5 nM MitoQ; (0.5 ± 0.1 and 0.04 ± 0.01 pmol/mg respectively). Pig kidneys retrieved using the controlled model (n = 8) were exposed to 10 min WIT and subsequently perfused on the back table with 500 mL Soltran® ± 500 nM MitoQ. Thereafter, the kidneys were preserved using CSS in 500 mL of Soltran® ± 500 nM MitoQ for 10 h and then placed on the EVNP circuit for 3 h. There were no significant differences between the 500 nM MitoQ group (n = 4) and the control group (n = 4) in renal blood flow (Figure 5.3), renal function (Figure 5.4) and formation of the oxidative damage marker protein carbonyl (Figure 5.5) throughout 3 h of EVNP.

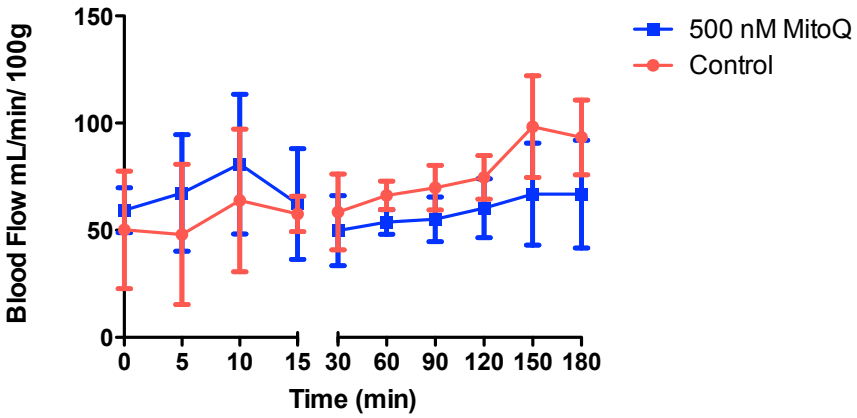

Figure 5.3. Renal blood flow during 3 h of EVNP. The kidneys were flushed and stored with or without 500 nM MitoQ (n = 4 per group) for 10 h using CSS. There was no significant difference between the MitoQ group and the control group at the end of 3 h EVNP (66.9 ± 25.1 vs. 93.3 ± 17.5 mL/min/100 g; p = 0.135; paired t-test). Data are mean ± SD.

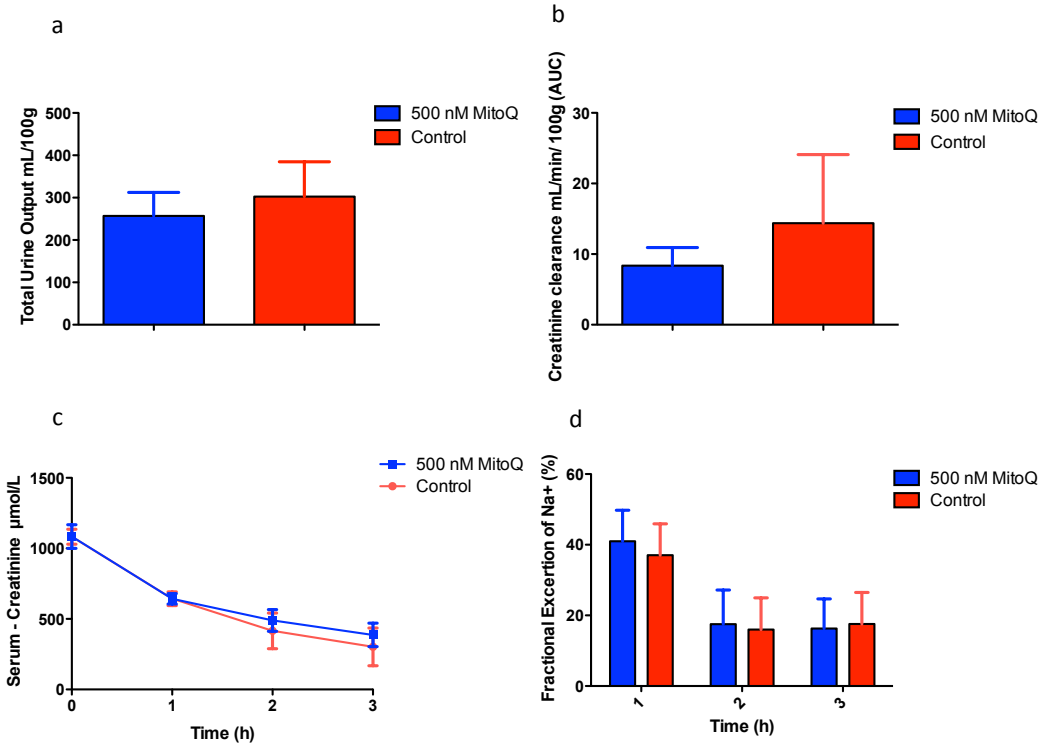

Figure 5.4. Renal function during 3 h of EVNP. The kidneys were flushed and stored with or without 500 nM MitoQ (n = 4 per group) for 10 h using CSS. There were no significant differences between the two groups at the end of 3h EVNP in (a) Total urine output (257 ± 56 vs. 302 ± 82 mL/100 g; p = 0.389; paired t-test), (b) Creatinine clearance (8.4 ± 2.6 vs. 14.4 ± 9.7 mL/min/100 gram area under the curve (AUC); p = 0.328; paired t-test), (c) Percentage of serum creatinine fall (63.9 ± 9.3 vs. 71.7 ± 13.2; p = 0.401; paired t-test) or (d) Fractional excretion of sodium (16.3 ± 8.4 vs. 17.6 ± 8.9 %; p = 0.842; paired t-test). Data are mean ± SD.

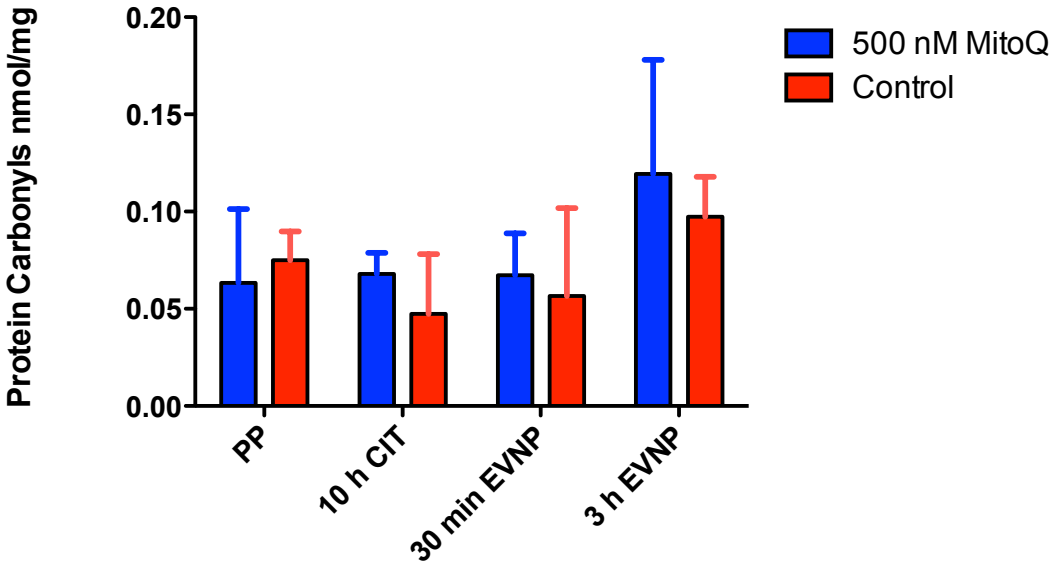

Figure 5.5. Protein carbonyl formation during 3 h of EVNP. The kidneys were flushed and stored with or without 500 nM MitoQ (n = 4 per group) for 10 h using CSS. Biopsy samples were taken immediately post-perfusion on the back table (PP), at 10 h CSS, and at 30 min and 3 h after the start of EVNP. There was no significant difference in protein carbonyl content in both groups at the end of 3 h EVNP (0.119 ± 0.059 vs. 0.097 ± 0.021 nmol/mg; p = 0.527; paired t-test). Data are mean ± SD.

5.4 Effect of 500 nM MitoQ on kidney function and IRI during 6 h of EVNP

Administration of 500 nM MitoQ to the flush solution and to the preservation solution during 10 h CIT did not significantly alter the functional markers of renal IRI at the end of 3 h EVNP. In addition, there was no significant difference at the cellular level (protein carbonyl formation) between the control group and the 500 nM MitoQ group. The ability to detect therapeutic efficacy of 500 nM MitoQ may be limited by the short duration of the reperfusion period on the EVNP circuit (3 h). I therefore decided to extend the duration of EVNP to 6 h in subsequent experiments. Pig kidneys retrieved using the controlled model were exposed to 10 min WIT and subsequently perfused on the back table with 500 mL Soltran® ± 500 nM MitoQ. Thereafter, the kidneys were preserved using CSS in 500 mL of Soltran® ± 500 nM MitoQ for 10 h. The kidneys were then placed on the EVNP for 6 h rather than 3 h. There were no significant differences between the 500 nM MitoQ group (n = 4) and the control group (n = 4) in renal blood flow (Figure 5.6), renal function (Figure 5.7) and the oxidative damage marker (protein carbonyl) throughout 6 h EVNP (Figure 5.8).

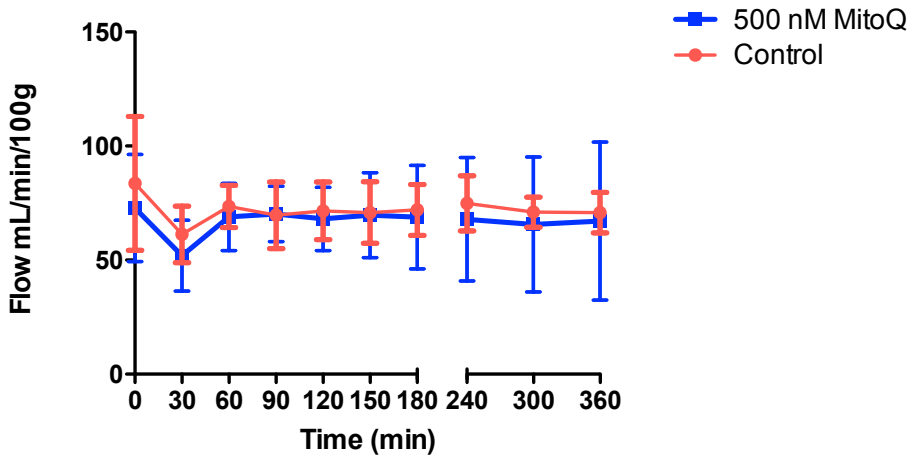

Figure 5.6. Renal blood flow during 6 h of EVNP. The kidneys were flushed and stored with or without 500 nM MitoQ (n = 4 per group) for 10 h using CSS. There was no significant difference between the MitoQ group and the control group at the end of 6 h EVNP (67.2 ± 34.6 vs. 70.8 ± 8.9 mL/min/100 g; p = 0.823; paired t-test). Data are mean ± SD.

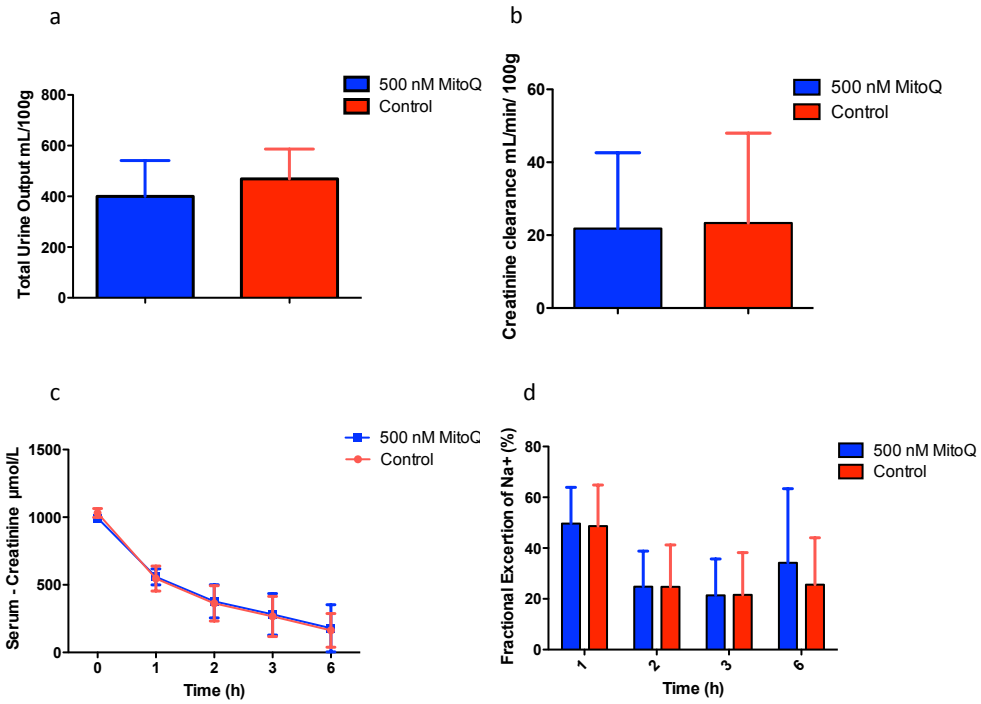

Figure 5.7. Renal function during 6 h of EVNP. The kidneys were flushed and stored with or without 500 nM MitoQ (n = 4 per group) for 10 h using CSS. There were no significant differences between the two groups (MitoQ vs. control) at the end of 6 h EVNP in (a) Total urine output (400 ± 141 vs. 469 ± 117 mL/100 g; p = 0.269; paired t-test), (b) Creatinine clearance (21.8 ± 20.8 vs. 23.4 ± 24.6 mL/min/100 gram area under the curve (AUC); p = 0.637; paired t-test), (c) Percentage of serum creatinine fall (82.0 ± 17.5 vs. 83.9 ± 12.6; p = 0.805; paired t-test) or (d) Fractional excretion of sodium (34.2 ± 29.2 vs. 25.6 ± 18.4 %; p = 0.827; paired t-test). Data are mean ± SD.

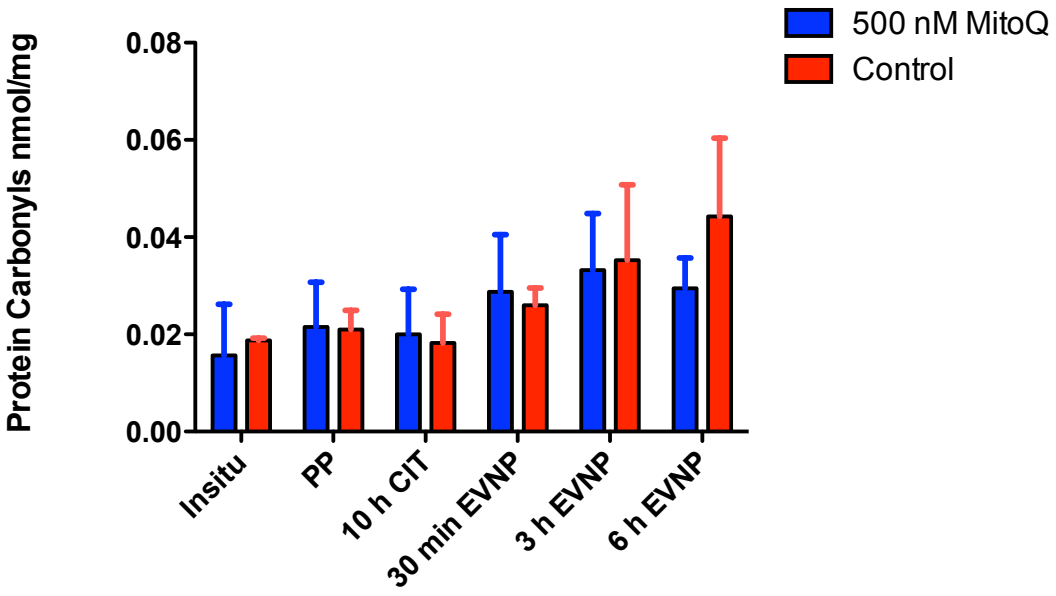

Figure 5.8. Protein carbonyl formation during 6 h of EVNP. The kidneys were flushed and stored with or without 500 nM MitoQ (n = 4 per group) for 10 h using CSS. Biopsy samples were taken immediately post-perfusion on the back table (PP), at 10 h CSS, and at 30 min, 3 h and 6 h after the start of EVNP. There was no significant difference in protein carbonyl content in both groups at the end of 6 h EVNP (0.030 ± 0.006 vs. 0.044 ± 0.016 nmol/mg; p = 0.127; paired t-test). Data are mean ± SD.

5.5 Effect of 5 µM MitoQ on kidney function and IRI during 6 h of EVNP

I next investigated the efficacy of 5 µM MitoQ in ameliorating renal IRI. Cold Soltran® (500 mL) was infused into the kidney containing 5 µM (n = 4) and kidney function and injury was compared with the contralateral kidney from the same pig that had been infused with cold Soltran® only (control group; n = 4). A pair of pig kidneys was then placed on the EVNP circuit for 6 h. 5 µM MitoQ had no effect on renal blood flow (Figure 5.9), renal function (Figure 5.10) or renal injury as measured by protein carbonyl formation during 6 h EVNP (Figure 5.11).

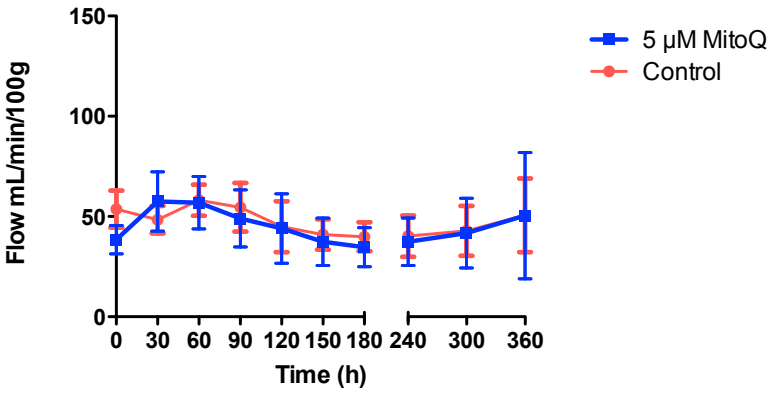

Figure 5.9. Renal blood flow during 6 h of EVNP. The kidneys were flushed and stored with or without 5 µM MitoQ (n = 4 per group) for 10 h using CSS. There was no significant difference between the MitoQ group and the control group at the end of 6 h EVNP. (50.5 ± 31.5 vs. 50.6 ± 18.3 mL/min/100g; p = 0.986; paired t-test). Data are mean ± SD.

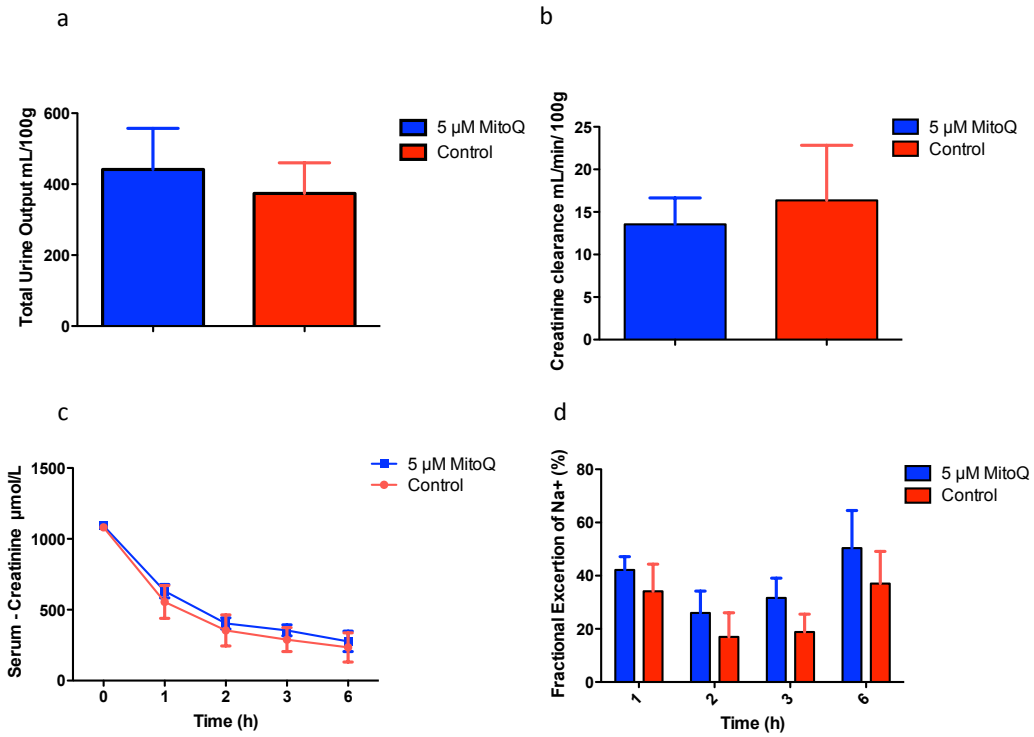

Figure 5.10. Renal function during 6 h of EVNP. The kidneys were flushed and stored with or without 5 µM MitoQ (n = 4 per group) for 10 h using CSS. There were no significant differences between the two groups (MitoQ vs. control) at the end of 6 h EVNP in (a) Total urine output (441 ± 116 vs. 374 ± 86 mL/100g; p = 0.109; paired t-test), (b) Creatinine clearance (13.5 ± 3.1 vs. 16.4 ± 6.5 mL/min/100 gram area under the curve (AUC); p = 0.319; paired t-test) (c) Percentage of serum creatinine fall (74.7 ± 6.3 vs. 78.2 ± 9.8 %; p = 0.241; paired t-test) or (d) Fractional excretion of sodium (50.4 ± 14.1 vs. 37.0 ± 12.1 %; p = 0.201; t-test). Data are mean ± SD.

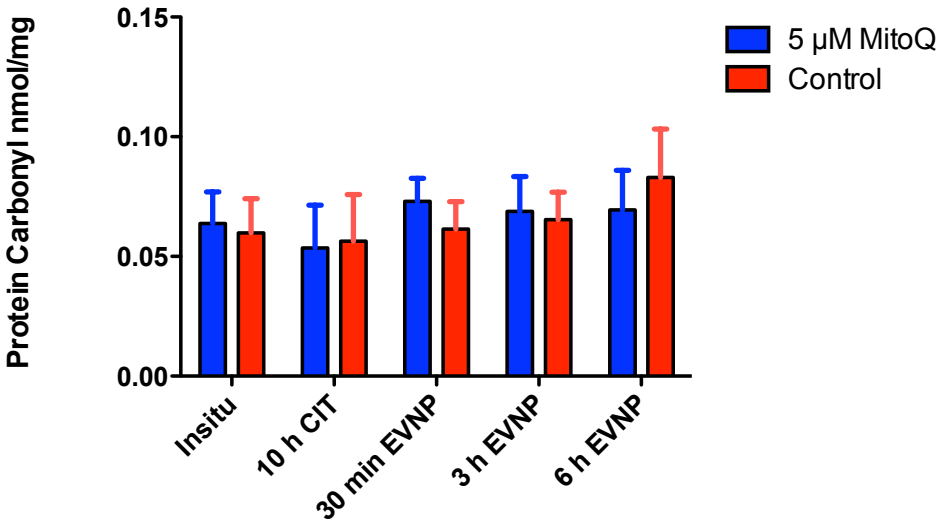

Figure 5.11. Protein carbonyl formation during 6 h of EVNP. The kidneys were flushed and stored with or without 5 µM MitoQ (n = 4 per group) for 10 h using CSS. The kidneys were flushed and stored with or without 5 µM MitoQ for 10 h using CSS. Biopsy samples were taken at the indicated times. There was no significant difference in protein carbonyl content in both groups at the end of 6 h EVNP (0.069 ± 0.017 vs. 0.083 ± 0.020 nmol/mg; p = 0.400; paired t-test). Data are mean ± SD.

5.6 Effect of 50 µM and 100 µM MitoQ on kidney function and IRI on EVNP

To assess the effect of 50 and 100 µM of MitoQ following 10 min WIT, pairs of pig kidneys were flushed with Soltran® ± 50 or 100 µM MitoQ and then subjected to 10 h CIT and the effect of MitoQ on kidney function and series of damage markers were assessed over 6 h EVNP. All kidneys appeared well perfused in the 50 µM and the 100 µM MitoQ groups during 6 h of EVNP (Figure 5.12). Renal blood flow was significantly increased in kidneys treated with 50 µM and 100 µM MitoQ at the end of 6 h EVNP compared to control kidneys (Figure 5.13). Total urine output increased significantly in the 50 µM MitoQ group compared to the control group. However, the difference between the 100 µM MitoQ group compared to the control group during 6 h EVNP did not reach statistical significance (Figure 5.14). Creatinine clearance was numerically higher in the 50 µM and 100 µM MitoQ groups but the difference did not reach statistical significance (Figure 5.15). There was no effect on fractional excretion of sodium in any of the groups (Figure 5.16). There were no significant effects of 50 µM and 100 µM MitoQ on total protein carbonyl formation (Figure 5.17) or on lipid peroxidation (isoprostanes; Figure 5.18).

a

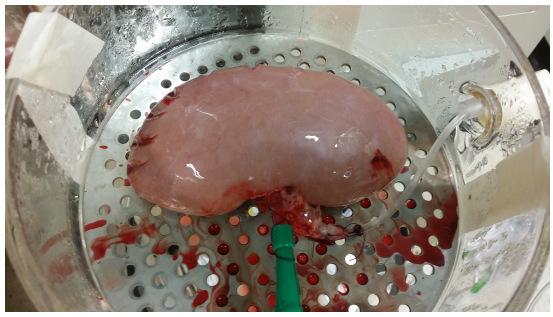

b

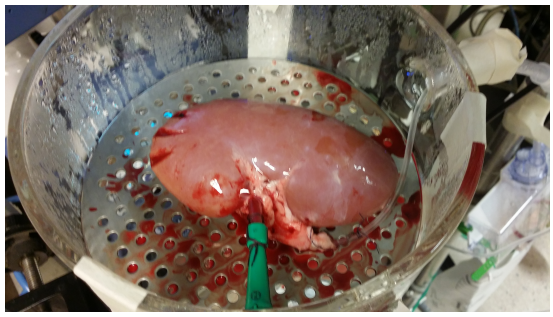

c

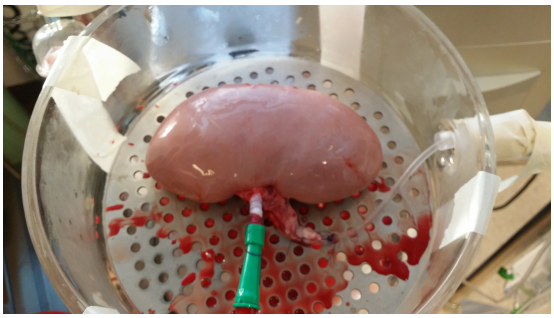

d

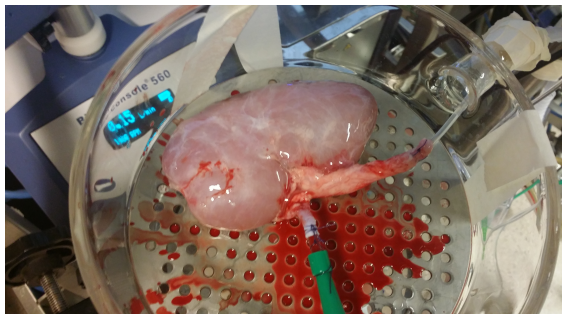

Figure 5.12. The quality of EVNP perfusion in the 50 and the 100 µM of MitoQ groups. All kidneys appeared well perfused during 6 h of EVNP in the group treated (a) with 50 µM of MitoQ, (b) without 50 µM of MitoQ (control), (c) with 100 µM of MitoQ and (d) without 100 µM of MitoQ (control). Images are representative examples and were repeated four times with similar appearance.

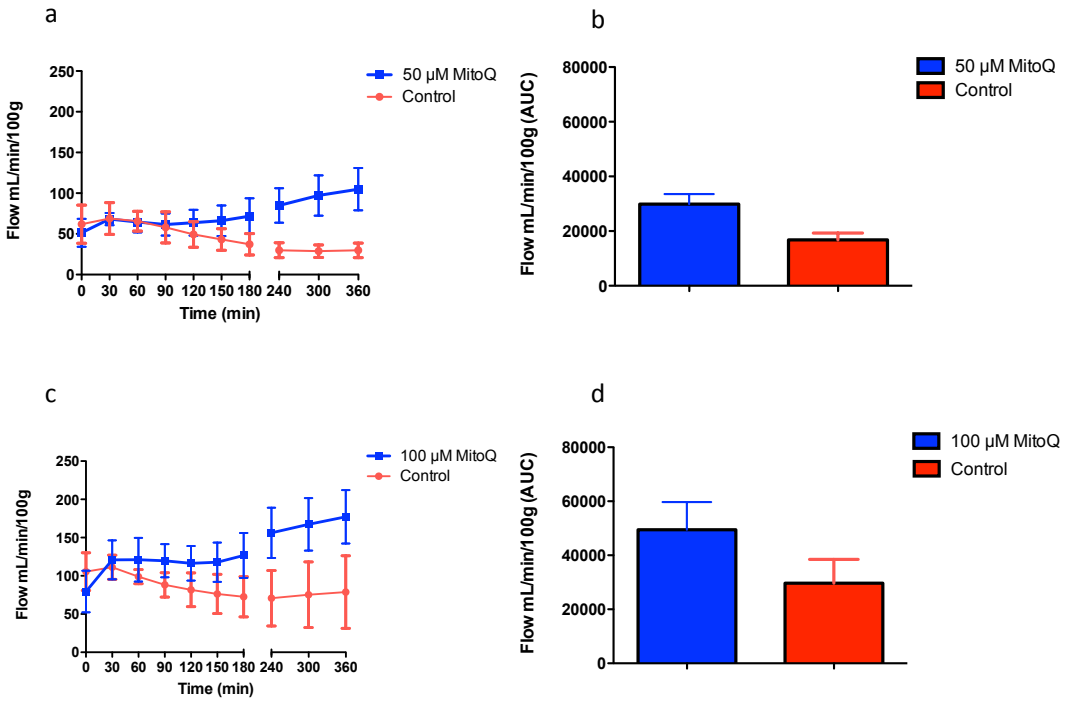

Figure 5.13. Effects of 50 µM and 100 µM MitoQ on renal blood flow during 6 h of EVNP. The kidneys were flushed and stored with or without MitoQ for 10 h using CSS. (a) The renal blood flow was significantly higher in the 50 µM MitoQ group (n = 4) compared to the control group (n = 4) at the end of 6 h EVNP (115 ± 15 vs. 33 ± 7 mL/min/100 g; p = 0.001; paired t-test) and (b) during 6 h of EVNP (AUC p = 0.006; paired t-test). (c) The 100 µM MitoQ group (n = 5) showed a similar trend when compared to the control group (n = 5) at the end of 6 h EVNP (177 ± 35 vs. 79 ± 48 mL/min/100 g; p = 0.032**;** paired t-test) and (d) during 6 h of EVNP (AUC p = 0.049; paired t-test). Data are mean ± SD.

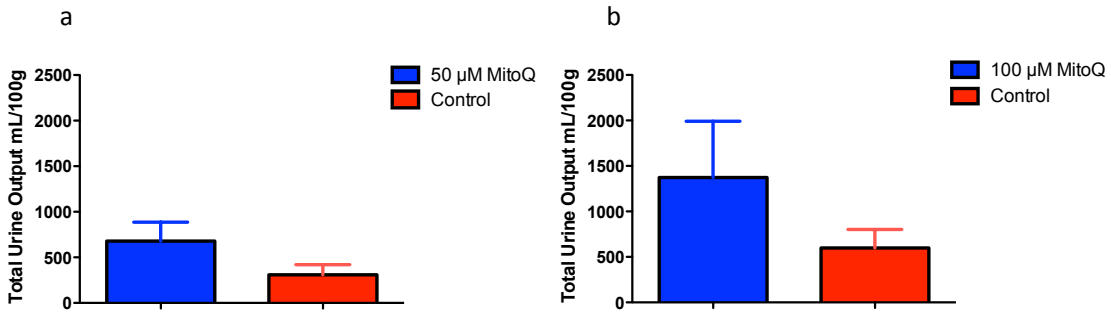

Figure 5.14. Effects of 50 and 100 µM MitoQ on total urine output during 6 h of EVNP compared to the control groups. The kidneys were flushed and stored with or without MitoQ for 10 h using CSS. (a) The total urine output was significantly higher in the 50 µM MitoQ group (n = 4) compared to the control group (n = 4) during 6 h of EVNP (678 ± 208 vs. 309 ± 112 mL/100 g; p = 0.007; paired t-test). (b) The difference between the 100 µM MitoQ group (n = 5) compared to the control group (n = 5) during 6 h of EVNP did not reach statistical significance (1374 ± 618 vs. 599 ± 203 mL/100 g; p = 0.054; paired t-test). Data are mean ± SD.

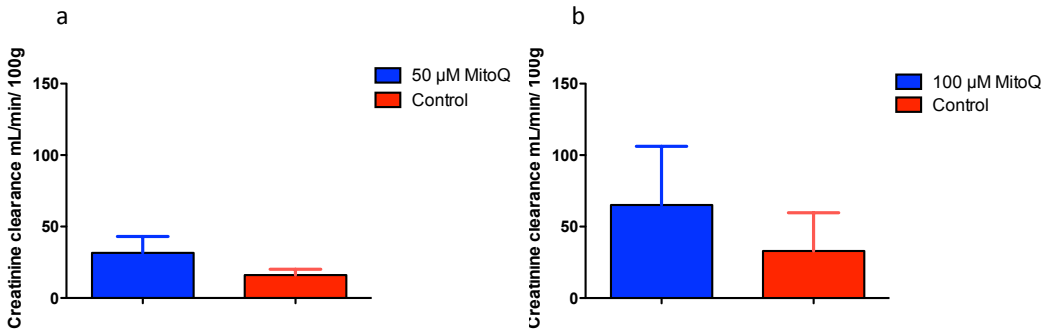

FIgure 5.15. Effects of 50 and 100 µM MitoQ on creatinine clearance during 6 h of EVNP compared to the control groups. The kidneys were flushed and stored with or without MitoQ for 10 h using CSS. (a) Creatinine clearance was numerically higher in the 50 µM MitoQ group (n = 4) compared to the control (n=4) during 6 h of EVNP, but the difference did not reach statistical significance (31.6 ± 11.4 vs. 16.1 ± 4.1mL/min/100 g area under the curve (AUC); p = 0.065; paired t-test). (b) The difference did not reach statistical significance in the 100 µM MitoQ group (n = 5) compared to the control group (n = 5) during 6 h of EVNP (65.1 ± 41.1 vs. 32.9 ± 26.7 mL/min/100 g area under the curve (AUC); p = 0.293; paired t-test). Data are mean ± SD.

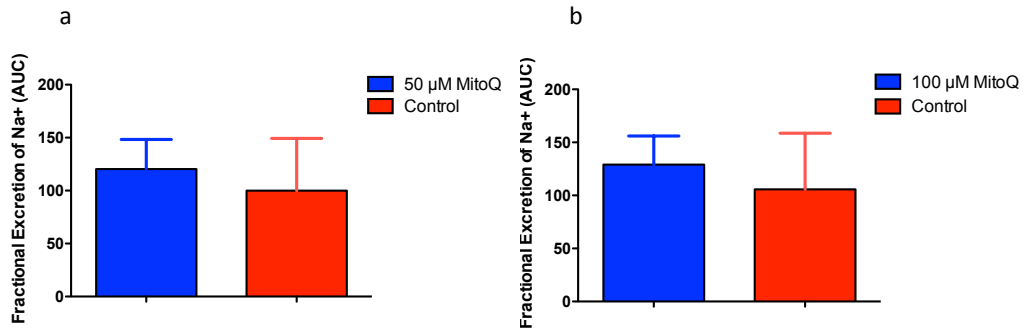

Figure 5.16. Effects of 50 and 100 µM MitoQ on fractional excretion of sodium during 6 h of EVNP compared to the control groups. The kidneys were flushed and stored with or without MitoQ for 10 h using CSS. (a) There was no significant difference in fractional excretion of sodium between the 50 µM MitoQ group (n = 4) and the control group (n = 4) during 6 h of EVNP (120 ± 28 vs.100 ± 49 % area under the curve (AUC); p = 0.618; paired t-test). (b) Similarly, there was no significant difference in fractional excretion of sodium between the 100 µM MitoQ group (n = 5) and the control group (n = 5) during 6 h of EVNP (129 ± 27 vs. 106 ± 53 % area under the curve (AUC); p = 0.312; paired t-test). Data are mean ± SD.

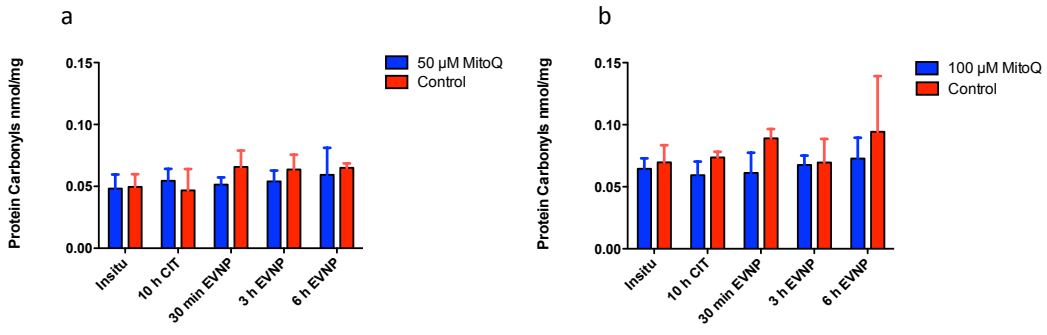

Figure 5.17. Effects of 50 and 100 µM MitoQ on protein carbonyls during 6 h of EVNP. The kidneys were flushed and stored with or without MitoQ for 10 h using CSS. Biopsy samples were taken at the indicated times. (a) There was no significant difference in the oxidative damage to proteins, measured by protein carbonyl formation between the 50 µM MitoQ group (n = 4) and the control group (n = 4) at the end of 6 h of EVNP (0.059 ± 0.022 vs. 0.065 ± 0.003 nmol/mg; p = 0.679; paired t-test). (b) Similarly, there was no significant difference in protein carbonyl formation between the 100 µM MitoQ group (n = 5) and the control group (n = 5) at the end of 6 h of EVNP (0.092 ± 0.041 vs. 0.073 ± 0.017 nmol/mg; p = 0.225; paired t-test). Data are mean ± SD.

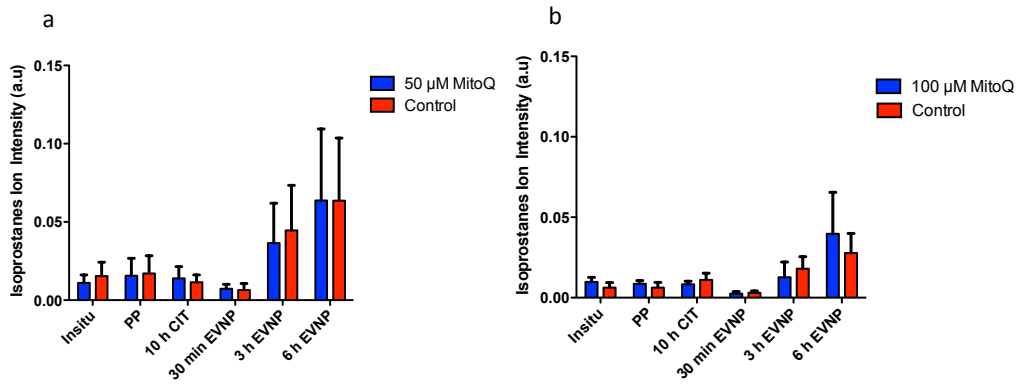

Figure 5.18. Effects of 50 and 100 µM MitoQ on isoprostanes during 6 h of EVNP compared to the control groups. The kidneys were flushed and stored with or without MitoQ for 10 h using CSS. Biopsy samples were taken at the indicated times. (a) There was no significant difference in the oxidative damage to lipids, measured by isoprostanes formation between the 50 µM MitoQ group (n = 4) and the control group (n = 4) at the end of 6 h of EVNP (0.064 ± 0.046 vs. 0.064 ± 0.040 nmol/mg; p = 0.997; paired t-test) or between (b) the 100 µM MitoQ group (n = 5) and the control group (n = 5) at the end of 6 h of EVNP (0.039 ± 0.026 vs. 0.028 ± 0.012 nmol/mg; p = 0.659; paired t-test). Data are mean ± SD.

5.7 Histological assessment of 50 µM MitoQ on IRI during EVNP

A wedge biopsy sample 5 mm x 10 mm (around 120 mg tissue wet weight) from cortex, medulla and inner medulla was taken from the pig kidneys immediately post-perfusion on the back table (PP), at the end of CIT (10 h) and at the end of EVNP (6 h). Collected biopsies were fixed in 10% formalin, sectioned, stained with haematoxylin and eosin. Samples were assessed for markers and degrees of IRI. No abnormalities seen in glomeruli, arterioles or arteries. In this context, scores were given according to the degree of tubular injury (Table 5.1). The total score ranged from 0 to 3, with 0 representing no pathological changes and 3 representing acute tubular necrosis (Figure 19). A histopathology consultant blinded to experimental group identity performed the histopathological assessment.

There were no significant differences between the control group (n = 4) and the MitoQ group (n = 4) in the total histopathology injury score for the pig kidney biopsies at the end of CIT (0.5 ± 0.57 vs. 0.75 ± 0.50; p = 0.638; paired t-test) or at the end of 6h of EVNP (3.00 ± 0.00 vs. 2.50 ± 0.57; p = 0.182; paired t-test).

Scores	The degree of tubular injury
0	No pathological changes
1	Minimal focal acute tubular injury
2	Moderate diffuse acute tubular injury
3	Acute tubular necrosis

Table 5.1. Histopathological scoring system for the degree of tubular injury in pig kidneys.

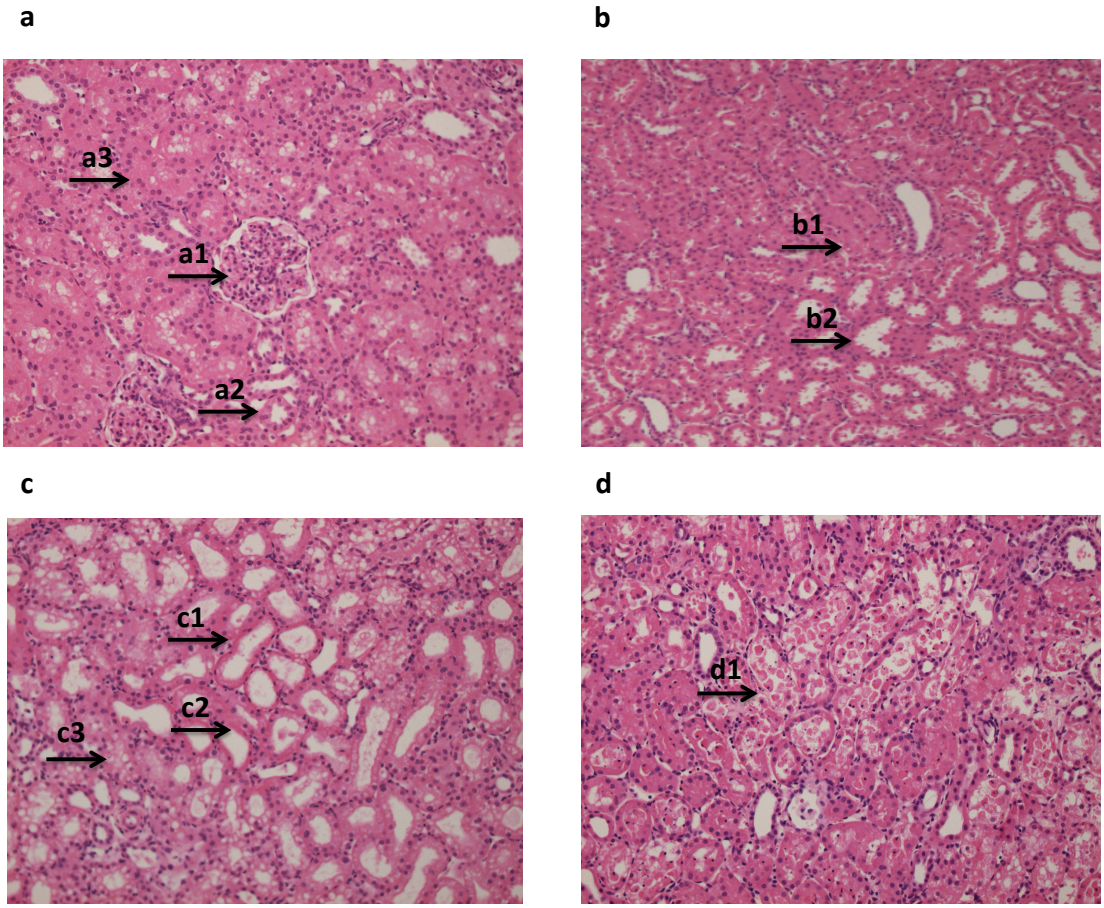

Figure 5.19. Histopathological assessment of pig kidneys tissue biopsies. Representative images of the degree of tubular injury. (a) Score 0; (a1) normal glomeruli , (a2) normal arterioles, (a3) normal parenchyma with tubules packed close together lined by tall eosinophilic cells with brush border. Haematoxylin and eosin x200 (b) Score 1; low power view to show area of normal tubules. (b1) adjoining focus of tubules lined by attenuated epithelium, (b2) loss of brush border and apparent luminal dilation. Haematoxylin and eosin x100. (c) Score 2; (c1) diffuse acute tubular injury with tubules lined by attenuated epithelium with loss of brush border and apparent luminal dilation, (c2) others with loss of nuclei, (c3) and some having extreme coarse vacuolisation (c3). Haematoxylin and eosin x100. (d) Score 3; (d1) tubules showing sloughed necrotic epithelial cells within the lumen (d1). Haematoxylin and eosin x100.

5.8 Effect of 250 µM MitoQ on kidney function and IRI during EVNP

To determine the therapeutic window of MitoQ in my controlled DCD pig model, I examined the effect of 250 µM MitoQ on pig kidneys. The use of 250 µM MitoQ in the first pair of kidneys demonstrated a toxic effect, with the MitoQ-treated kidney slowly developing large areas of patchy and dusky reperfusion during 6 h of EVNP (Figure 5.20). The renal blood flow was similar between the kidney treated with 250 µM MitoQ and the control kidney in the first pair of pig kidneys during 6 h of EVNP. However, the renal blood flow was less than 50 mL/min/100 g for both kidneys at the end of 6 h EVNP (Figure 5.21a). Total urine output was higher in the 250 µM MitoQ kidney compared to the control kidney at the end of 6 h EVNP (291 vs. 177 mL/min/100; Figure 5.21b). However, creatinine clearance was similar in the MitoQ kidney and the control kidney during 6 h of EVNP (5.4. vs. 4.3 mL/min/100g AUC; Figure 5.21c). Of note, the fractional excretion of sodium was higher in the 250 µM MitoQ kidney compared to the control kidney at the end of 6 h EVNP (94.4 % vs. 71.2 %; Figure 5.21d). The 250 µM MitoQ kidney in the second pair of pig kidneys showed a clear toxic effect, with large areas of necrosis once placed on the EVNP circuit (Figure 5.22). I therefore terminated the normothermic perfusion and only two pairs of kidneys were flushed with 250 µM of MitoQ.

a

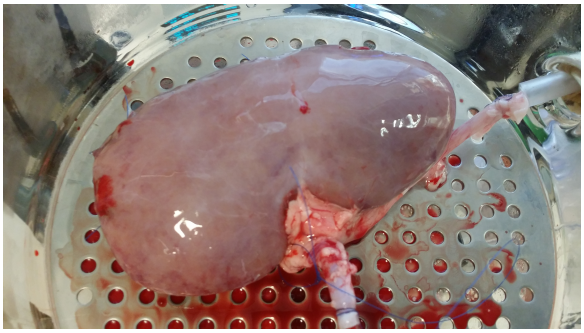

b

c

d

Figure 5.20. MitoQ toxicity following the use of 250 µM dose in the first pair of pig kidneys. The 250 µM MitoQ pig kidney was slowly developing large areas of patchy and dusky reperfusion during 6 h EVNP (a-d).

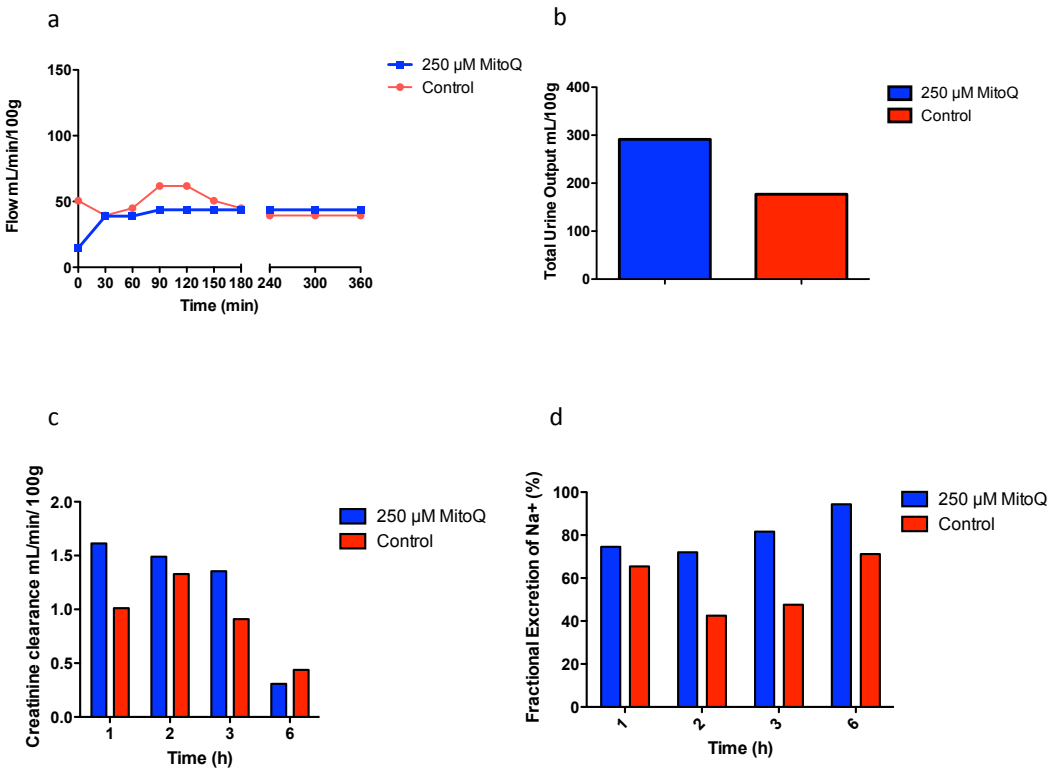

Figure 5.21. Effect of 250 µM MitoQ dose on renal functions in the first pair of pig kidneys during 6 h EVNP. The kidneys were exposed to 10 min WIT then flushed and stored with or without MitoQ for 10 h using CSS. (a) Renal blood flow. (b) Total urine output. (c) Creatinine clearance. (d) Fractional excretion of sodium.

Figure 5.22. MitoQ toxicity following the use of 250 µM dose in the second pair of pig kidneys during 1 h of EVNP. The 250 µM MitoQ kidney developed large areas of necrosis once placed on the EVNP circuit.

5.9 Effect of control compounds on kidney function and IRI on EVNP

5.9.1 Efficacy of 'control' TPMP compound

As outlined in chapter 1, the MitoQ molecule consists of a TPP cation covalently linked to the antioxidant moiety (ubiquinone) by a 10-carbon alkyl chain. The ability of the TPP cation to move directly through phospholipid bilayers enables the selective accumulation of the MitoQ molecule within the mitochondrial matrix. To examine if the therapeutic efficacy of MitoQ in ameliorating renal IRI was solely due to its antioxidant effect produced by the antioxidant moiety (ubiquinone), I next compared the effects of a simple TPP compound methyl triphenyl phosphonium bromide (TPMP) to that of MitoQ (Figure.523). Since the greatest therapeutic efficacy of MitoQ was at a dose of 50 µM, I used this dose (50 µM) for the control TPMP compound and for subsequent control compound experiments.
The control TPP compound TPMP had no effect on renal blood flow (Figure 5.24a), total urine output (Figure 5.24b), creatinine clearance (Figure 5.24c) or fractional excretion (Figure 5.24d) of sodium when compared to kidneys perfused with Soltran® only.

a

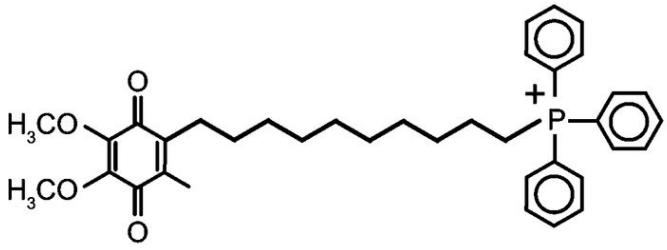

b

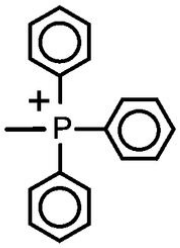

Figure 5.23. Chemical structures of MitoQ (a) and simple control TPMP compound (b).

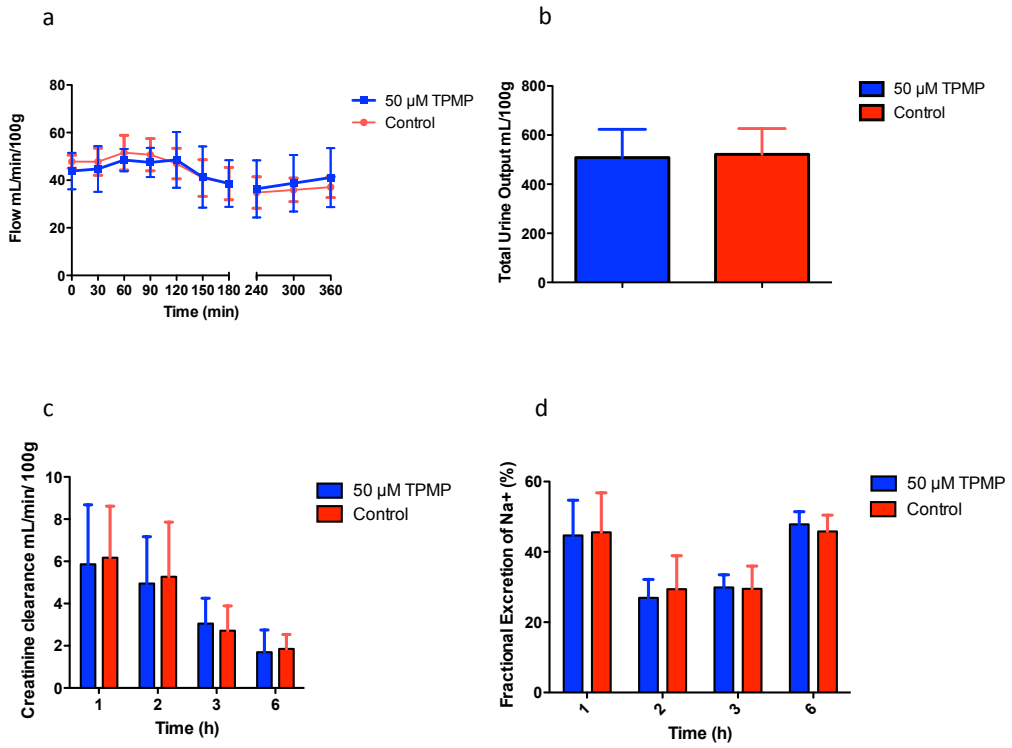

Figure 5.24. Effect of the control TPMP compound group on renal function. The kidneys were flushed and stored with or without 50 µM TPMP (n = 4 per group) for 10 h in CSS and subsequently underwent 6 h of EVNP. At the end of 6 h of EVNP, 50 µM TPMP had no significant effect on (a) renal blood flow (41.1 ± 12.4 vs. 37.1 ± 4.4 mL/100 g; p =0.424; paired t-test), (b) total urine output (509 ± 115 vs. 522 ± 105 mL/100 g; p = 0.730; paired t-test), (c) creatinine clearance (1.7 ± 1.1 vs. 1.9 ± 0.7 mL/min/100 g; p = 0.538) or (d) fractional excretion of sodium (47.8 ± 3.6 vs. 45.8 ± 4.6 %; p = 0.545; paired t-test). Data are mean ± SD.

5.9.2 Assessment of DecylTPP and MitoTMB as control compounds

The lack of TPMP efficacy to ameliorate renal IRI suggests that the antioxidant moiety on MitoQ was responsible for protection, rather than the TPP cation. To explore this further, I also examined more hydrophobic TPP compounds; DecylTPP and MitoTMB (Figure 5.25) using the same concentration (50 µM) that was used previously for the simple TPP compound (TPMP). Pairs of pig kidneys were exposed to 10 min of WIT, flushed with Soltran® ± DecylTPP or MitoTMB and then subjected to 10 h CIT using CSS. The kidneys were then placed on EVNP for 6 h. There was a trend towards better renal blood flow (Figure 5.26a) and renal function (higher total urine output and higher creatinine clearance) in the DecylTPP group compared to the control group at the end of 6 h EVNP (Figure 5.26b, Figure 5.26c). DecylTPP had no effect on fractional excretion of sodium (Figure 5.26d).

50 µM MitoTMB had a significant effect on kidney function. Renal blood flow was significantly higher in the 50 µM MitoTMB group compared to the control group (Figure 5.27a). In addition, total urine output and creatinine clearance were significantly higher in the MitoTMB group compared to the control group (Figure 5.27b, 5.27c). Similar to DecylTPP, MitoTMB had no effect on fractional excretion of sodium (Figure 5.27d).

a

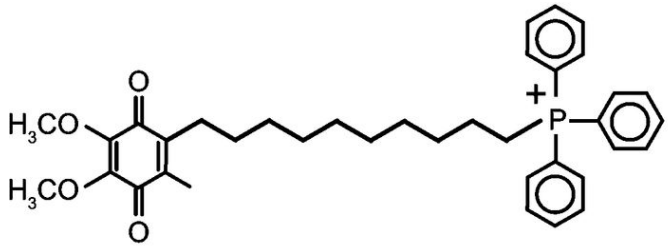

b

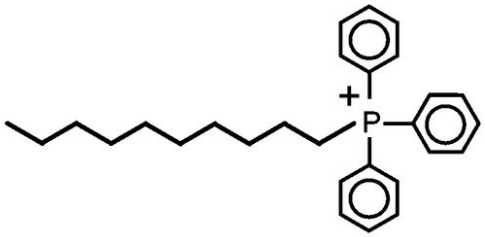

c

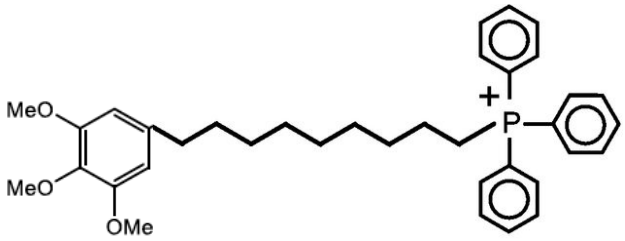

Figure 5.25. Chemical structures of MitoQ and control compounds. (a) MitoQ. (b) DecylTPP. (c) MitoTMB.

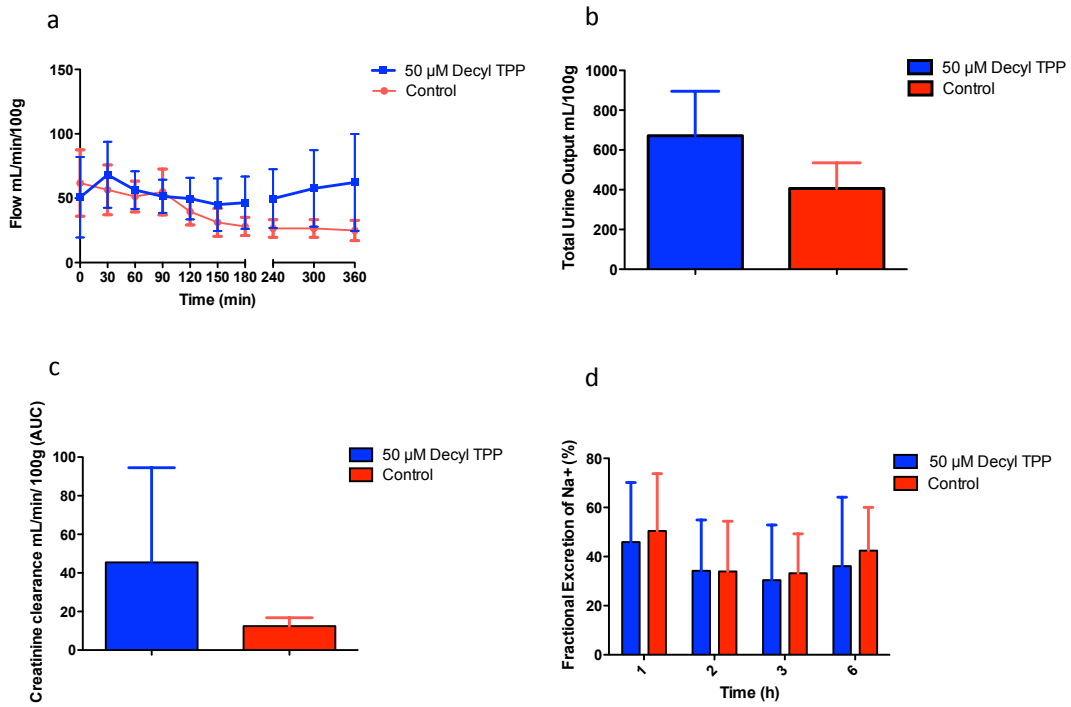

Figure 5.26. Effect of the control compound DecylTPP group on renal function. The kidneys were flushed and stored with or without 50 µM TPMP (n = 4 per group) for 10 h in CSS and subsequently underwent 6 h of EVNP. (a) At the end of 6 h EVNP there was a trend towards better renal blood flow in the DecylTPP group compared to the control group, but the difference was not statistically significant (62.3 ± 37.6 vs. 24.9 ± 7.9 mL/min/100 g; p = 0.092; paired t-test). (b) The total urine output was numerically higher in the Decyl TPP group compared to the control kidneys group, but the difference was not statistically significant (671 ± 224 vs. 407 ± 129 mL/100 g; p = 0.087; paired t-test). (c) There was no significant difference in creatinine clearance between the DecylTPP group compared to the control group (45.5 ± 49.1 vs. 12.5 ± 4.3 mL/min/100 g area under the curve (AUC); p = 0.268). (d) There was no significant difference in fractional excretion of sodium between the Decyl TPP group compared to the control group (36.1 ± 28.1 vs. 42.4 ± 17.6%; p = 0.662; paired t-test). Data are mean ± SD.

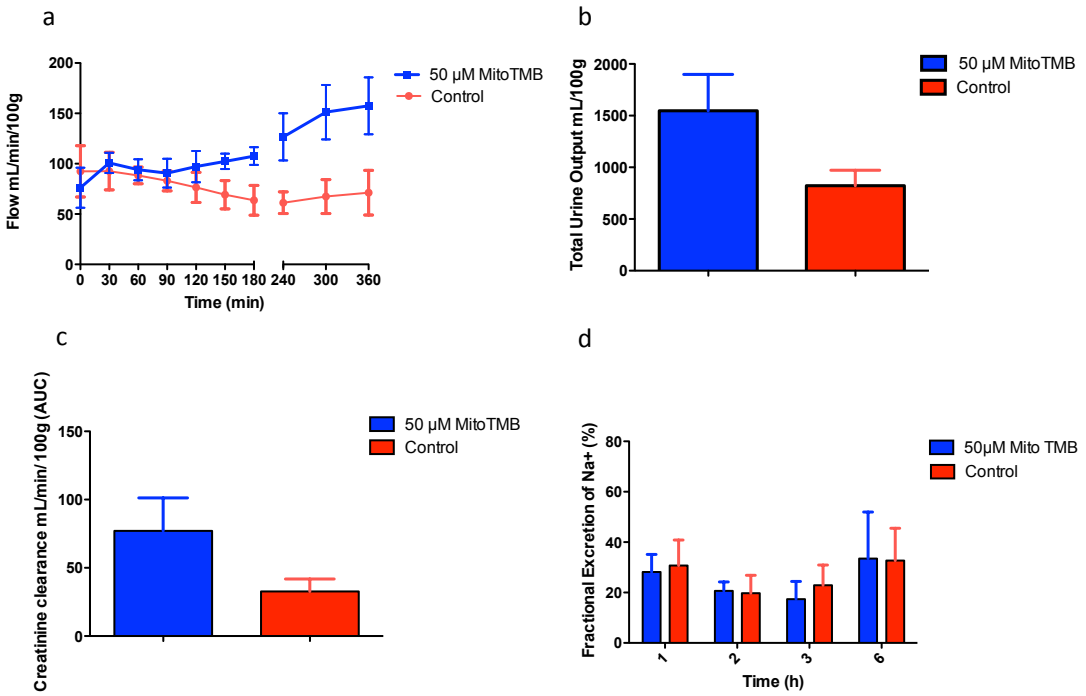

Figure 5.27. Effect of the control compound MitoTMB group on renal function. The kidneys were flushed and stored with or without 50 µM MitoTMB (n = 4 per group) for 10 h in CSS and subsequently underwent 6 h of EVNP. (a) At the end of EVNP the renal blood flow was significantly higher in the MitoTMB group compared to the control group (158 ± 28 vs. 71 ± 22 mL/min/100 g; p = 0.003; paired t-test). (b) The total urine output was significantly higher in the MitoTMB group compared to the control group (1547 ± 352 vs. 823 ± 149 mL/100 g; p = 0.009; paired t-test). (c) The creatinine clearance was significantly better in the MitoTMB group compared to the control group (77.1 ± 24.1 vs. 32.7 ± 9.1 mL/min/100 g area under the curve (AUC); p = 0.023). (d) There was no significant difference in fractional excretion of sodium between the MitoTMB group compared to the control group (33.5 ± 18.5 vs. 32.7 ± 12.8%; p =0.951; paired t-test). Data are mean ± SD.

5.10 Discussion

In this chapter I was able to successfully:

1. Characterise MitoQ uptake and tissue concentrations during 10 h CSS and 6 h of EVNP in the 5 µM, 50 µM and 100 µM MitoQ groups.
2. Characterise the therapeutic window for MitoQ and assess its efficacy in ameliorating renal IRI using 50 and 100 µM MitoQ concentrations.
3. Extend the duration of EVNP to 6 h.

There were dose-dependent increases in MitoQ tissue concentrations in the 5 µM, 50 µM and 100 µM Mito Q groups. In addition, there were non-significant increases in the MitoQ tissue concentrations during the first 6 h of CSS preservation, after which MitoQ tissue concentrations were relatively stable and did not markedly alter upon preservation for up to 10 h in CSS. This indicates that MitoQ tissue uptake occurs primarily during the initial flushing and cold preservation period and that the tissue concentration of MitoQ is then stable over at least 10 hours of CSS. This suggests that a single dose of MitoQ, administered at the time of kidney retrieval, results in stable tissue concentrations. This is of clinical importance as kidneys are exposed to a variable period of CIT in clinical transplantation, and MitoQ tissue concentrations must therefore remain within the safe therapeutic window during that period.

MitoQ tissue concentrations also remained relatively stable during 6 h of EVNP in the 5 µM, 50 µM and 100 µM MitoQ groups. This may be because MitoQ, once taken up by organs is retained for 6 h with no losses during reperfusion with blood. However, this needs to be considered in the context of mouse experiments, where the half-life for loss of MitoQ from the liver and kidneys was both around 3 h after a bolus i.v. injection (43). This loss from the organs is due to the equilibration of MitoQ from the mitochondria to the cytosol and from there to the circulation. Therefore, although there are very large concentration gradients from the extracellular medium to the cytosol and again from the cytosol to the mitochondria, these are all in an equilibrium that is determined by the magnitude of the mitochondrial and plasma membrane potentials. In vivo the excretion of MitoQ to the urine and bile will mean that there will be a gradual loss of MitoQ from the circulation (10), and thus via equilibration from the organs. The reason why this did not occur in the EVNP system may be because of differences in organ size and perfusion rate between the mouse kidney in vivo and the pig kidney in the EVNP system. Alternatively it could be because the EVNP is a closed, recirculating system, thus once some of the MitoQ had been lost from the tissue it would establish a concentration in the circulating medium that equilibrated with that in the kidney, preventing further loss of MitoQ. In this context, I have collected EVNP perfusate samples for future analysis of MitoQ concentrations in the EVNP perfusate.

As outlined in chapter 1, mitochondria play a key role in IRI through the production of ROS during reperfusion. Oxidative damage to mitochondria is an early event in IRI. The process of IRI contributes significantly to graft damage and impacts on the short and long-term graft survival outcomes in kidney transplantation. Acute kidney injury (AKI) is the clinical manifestation of kidney IRI. AKI is characterized by a rapid decrease in renal excretory function, with the accumulation of nitrogenous metabolic end products such as creatinine or decreased urine output, or both. In this context, creatinine clearance and urine output are key clinical markers of AKI and are widely used to assess renal function in clinical practice and in renal IRI experiments. In my controlled DCD pig model, total urine output increased significantly in the 50 µM MitoQ group compared to the control group. Creatinine clearance was numerically higher in the 50 µM MitoQ group but the difference did not reach statistical significance. MitoQ protective effect on total urine out put and the trend toward better creatinine clearance suggest a protective role against IRI and AKI in clinical transplantation. In chapter 4, fractional excretion of sodium was shown to be a sensitive marker when the relative effects of warm ischaemic time (WIT) and cold ischaemic time (CIT) were assessed. MitoQ had no effect on fractional excretion of sodium suggesting that MitoQ was protective against some functional deficits, but not all.

MitoQ has been shown to have a protective effect in ameliorating vascular endothelial dysfunction in mice (87). As outlined in chapter 1, superoxide radical ($O_2^{\bullet -}$) can react with NO to generate peroxynitrite ($ONOO^-$). In this context, increased $O_2^{\bullet -}$ production at reperfusion may lead to reduce the bioavailability of the endothelium-synthesized dilating molecule NO and impaired endothelial dilatation function. This might explain the significantly higher renal blood flow noticed in the 50 µM and 100 µM MitoQ groups compared to the control groups at the end of 6 h EVNP.

Of note, there were significant differences in the two control groups from the 50 and 100 µM MitoQ groups in terms of renal flow, renal functions (urine output and creatinine clearance) and oxidative damage markers (protein carbonyl formations and isoprostanes). In this context, the use of paired kidneys from the same animal, and paired statistical testing, eliminated a potential source of bias could otherwise compromise the validity of the experimental findings.

MitoQ is a selective mitochindria-targeted antioxidant and is expected to protect against oxidative damage during reperfusion by blocking reactive oxygen species. I therefore investigated protein carbonyl formation and lipid peroxidation (isoprostanes) as markers of oxidative damage. There were increases in protein carbonyl formation and isoprostanes after reperfusion, albeit not statistically significant. This is consistent with the expected burst of mitochondrial ROS production that occurs upon reperfusion of ischaemic renal tissue resulting in oxidative damage to proteins and lipids. However more data is required before this can be concluded. Of note, treatment with MitoQ during cold storage and prior to ischaemia did not result in a significant reduction of the protein carbonyls content or isoprostanes formation in renal tissue during 6 h of EVNP, compared to the control group. The absence of a significant reduction in the formation of protein carbonyl and isoprostanes in the MitoQ group

might be partially explained by the short duration of EVNP. Despite extending the duration of EVNP from 3 h to 6 h, no protective effect at the cellular level was evident at these relatively early time points. The MitoQ antioxidant effect at the cellular level might be a slow and progressive process, thus the beneficial effect may not manifest during the current limited duration of EVNP. In support of this, there were no significant differences in oxidative damage markers for samples taken 60 min post reperfusion using a small animal model of renal IRI. The differences in oxidative damage markers were only significant at 24 hours post renal IRI (40).

Histological assessment of renal graft biopsies can be used to determine the severity of IRI. Acute tubular necrosis (ATN) is the most common cause of ischaemic acute kidney injury (AKI). The recovery from ATN depends on the kidney's ability to carry out cellular repair and regeneration to overcome the structural damage to the renal parenchyma and cellular death induced by IRI. The recovery from ATN may continue for several days or weeks. Therefore, it is not surprising that MitoQ did not demonstrate a beneficial effect in the histological assessment of pig kidney biopsies after the limited duration of EVNP reperfusion (6 h).

EVNP played a vital role in examining the safety and the efficacy of MitoQ in ameliorating renal IRI. Extending the duration of EVNP beyond 6 h might help to assess if the MitoQ demonstrates therapeutic efficacy in ameliorating cellular oxidative damage at a later time point. However, it is technically difficult to extend the reperfusion period beyond 6 h in the EVNP system. Blood haemolysis during cardiopulmonary bypass and EVNP has been reported, whether a standard roller pump or centrifugal pump were used (88). Haemolysis can potentially be increased by extending the duration of EVNP beyond 6 h. Blood haemolysis leads to a higher estimation of creatinine by interfering with the colorimetric method (Jaffe reaction) used in clinical practice to determine creatinine levels in blood and urine (89), which can affect the validity of the data. In addition, the use of creatinine as a marker of AKI relies on the presence of an adequate level of creatinine in the EVNP circuit to calculate creatinine clearance. As outlined in chapter 2, creatinine was added to the perfusate to achieve an initial circulating concentration of 1000 µmol/L. There was enough creatinine to allow creatinine clearance to be calculated at the end of 6 h EVNP. However, as there is no external metabolic source of creatinine in the isolated perfused kidney, the majority of the creatinine was cleared from the EVNP circuit at the end of 6 h period of EVNP. To extend the current duration of EVNP beyond 6 h, the issue of maintaining an adequate creatinine concentration must be addressed and overcome. Creatinine infusion at a constant rate is one experimental approach and may be a better alternative to bolus loading of the EVNP circuit with creatinine. Further work is required to characterise the rate and the concentration of the creatinine infusion before extending the current duration beyond 6 h.

EVNP provided important data on MitoQ uptake, safety and efficacy. However, this model was limited by the relatively short duration of reperfusion (6 h). In addition, pig kidneys on the EVNP were not

exposed to systemic neuro-hormonal and immunological factors that influence the severity of renal IRI in clinical practice. Therefore, a full auto- or allo-transplantation pig model would be required to overcome these limitations and assess the long term effects of MitoQ on functional and cellular renal IRI. However, this is a technically complex and costly model and was not within the scope of this project.

The MitoQ molecule comprises a lipophilic triphenylphosphonium (TPP) cation covalently linked to an antioxidant ubiquinone moiety by a 10-carbon alkyl chain. TPP cations have the ability to pass rapidly through the plasma and mitochondria membrane and accumulate within the mitochondria up to several hundred fold. In this context, TPP has been used to target the antioxidant MitoQ selectively to the mitochondria. The simple control compound TPMP did not protect against renal IRI, suggesting the MitoQ antioxidant moiety (ubiquinone) was responsible for protection and not the TPP targeting cation. However, more hydrophobic TPP compounds; DecylTPP and MitoTMB demonstrated apparent efficacy in ameliorating renal IRI. The effect of DecylTPP was minor and may indicate a small effect of mitochondrial membrane disruption due to the accumulation of DecylTPP. The effect of MitoTMB was more puzzling, as it showed significant protection. This led my collaborators (T. Bright in the Murphy lab) to assess whether MitoTMB may have other biological activity. Surprisingly, it was found that the moiety targeted to mitochondria in MitoTMB, which had been initially thought to be inactive, also had some antioxidant effect in vitro and thus its effects in vivo were likely to be due to this antioxidant function, making MitoTMB an inappropriate control for MitoQ. These data indicate that the main mode of action of MitoQ in the EVNP system is likely to be due to its antioxidant effects in mitochondria.

The use of 250 µM MitoQ in my controlled DCD pig model demonstrated a toxic effect, with the MitoQ-treated kidney developing large areas of necrosis. MitoQ is largely adsorbed to the inner membrane of mitochondria and the linker chain (10-carbon alkyl) enables the active antioxidant component (ubiquinol) to penetrate into the membrane core. The accumulation of high concentrations of MitoQ within the inner mitochondria membrane might interfere with the membrane structure and oxidative phosphorylation and ATP synthesis. This might lead to the induction of the mitochondrial permeability transition pore (MPTP) and cell death (necrosis/apoptosis). More generally, these data indicate the likely therapeutic window for MitoQ to be between 5 and 250 µM.

In conclusion the data from pig kidneys suggest that MitoQ was protective against some functional deficits, but not all and may have efficacy in ameliorating the detrimental effects of renal IRI. Therefore, I next examined if this protection could be extended to human kidneys.

Chapter 6

Evaluation of efficacy of MitoQ in ameliorating renal IRI using declined human kidneys

6.1 Introduction

The data presented in chapter 5 demonstrate that MitoQ can protect against some functional renal IRI deficits, but not all in a controlled DCD pig model. The focus of this chapter is to evaluate the efficacy of MitoQ in ameliorating renal IRI using the declined deceased human kidneys.

In clinical practice, deceased human kidneys that have been retrieved may subsequently be declined for transplantation. Kidneys are declined for a number of reasons, including:

- Significant donor vascular disease (evidence on gross macroscopic examination) such as severe aortic atherosclerosis
- Poor perfusion
- Malignancy (renal or extra-renal)
- Poor pre-implantation kidney biopsy score (according to Remuzzi et al.2006 score) indicating chronic disease and predicting graft failure (90)
- Damage during retrieval

Human kidneys that are retrieved for transplantation but subsequently declined have much greater variability in their characteristics than pig kidneys due to the inherent differences in donors (including age, past medical history, cause of death and type of donation [DCD v DBD]) and the process they go through prior to being declined for use in transplantation (including quality of perfusion, WIT and CIT). In addition, pairs of declined deceased human kidneys from the same donor are only rarely available for research use. Therefore, I used single declined deceased human kidneys to investigate MitoQ uptake, and declined pairs of deceased human kidneys were used to investigate efficacy of MitoQ on the EVNP circuit.
In order to ensure that the declined kidneys were suitable for investigation of the safety and the efficacy of MitoQ on the EVNP circuit, the following exclusion criteria were applied:

- More than two renal arteries, which presents technical difficulties for placement of the kidney on the EVNP circuit
- Occlusion in the renal artery or one of the main branches due to dissection
- Expected CIT > 24 h at the time of placing the kidney on the EVNP circuit

As outlined in chapter 2, declined deceased human kidneys were placed in a kidney dish filled with ice and cold Soltran® solution. The kidneys were flushed with 500 mL Soltran® ± MitoQ at 4 °C. The kidneys were then preserved in CSS in 500 mL of Soltran® ± MitoQ for 6 h to characterise MitoQ uptake during CSS. Deceased human kidneys that were retrieved and subsequently declined for transplantation were received from centres across the UK and were thus exposed to variable length of WIT and CIT due to

several factors (including time taken for assessment of kidney by the original centre and the distance of the declining transplant centre from Cambridge). Having previously demonstrated that MitoQ tissue concentrations are stable over time (see chapter 3), I limited storage of declined deceased human kidneys in CSS to 6 h so that perfusion of the kidney on the EVNP circuit could be commenced within 24 h CIT.

Pairs of declined deceased human kidneys were placed on two EVNP circuits and the kidney function of the MitoQ-treated kidney was compared with the control kidney from the same donor over 3 h or 6 h of EVNP with ABO-compatible packed red cells. A maximum of six wedge biopsies (approximately 120 mg tissue wet weight each) were obtained at different times to measure MitoQ tissue concentration and an oxidative damage marker. A typical biopsy schedule consisted of biopsy post-perfusion (PP) with Soltran® ± MitoQ, at 6 h CSS, 30 min EVNP, 3 h EVNP and 6 h EVNP. Wedge biopsies were snap-frozen in liquid nitrogen and stored at -80 °C until analysed (Figure 6.1).

In this chapter I sought to:

1. Investigate the uptake of MitoQ into the declined deceased human kidney tissue
2. Evaluate the efficacy of MitoQ in ameliorating renal IRI using the declined deceased human kidneys
3. Investigate the therapeutic window for MitoQ using a series of dose-response experiments
4. Generate sufficient data to support commencement of a human clinical trial

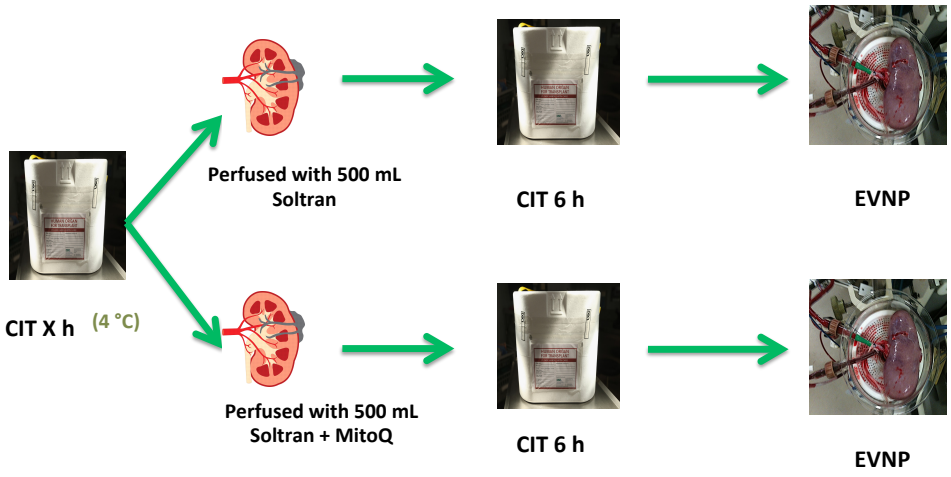

Figure 6.1. Cold static storage of pairs of declined deceased human kidneys with or without MitoQ and subsequent analysis of kidney function by EVNP. Pairs of declined deceased human kidneys were received after having been exposed to a variable period of ischaemia. Pairs of kidneys were flushed and stored in Soltran® with or without MitoQ at ~ 4 ˚C for 6 h. The kidneys were then placed on EVNP circuit and perfused with normothermic oxygenated ABO compatible donated human blood (packed red cells). The effect of MitoQ on kidney function (urine production, blood flow and creatinine clearance) was compared with the contralateral kidney from the same donor that had been flushed and stored in Soltran® only. In addition, cellular injury was assessed by analysis of biopsies for the formation of protein carbonyls as a marker of oxidative damage.

6.2 Uptake of MitoQ

Declined deceased human kidneys, which were received after a variable length of CIT, were flushed with 500 mL Soltran® cold preservation solution supplemented with MitoQ (500 nM - 100 μM). The range of MitoQ dose used in these experiments (500 nM - 100 μM) was based on my controlled DCD pig model results which demonstrated 50 μM of MitoQ to be safe and effective in reducing renal IRI. The kidneys were then placed in 500 mL of fresh cold Soltran® containing the same concentration of MitoQ and preserved at 4 °C for 6 h. I measured the concentration of MitoQ in the kidney by analysing biopsies (~ 120 mg wet weight) using Liquid Chromatography Mass Spectrometry and Liquid Chromatography – Tandem Mass Spectrometry (LC-MS/MS).

To assess the retention of MitoQ in the kidney following reperfusion on the EVNP circuit, I also measured the concentration in the kidney tissue biopsies following 30 min, 3 h and 6 h of reperfusion on the EVNP circuit.

In preliminary experiments, I investigated the uptake of MitoQ at a concentration of 500 nM (n = 4). The MitoQ concentrations in the cold declined deceased human kidney tissue post-perfusion with 500 nM MitoQ were below the level expected to ameliorate renal IRI (Figure 6.2). I therefore investigated uptake and efficacy of a higher range of MitoQ concentrations (5 μM – 100 μM) in subsequent experiments.

There were dose-dependent rises in MitoQ tissue concentrations in the in the 5 μM (n = 3), 50 μM (n = 3) and 100 μM (n = 3) MitoQ groups and the majority of MitoQ uptake took place immediately after flushing. MitoQ tissue concentrations were not statistically different at the end of 6 h CSS preservation compared to the immediate post-perfusion (PP) tissue concentrations. MitoQ tissue concentrations also did not significantly change upon 6 h of EVNP in the 5 μM, 50μM and 100 μM Mito Q groups (Figure 6.3).

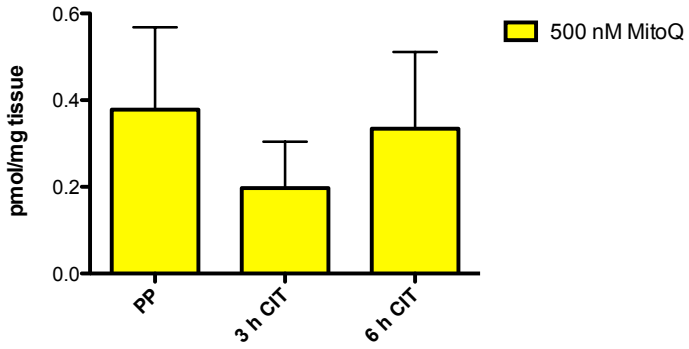

Figure 6.2. MitoQ tissue levels in declined deceased human kidneys during cold static storage. Declined deceased human kidneys were flushed with 500 mL cold Soltran® supplemented with 500 nM of MitoQ (n = 4), and then stored in 500 mL cold Soltran® containing the same concentration of MitoQ (500 nM) in CSS. Wedge biopsies of the kidney (~ 120 mg wet weight) were obtained at the indicated times. Most MitoQ uptake occurred immediately post-perfusion (PP) and there were no significant changes in the MitoQ tissue concentrations at the end of 6 h of CSS (PP 0.4 ± 0.2 vs. 6 h CSS 0.3 ± 0.2 pmol/mg; p = 0.605; paired t-test). Data are mean ± SD.

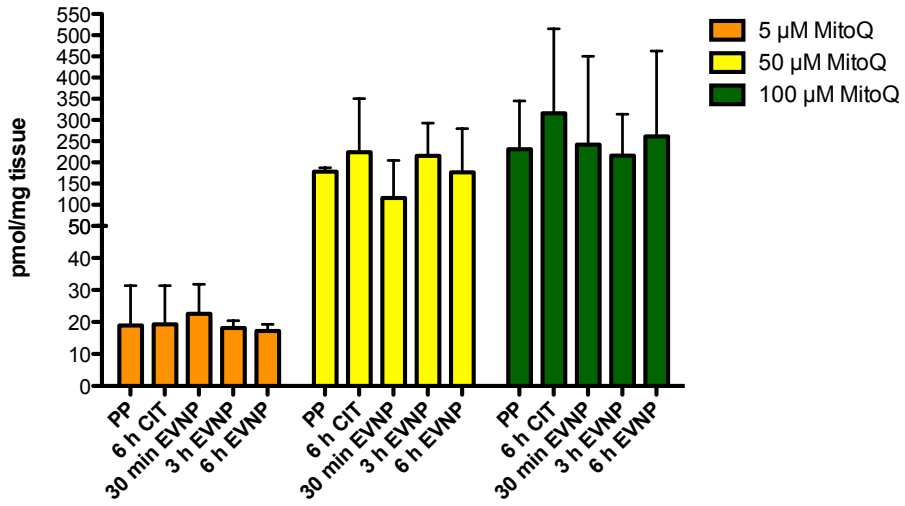

	PP pmol/mg	6 h CIT pmol/mg	6 h EVNP pmol/mg
5 µM MitoQ (n = 3)	18.9 ± 12.5	19.3 ± 12.1	17.2 ± 2.1
50 µM MitoQ (n = 3)	178.2 ± 9.1	224.4 ± 126.4	176.4 ± 103.3
100 µM MitoQ (n = 3)	231.1 ± 113.9	315.7 ± 199.3	261.6 ± 201.1

Figure 6.3. MitoQ tissue levels in declined deceased human kidneys during cold static storage and during 6 h of EVNP. Declined deceased human kidneys were flushed with 500 mL cold Soltran® supplemented with various concentrations of MitoQ as indicated, and then stored in 500 mL cold Soltran® containing the same concentration of MitoQ in CSS. Wedge biopsies were obtained at the indicated times. In the 5 µM (n = 3), 50 µM (n = 3) and 100 µM (n = 3) groups, there were dose-dependent rises in MitoQ tissue concentrations. However, there were no significant changes in MitoQ tissue concentrations at the end of 6 h of CSS compared to the immediate post-perfusion (PP) levels ($p > 0.567$ in all comparisons; paired t-test). Of note, there were no significant changes in MitoQ tissue concentrations at the end of 6 h EVNP compared to the MitoQ tissue concentrations at the end of 6 h CSS ($p > 0.284$ in all comparisons; paired t-test). Data are mean ± SD.

6.3 Effect of 5 µM MitoQ on kidney function and damage during 6 h of EVNP

To assess the efficacy of 5 µM of MitoQ to ameliorate renal IRI, declined deceased human kidneys (n = 4 pairs) were perfused with 500 mL Soltran® ± 5 µM MitoQ. Thereafter, the declined deceased human kidneys were preserved using CSS in 500 mL of Soltran® ± 5 µM MitoQ for 6 h and then placed on the EVNP circuit for 6 h. The donor demographic details are outlined in table 6.2.

There were no significant differences between the 5 µM MitoQ group (n = 4) and the control group (n = 4) in renal blood flow (Figure 6.4), renal function (Figure 6.5) and formation of the oxidative damage marker protein carbonyl (Figure 6.6) throughout 6 h of EVNP.

Variable	1st pair	2nd pair	3rd pair	4th pair
Donor age (years)	72	75	60	80
Donor type	DCD	DCD	DCD	DBD
Reason for decline	Malignancy (renal)	Malignancy (renal)	Malignancy (renal)	Poor biopsy score (5)
Cold ischaemic time (hours)*	18	21	19	23

* The cold ischaemic time (CIT) before placing the kidney on the EVNP circuit

Table 6.1. Donor demographics of the 4 pairs of the declined deceased human kidneys used to assess the efficacy of 5 µM MitoQ to ameliorate renal IRI during 6 h of EVNP.

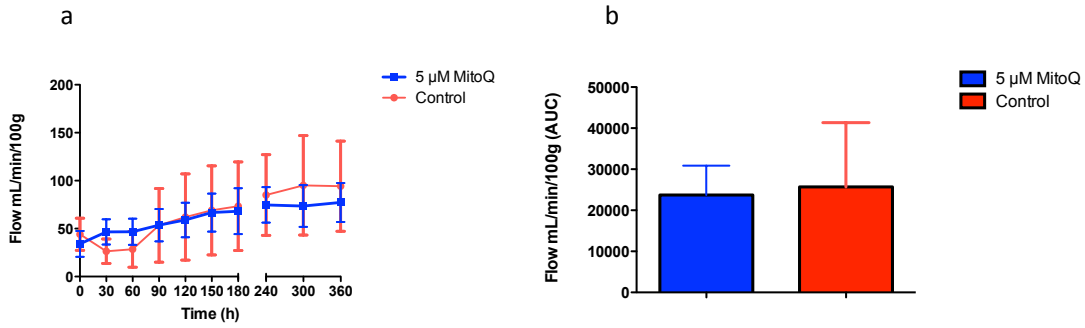

Figure 6.4. Renal blood flow in deceased declined human kidneys during 6 h of EVNP. The kidneys were flushed and stored with or without 5 µM MitoQ (n = 4 per group) for 6 h using CSS. (a) There was no significant difference between the MitoQ group and the control group at the end of 6 h EVNP (77.3 ± 20.3 vs. 94.3 ± 46.9 mL/min/100 g; p = 0.422; paired t-test) or (b) during 6 h of EVNP (AUC; p = 0.738). Data are mean ± SD.

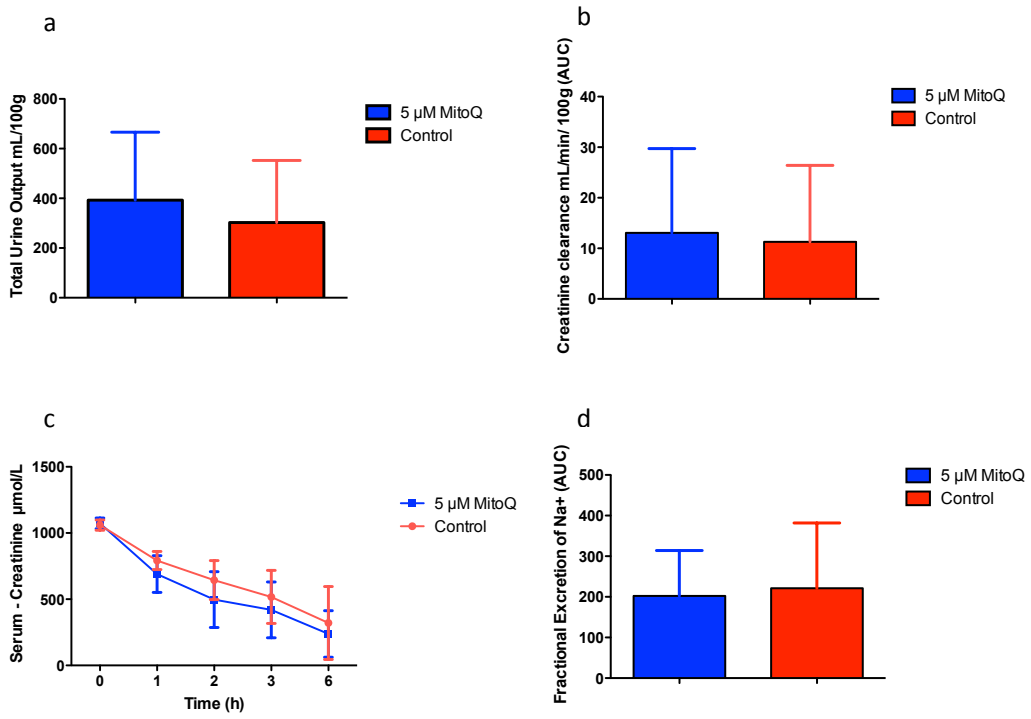

Figure 6.5. Renal function in deceased declined human kidneys during 6 h of EVNP. The kidneys were flushed and stored with or without 5 µM MitoQ (n = 4 per group) for 6 h using CSS. There were no significant differences between the two groups at the end of 6 h EVNP in (a) total urine output (393 ± 274 vs. 302 ± 250 mL/100 g; p = 0.244; paired t tests.), (b) creatinine clearance (13.1 ± 16.7 vs. 11.3 ± 15.1 mL/min/100 gram AUC; p = 0.308; paired t tests.), (c) percentage of serum creatinine fall (77.9 ± 17.3 vs. 69.2 ± 27.2; p = 0.474; paired t tests.) or (d) fractional excretion of sodium (202 ± 106 15 vs. 221 ± 160 AUC; p = 0.615; paired t tests.). Data are mean ± SD.

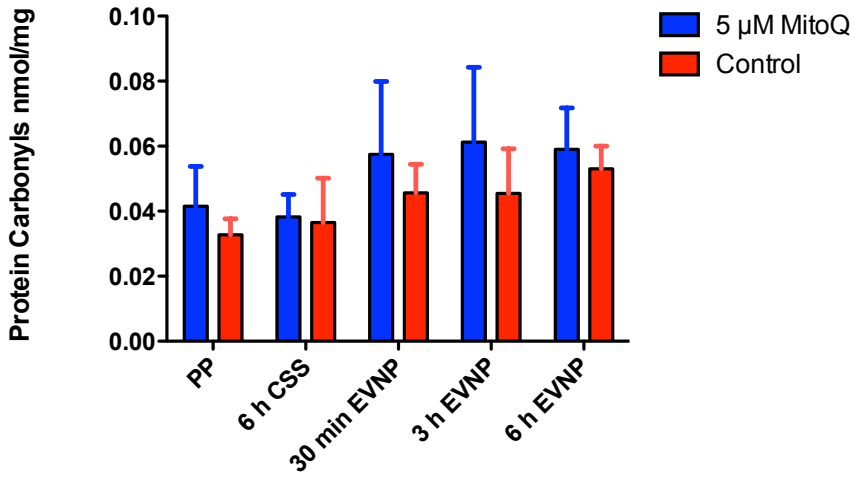

Figure 6.6. Protein carbonyl formation in deceased declined human kidneys during 6 h of EVNP. The kidneys were flushed and stored with or without 5 µM MitoQ (n = 4 per group) for 6 h using CSS. Biopsy samples were taken immediately post-perfusion on the back table (PP), at 6 h CSS, and at 30 min, 3 h and 6 h after the start of EVNP. There was no significant difference in protein carbonyl content in both groups at the end of 6 h EVNP (0.059 ± 0.013 vs. 0.053 ± 0.007 nmol/mg; p = 0.286; paired t-test). Data are mean ± SD.

6.4 Effect of 50 µM MitoQ on kidney function and damage

I next investigated the efficacy of 50 µM MitoQ in ameliorating renal IRI. Cold Soltran® (500 mL) was infused into the kidney containing 50 µM MitoQ (n = 7) and kidney function and injury was compared with the contralateral kidney from the same deceased donor that had been infused with cold Soltran® only (control group; n = 7). Thereafter, the declined deceased human kidneys were preserved using CSS in 500 mL of Soltran® ± 50 µM MitoQ for 6 h. The first 3 pairs of declined deceased human kidneys were placed on the EVNP circuit for 3 h rather 6 h, as those kidneys were recruited at an early stage (before the decision to extend the duration of EVNP to 6 h based on my controlled DCD pig model results). The last 4 pairs of declined deceased human kidneys were placed on the EVNP circuit for 6 h. Therefore, I will present the results of the deceased human kidneys placed on the EVNP circuit for 3 h first (n = 7 pairs), followed by the results of the deceased human kidneys that were placed on the EVNP circuit for 6 h (n = 4 pairs).

6.4.1 Effect of 50 µM MitoQ on kidney function and damage during 3 h of EVNP

The donor demographic details of the 7 pairs of the declined deceased human kidneys used to assess the efficacy of 50 µM MitoQ to ameliorate renal IRI during 3 h of EVNP are outlined in table 6.2.

The renal blood flow remained stable during the first hour of EVNP in the MitoQ group and was significantly higher in the MitoQ group compared to the control group at the end of the first hour of EVNP. Thereafter, the renal blood flow increased in the control group and there was no significant difference between the two groups at the end of 3 h of EVNP (Figure 6.7).

The total urine output was numerically higher in the 50 µM MitoQ group compared to the control group but the difference did not reach statistical significance during 3 h of EVNP (Figure 6.8a). Creatinine clearance (Figure 6.8b) and percentage of serum creatinine fall (Figure 6.8c) were numerically higher in the 50 µM MitoQ groups compared to the control groups but the difference did not reach statistical significance. There was no significant effect of 50 µM MitoQ compared to the control group on fractional excretion of sodium (Figure 6.8d) or total protein carbonyls formation (Figure 6.9) at the end of 3 hour of EVNP using 7 pairs of declined deceased human kidneys.

Variable	1st pair	2nd pair	3rd pair	4th pair	5th pair	6th pair	7th pair
Donor age (years)	54	64	76	60	70	58	78
Donor type	DCD	DCD	DCD	DCD	DCD	DCD	DBD
Reason for decline	Malignancy (renal)	Poor perfusion	Malignancy (renal)	Poor perfusion	Age/Past medical history	Malignancy (renal)	Age/Past medical history
Cold ischaemic time (hours)*	17	12	23	17	18	24	22

* The (CIT) before placing the kidney on the EVNP circuit.

Table 6.2. Donor demographics of the 7 pairs of the declined deceased human kidneys used to assess the efficacy of 50 µM of MitoQ to ameliorate renal IRI during 3 h of EVNP.

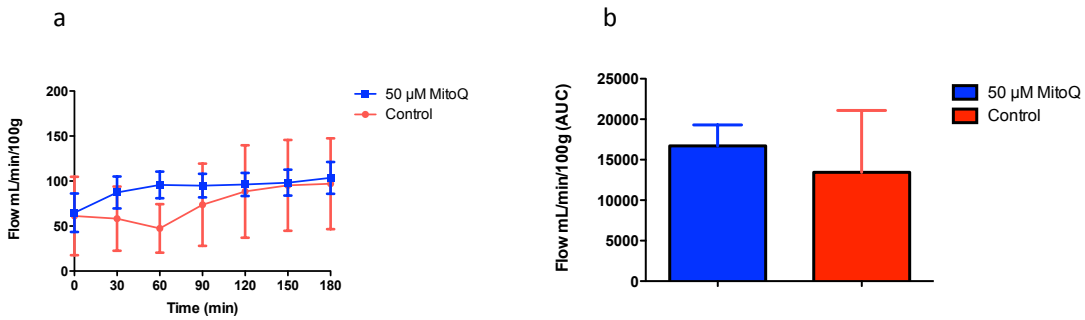

Figure 6.7. Renal blood flow in deceased declined human kidneys during 3 h of EVNP. The kidneys were flushed and stored with or without 50 µM MitoQ (n = 7 per group) for 6 h in CSS and subsequently underwent 3 h of EVNP (a) There was a significant difference between the MitoQ group and the control group at the end of the first hour of EVNP (95.7 ± 14.7 vs. 47.4 ± 26.9 mL/min/100 g; Bonferroni adjusted p = 0.007; paired t-test). However there was no significant difference between the two groups (MitoQ vs. control) (a) at the end of 3 h of EVNP (103.6 ± 17.6 vs. 97.0 ± 50.5 mL/min/100 g; Bonferroni adjusted p = 1.000; paired t-test) or (b) during 3 h of EVNP (AUC p = 0.216; paired t-test). Data are mean ± SD.

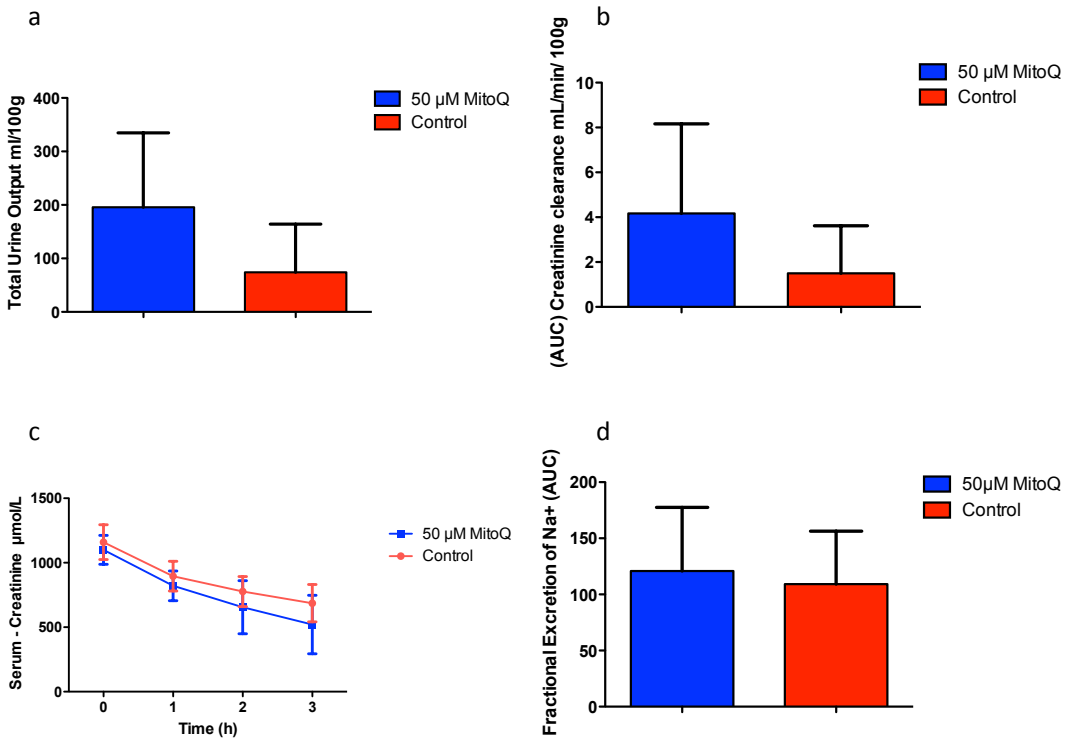

Figure 6.8. Effect of MitoQ on renal function. The kidneys were flushed and stored with or without 50 µM MitoQ (n = 7 per group) for 6 h in CSS and subsequently underwent 3 h of EVNP. (a) The total urine output was numerically higher in the 50 µM MitoQ group compared to the control during 3 h of EVNP, but the differences did not reach statistical significance (196 ± 139 vs. 74 ± 90 mL/100g; p = 0.054; paired t-test). (b) The creatinine clearance was numerically higher in 50µM MitoQ group compared to the control during 3 h of EVNP, but the difference did not reach statistical significance (4.0 ± 4.1 vs. 1.5 ± 2.1 mL/min/100g AUC p = 0.152; paired t-test) (c) Percentage of serum creatinine fall was higher in the MitoQ group compared to the control group at the end of 3 h of EVNP but the difference did not reach statistical significance (51.4 ± 20.8 vs. 37.4 ± 14.4; p = 0.157; paired t tests). (d) There was no significant difference between the MitoQ group and the control group during 3 h of EVNP in fractional excretion of sodium (121 ± 57 vs. 109 ± 47 AUC; p = 0.392; paired t tests). Data are mean ± SD.

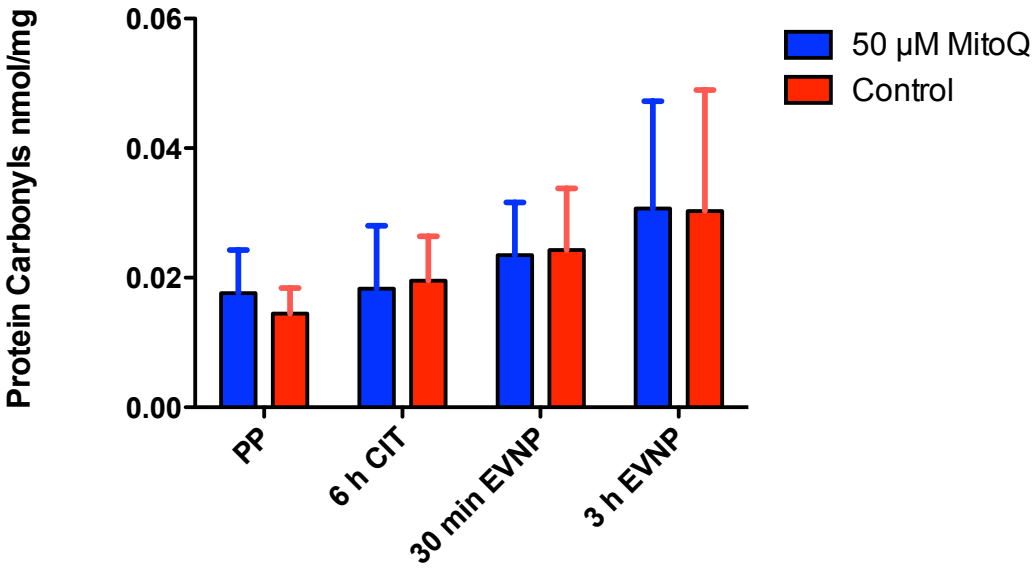

Figure 6.9. Protein carbonyl formation during 3 h of EVNP. The kidneys were flushed and stored with or without 50 µM MitoQ (n = 7 per group) for 6 h using CSS. Biopsy samples were taken immediately post-perfusion (PP) on the back table, at 6 h CSS, and at 30 min and 3 h after the start of EVNP. There was no significant difference in protein carbonyl content in both groups at the end of 3 h of EVNP (0.031 ± 0.017 vs. 0.030 ± 0.019 nmol/mg; p = 0.941; paired t-test). Data are mean ± SD

6.4.2 Effect of 50 µM MitoQ on kidney function and damage during 6 h of EVNP

The donor demographic details of the subset 4 pairs of the declined deceased human kidneys used to assess the efficacy of 50 µM MitoQ to ameliorate renal IRI during 6 h of EVNP are outlined in table 6.3.

The renal blood flow was numerically higher at the end of the first hour of EVNP in the MitoQ group compared to the control group but the difference did not reach statistical significance (Figure 6.10a). The renal blood flow was similar between the two groups at the end of 6 h of EVNP (Figure 6.10b). The total urine output was numerically higher in the 50 µM MitoQ group compared to the control group but the difference did not reach statistical significance during 6 h of EVNP (Figure 6.11a).

There were no significant differences between the MitoQ group and the control group at the end of 6 h of EVNP in creatinine clearance (Figure 6.11b), percentage of serum creatinine fall (Figure 6.11c), fractional excretion of sodium (Figure 6.11d) or protein carbonyl formation (Figure 6.12).

Variable	1st pair	2nd pair	3rd pair	4th pair
Donor age (years)	60	70	58	78
Donor type	DCD	DCD	DCD	DBD
Reason for decline	Poor perfusion	Age/Past medical history	Malignancy (renal)	Age/Past medical history
Cold ischaemic time (hours)*	17	18	24	22

* The cold ischaemic time (CIT) before placing the kidney on the EVNP circuit

Table 6.3. Donor demographics of the 4 pairs of declined human kidneys used to assess the efficacy of 50 μM of MitoQ to ameliorate renal IRI during 6 h of EVNP.

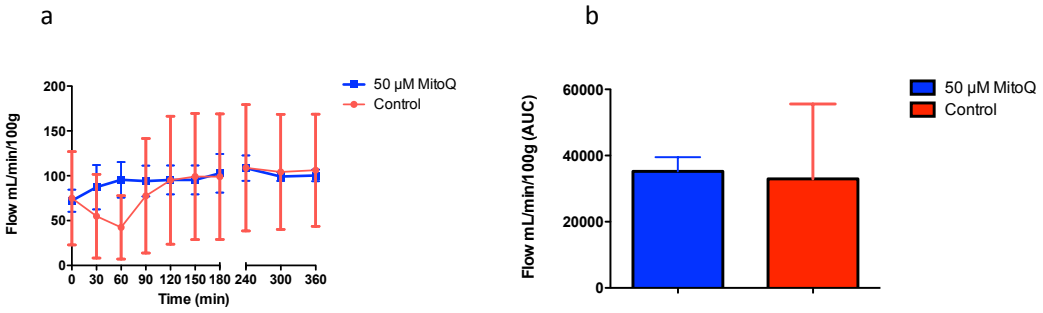

Figure 6.10. Renal blood flow in deceased declined human kidneys during 6 h of EVNP. The kidneys were flushed and stored with or without 50 µM MitoQ (n = 4 per group) for 6 h in CSS before EVNP for 6 h. (a) The renal blood flow was numerically higher in the MitoQ group compared to the control group but the difference did not reach statistical at the end of the first hour of EVNP (96 ± 20 vs. 43 ± 35 mL/min/100 g; Bonferroni adjusted p = 0.160; paired t tests). However, there was no significant difference between the two groups (MitoQ vs. control) at the end of 6 h of EVNP (100 ± 7 vs. 106 ± 63 mL/min/100 g; Bonferroni adjusted p = 1.000; paired t tests). (b) There was no significant difference between the MitoQ group and the control group in renal blood flow during 6 h of EVNP (b; AUC p = 0.835). Data are mean ± SD.

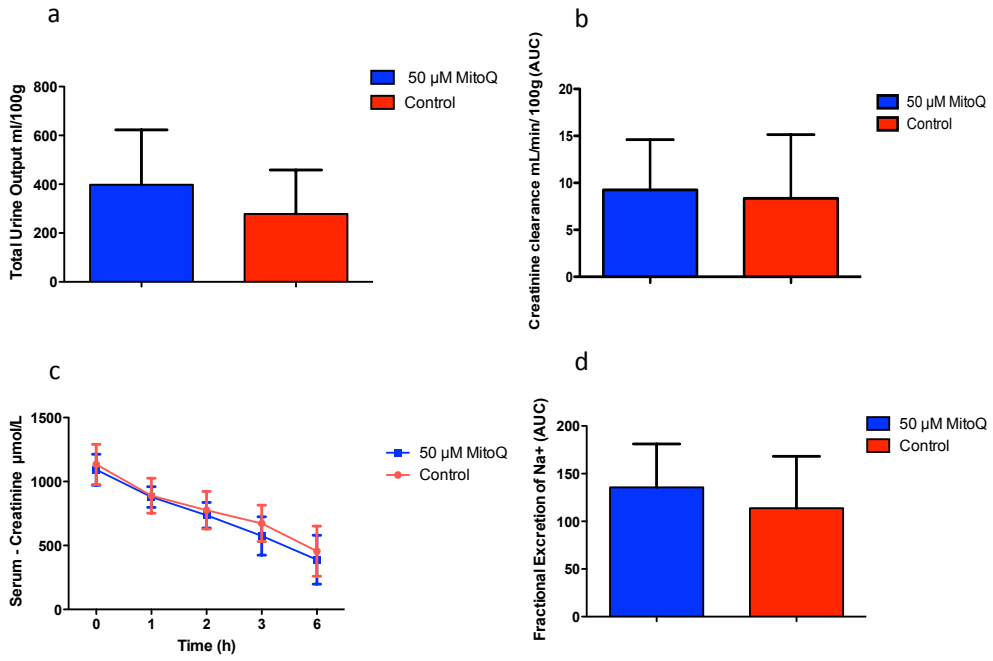

Figure 6.11. Renal function in deceased declined human kidneys during 6 h of EVNP. The kidneys were flushed and stored with or without 50 µM MitoQ (n = 4 per group) for 6 h using CSS. (a) The total urine output was numerically higher in the 50 µM MitoQ group compared to the control group but the difference did not reach statistical significance during 6 h of EVNP (398 ± 225 vs. 278 ± 180 mL/100 g; p = 0.241; paired t tests.). There were no significant differences between the two groups (MitoQ vs. control) at the end of 6 h EVNP in (b) creatinine clearance (9.3 ± 5.4 vs. 8.4 ± 6.8 mL/min/100 gram AUC; p = 0.767; paired t test), (c) percentage of serum creatinine fall (63.5 ± 19.1 vs. 57.6 ± 22.5; p = 0.557; paired t test) or (d) fractional excretion of sodium (135 ± 64 vs. 114 ± 54 AUC; p = 0.302; paired t test). Data are mean ± SD.

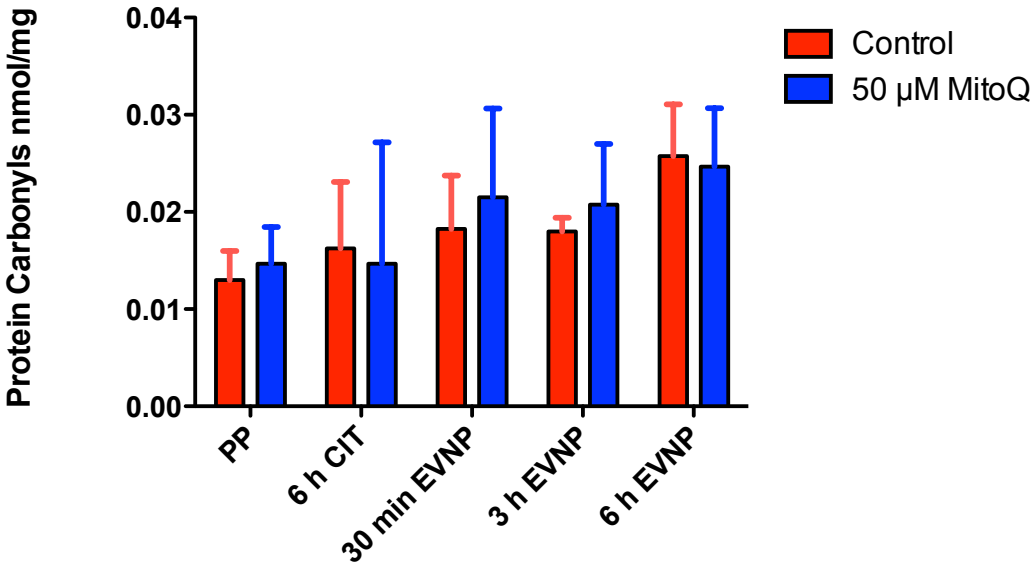

Figure 6.12. Protein carbonyl formation in deceased declined human kidneys during 6 h of EVNP. The kidneys were flushed and stored with or without 50 µM MitoQ (n = 4 per group) for 6 h using CSS. Biopsy samples were taken immediately post-perfusion on the back table (PP), at 6 h CSS, and at 30 min, 3 h and 6 h after the start of EVNP. There was no significant difference in protein carbonyl content in both groups at the end of 6 h EVNP (0.025 ± 0.006 vs. 0.026 ± 0.005 nmol/mg; p = 0.624; paired t-test). Data are mean ± SD.

6.5 Effect of 100 µM MitoQ on kidney function and damage on EVNP

To assess the effect of 100 µM of MitoQ, 3 pairs of declined deceased human kidneys were flushed with Soltran® ± 100 µM MitoQ and then subjected to 6 h CIT and the effect of MitoQ on kidney function and series of damage markers was assessed over 6 h of EVNP.

The renal blood flow remained relatively stable in the MitoQ group compared to the control group during 6 h of EVNP. The renal blood flow was numerically higher in the MitoQ group compared to the control group at the end of the first hour of EVNP but the difference did not reach statistical significance. Of note, the renal blood flow in the control group improved afterward and became numerically higher compared to the MitoQ group at the end of 6 h of EVNP but the difference did not reach statistical significance (Figure 6.13a). However, there was no significant difference in renal blood flow between the two groups (MitoQ vs. Control) during 6 h of EVNP (Figure 6.13b).

The total urine output was higher in the 100 µM MitoQ kidney compared to the control kidney at the end of 6 h EVNP but the difference did not reach statistical significance (Figure 6.14a). However, the level of creatinine clearance and percentage of serum creatinine fall were similar in the MitoQ kidney and the control kidney during 6 h of EVNP (Figure 6.14b, Figure 6.14c). Of note, the fractional excretion of sodium was numerically higher in the 100 µM MitoQ kidney compared to the control kidney at the end of 6 h EVNP but the difference did not reach statistical significance (Figure 6.14d). There was no significant difference between the MitoQ group and the control group at the end of 6 h of EVNP in protein carbonyl formation (Figure 6.15).

Variable	1st pair	2nd pair	3rd pair
Donor age (years)	67	75	76
Donor type	DBD	DBD	DCD
Reason for decline	Malignancy (renal)	Malignancy (extra renal; lung)	Poor biopsy score (6)
Cold ischaemic time (hours)*	19	21	24

* The (CIT) before placing the kidney on the EVNP circuit.

Table 6.4. Donor demographics of the 3 pairs of the declined deceased human kidneys used to assess the efficacy of 100 µM of MitoQ to ameliorate renal IRI during 6 h of EVNP.

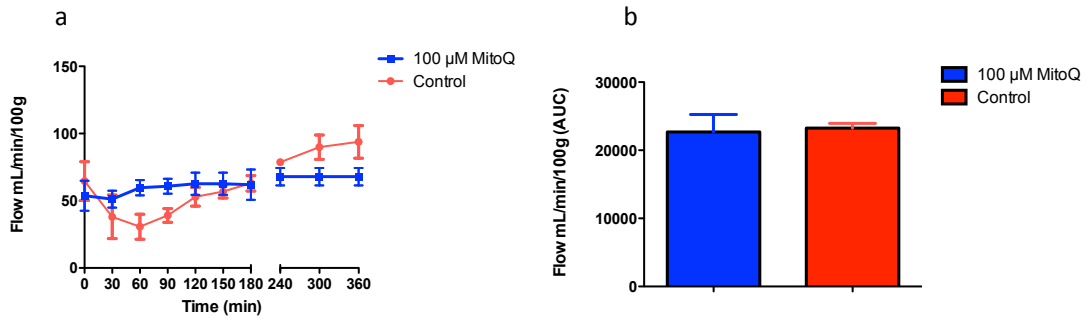

Figure 6.13. Renal blood flow in deceased declined human kidneys during 6 h of EVNP. The kidneys were flushed and stored with or without 100 µM MitoQ (n = 3 per group) for 6 h using CSS. (a) The renal blood flow was numerically higher in the 100 µM MitoQ group compared to the control group at the end of the first hour of EVNP but the difference did not reach statistical significance (67.9 ± 6.5 vs. 30.7 ± 9.3 mL/min/100 g; Bonferroni adjusted p = 0.770; paired t-test). Thereafter, the renal blood flow improved in the control group and became numerically higher at the end of 6 h of EVNP compared to the MitoQ group but the difference did not reach statistical significance (93.8 ± 12.2 vs. 67.9 ± 6.5 mL/min/100 g; Bonferroni adjusted p = 0.790; paired t-test). (b) There was no significant difference between the MitoQ group and the control group during 6 h of EVNP (AUC p = 0.665; paired t-test). Data are mean ± SD.

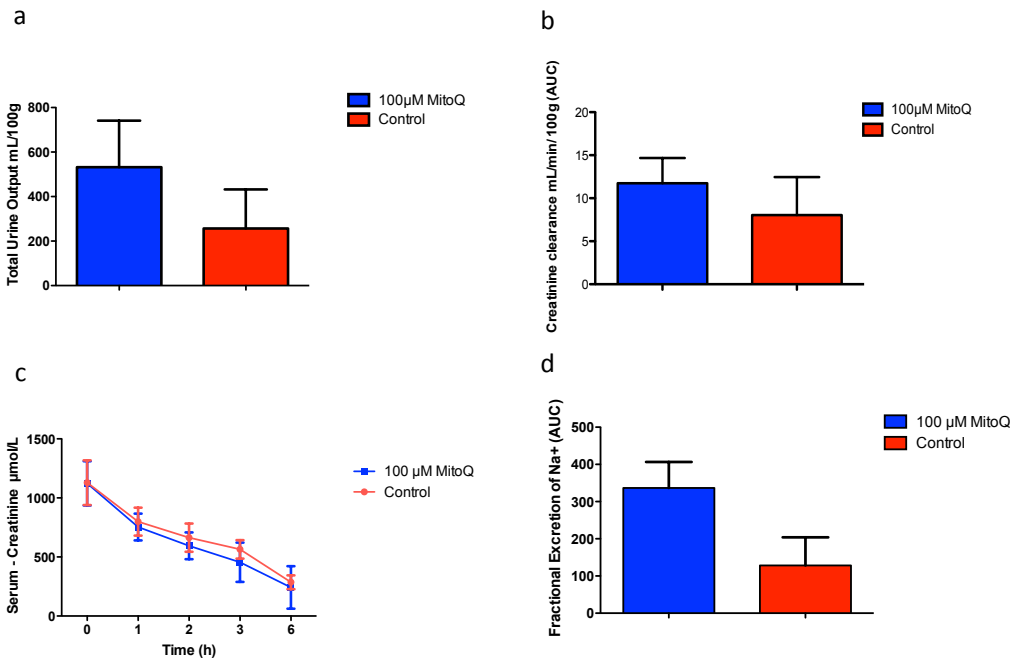

Figure 6.14. Renal function in deceased declined human kidneys during 6 h of EVNP. The kidneys were flushed and stored with or without 100 µM MitoQ (n = 3 per group) for 6 h using CSS. (a) The total urine output was numerically higher in the 100 µM MitoQ group compared to the control group but the difference did not reach statistical significance during 6 h of EVNP (532 ± 209 vs. 257 ± 176 mL/100 g; p = 0.063; paired t-test). There were no significant differences between the two groups (MitoQ vs. control) at the end of 6 h EVNP in (b) creatinine clearance (11.7 ± 2.9 vs. 8.0 ± 4.4 mL/min/100 gram AUC; p = 0.141; paired t-test), (c) or percentage of serum creatinine fall (77.4 ± 17.8 vs. 73.9 ± 8.5; p = 0.788; paired t-test). (d) Fractional excretion of sodium was numerically higher in the MitoQ group compared to the control group but the difference did not reach statistical significance (337 ± 70 vs. 128 ± 76 AUC; p = 0.119; paired t-test). Data are mean ± SD.

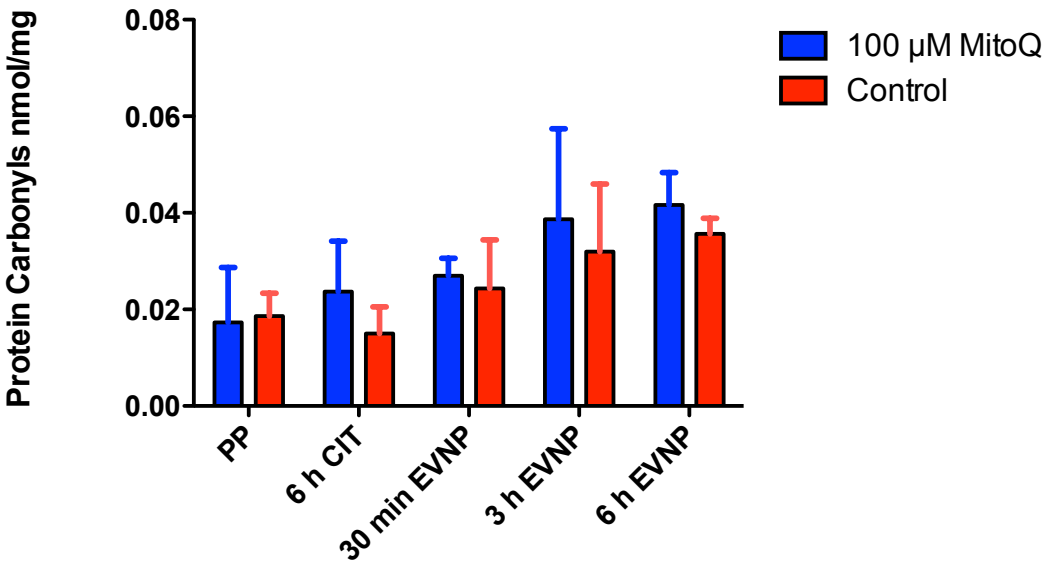

Figure 6.15. Protein carbonyl formation in declined deceased human kidneys during 6 h of EVNP. The kidneys were flushed and stored with or without 100 µM MitoQ (n = 3 per group) for 6 h using CSS. Biopsy samples were taken immediately post-perfusion on the back table (PP), at 6 h CSS, and at 30 min, 3 h and 6 h after the start of EVNP. There was no significant difference in protein carbonyl content in both groups at the end of 6 h of EVNP (0.042 ± 0.007 vs. 0.036 ± 0.003 nmol/mg; p = 0.375; paired t-test). Data are mean ± SD.

6.6 Discussion

In this chapter I was able to successfully:

1. Demonstrate that MitoQ is taken up efficiently by cold declined deceased human kidneys
2. Characterise MitoQ uptake and tissue concentrations during 6 h CSS and 6 h of EVNP at 5 μM, 50 μM and 100 μM doses
3. Characterise the therapeutic window of MitoQ and efficacy of 50 μM MitoQ in ameliorating renal IRI

In this chapter, I was able to demonstrate that MitoQ can be taken up efficiently by the cold declined deceased human kidneys after a variable period of CSS preservation. MitoQ uptake by the declined deceased human kidneys was dose-dependent, and most of the uptake happened rapidly upon perfusion then remained relatively stable upon CSS preservation for up to 6 h. The stability of MitoQ tissue concentrations during CSS preservation is of significant clinical importance, as in clinical practice the kidneys are exposed to variable period of CIT due to several factors (e.g. the distance between the donor and the recipient hospital, availability of operating theatre). Maintaining stable, safe and effective MitoQ tissue concentrations will greatly facilitate the administration of MitoQ to the cold human kidneys as a single dose during cold preservation prior to transplantation.

Of note, the trend of MitoQ tissue concentrations during 6 h of EVNP in the declined deceased human kidneys was similar to the controlled DCD pig kidneys. MitoQ tissue concentrations also remained relatively stable during 6 h of EVNP in the 5 μM, 50 μM and 100 μM MitoQ groups.

Total urine output, creatinine clearance and percentage fall of serum creatinine were numerically higher in the 50 μM MitoQ group compared to the control group, although the differences did not reach statistical significance during 3 h of EVNP. The effect of MitoQ on renal function (urine output, creatinine clearance and percentage of creatinine fall) was more prominent in the 7 pairs of declined deceased human kidneys placed on the EVNP circuit for 3 h compared to the results of the 4 pairs of declined deceased human kidneys placed on the EVNP circuit for 6 h, raising the possibility of a type II statistical error (i.e. a false negative). However, more data is required before this can be concluded. MitoQ had no effect on fractional excretion of sodium or protein carbonyls formation during 3 h or 6 h of EVNP similar to the controlled DCD pig model results presented in chapter 5.

Of note, there was a significant difference in the renal blood flow between the 50 μM MitoQ group and the control group at the end of the first hour of EVNP. The renal blood flow remained relatively stable during the first hour of EVNP in the 50 μM MitoQ group compared to a significant decrease in renal blood flow in the control group. This suggests that MitoQ may have a protective role in stabilising the renal blood flow during the initial period of IRI and ameliorating vascular endothelium dysfunction.

However, the renal blood flow improved in the control kidneys and there were no significant difference between the two groups (MitoQ vs. control) at the end of 3 h or 6 h of EVNP.

Total urine output was numerically higher in the 100 µM MitoQ group compared to the control group, although the difference did not reach statistical significance during 6 h of EVNP. The renal blood flow was numerically lower in the 100 µM MitoQ kidney compared to the control kidney at the end of 6 h EVNP but the difference did not reach statistical significance. In addition, the level of creatinine clearance and percentage of serum creatinine fall were similar in the MitoQ kidney and the control kidney during 6 h of EVNP. Of note, the fractional excretion of sodium was numerically higher in the 100 µM MitoQ kidney compared to the control kidney at the end of 6 h EVNP but the difference did not reach statistical significance. Taken together these results suggested that treating kidneys with 100 µM MitoQ during cold preservation may have reached or surpassed the upper limit of the MitoQ therapeutic window.

In chapter 3, I demonstrated that the uptake of MitoQ by the cold kidneys was less than the uptake of MitoQ by warm kidneys at the start of the cold preservation using the controlled DCD pig kidneys model. However, the uptake of MitoQ in the 5 µM, 50 µM and 100 µM MitoQ groups in the cold declined deceased human kidneys were comparable to the corresponding groups in the warm controlled DCD pig kidneys, with a mean tissue concentration of (19.3 ± 12.1 vs. 22.6 ± 9.2 pmol/mg), (224.4 ± 126.4 vs. 166.8 ± 84.4 pmol/mg) and (315.7 ± 199.3 vs. 461.3 ± 195.5 pmol/mg) at 6 h CSS samples for the 5, 50 and 100 µM doses, respectively. In addition, 100 µM MitoQ was shown to be safe and effective in ameliorating renal IRI using the controlled DCD pig model unlike the adverse effect observed using the same dose in declined deceased human kidneys. As outlined in chapter 1, MitoQ uptake is driven by the mitochondrial membrane potential, which may vary between the conditions used for the pig and human experiments. These differences may contribute to the differences in MitoQ uptake, efficacy and toxicity level observed in the declined deceased human kidneys compared to the controlled DCD pig kidneys.

In this chapter I was able to successfully characterise the uptake of MitoQ into the declined deceased human kidney tissue. While more declined deceased human kidneys need to be analysed to fully explore the potential efficacy of MitoQ in ameliorating renal IRI, this study provides important data that will help inform future studies and ultimately a clinical trial for assessing the efficacy of the mitochondria-targeted antioxidant MitoQ in human kidney transplantation. MitoQ has the potential to increase the use of marginal kidneys and to improve graft and patient outcomes.

Chapter 7

Discussion and future directions

7.1 General discussion

The relative shortage of optimal donors over the last 10 years and long waiting lists have necessitated the increased use of kidneys from sub-optimal donors, such as DCD donors. The use of kidneys from DCD donors has been shown to be associated with worse short-term graft outcomes (6, 7). The additional and inevitable period of warm ischaemia in DCD kidneys significantly increases the IRI and may partially explain the inferior short-term outcomes in DCD kidneys compared to DBD kidneys (7). In addition, the initial IRI may trigger an early antigen-independent inflammatory response which may amplify the subsequent adaptive immune response and potentially lead to chronic rejection. Therefore, preventing IRI could improve both the short- and long-term outcomes of transplanted organs and also allow the use of more marginal organs. However, there are currently no established treatments to ameliorate IRI and DGF. Mitochondria play a central role in the pathogenesis of IRI through the production of reactive oxygen species (ROS) (9). ROS production contributes to mitochondrial damage in organ transplantation and a range of other pathologies. Mitochondria are therefore promising therapeutic targets for ameliorating IRI and a number of mitochondria-targeted antioxidants have been developed by our laboratory at the MRC Mitochondrial Biology Unit. MitoQ is currently the best–characterised mitochondria-targeted antioxidant (10).

The overall aim of my thesis was to help translate the use of mitochondria-targeted antioxidants such as MitoQ from bench to bedside. In this context, it is important to determine whether they are safe and effective in large animal models, and in human organs. To assess the safety and efficacy of MitoQ in preserving organ function prior to full transplantation, I decided to use the *ex vivo* normothermic perfusion (EVNP) circuit. EVNP has been established as a valid model for investigating IRI (34, 51). The organ is subjected to several hours of reperfusion on EVNP under conditions that mimic transplantation and during which organ function and damage can be measured. To assess the efficacy of MitoQ in protecting pig and human kidneys during storage, the first step was to determine how effectively I could load the organs with MitoQ during cold storage. In chapter 5 and 6, I demonstrated that MitoQ is taken up efficiently by pig and human kidneys. MitoQ uptake occurs primarily during the initial flushing and is then stable, greatly facilitating the administration of MitoQ to the organ in a clinical situation prior to storage as a single dose that is then stable. I subsequently showed that pre-treating pig kidneys during cold storage was protective against some functional deficits, but not all and may have efficacy in ameliorating the detrimental effects of renal IRI. Therefore, I next examined if this protection could be extended to human kidneys. Total urine output, creatinine clearance and percentage fall of serum creatinine were numerically higher in the 50 μM MitoQ group compared to the control group, although the differences did not reach statistical significance during 3 h of EVNP. This might be due to type II statistical error (i.e. a false negative). However, more declined deceased human kidneys need to be analysed before this can be concluded.

I also characterised the therapeutic window of MitoQ, although further investigations to characterise and evaluate the full potential efficacy of MitoQ in ameliorating renal IRI are required, and this is discussed in the next section.

These findings provide important data that will help inform future studies and ultimately a clinical trial for assessing the efficacy of the mitochondria-targeted antioxidant MitoQ in human kidney transplantation. MitoQ has the potential to increase the use of marginal kidneys and to improve graft and patient outcomes.

7.2 Uptake of MitoQ

As outlined in chapter 3, there was significant uptake of MitoQ into the pig kidney parenchymal tissue when measured immediately after flushing. This level of uptake was relatively stable and did not alter markedly upon preservation for up to 24 h in CSS. Subsequent experiments showed that incubation of kidneys in cold Soltran® supplemented with MitoQ did not lead to additional MitoQ uptake into the kidney, thus the addition of MitoQ to the storage solution is not necessary. In addition, cold pig kidneys were able to take up MitoQ successfully after 12 h CSS. However, the uptake of MitoQ by cold pig kidneys was half that by warm pig kidneys. This suggests mitochondria are able to maintain a sufficient membrane potential during cold preservation to drive the uptake of MitoQ at 4 °C. In support of this, a significant uptake of MitoQ at 4 °C was demonstrated using isolated rat mitochondria, albeit less than at 37 °C (50). This is of a particular importance in clinical practice, where the MitoQ can be administered efficiently after a period of cold preservation prior to the onset of reperfusion. However, the therapeutic dose of MitoQ may need to be adjusted according to the temperature of the organ at the time of MitoQ delivery.

In clinical practice, kidneys are exposed to a variable period of CIT, and the MitoQ tissue concentrations should remain within the safe therapeutic window during that period. The trend of MitoQ uptake was similar in the cold declined deceased human kidneys. The majority of the MitoQ uptake by the declined deceased human kidneys happened rapidly upon perfusion, and remained relatively stable upon CSS preservation for up to 6 h. Of note, the trend of MitoQ tissue concentrations during 6 h of EVNP in the declined deceased human kidneys was similar to the controlled DCD pig kidneys. Either MitoQ does not leave the tissue during the limited duration of EVNP (6 h), or MitoQ leaves the tissue, but because the EVNP is a closed circuit, it recirculates in the perfusate and is taken up again by the tissue. In this context, I have collected EVNP perfusate samples for future analysis of MitoQ concentrations in the EVNP perfusate.

As discussed in chapter 5, the half-life of MitoQ in the mouse kidney in vivo was around 4 h after a bolus i.v. injection. The MitoQ was rapidly cleared from the blood and accumulated selectively by the mitochondria within 5 min of i.v. injection. Thereafter, the MitoQ was slowly re-equilibrated back to the blood and subsequently excreted in the urine and bile. The degree of MitoQ equilibration back to the

blood is determined by the mitochondrial content and the magnitude of the mitochondrial and plasma membrane potentials. Thus, it is difficult to anticipate the half-life of MitoQ in human kidneys after transplantation, as mitochondria content and potential may vary between species and with the condition of the organ. In support of this hypothesis, I have shown the uptake of MitoQ by the cold kidneys was less than the uptake of warm kidneys using the controlled pig model. Therefore I anticipated that the uptake of MitoQ by the cold declined human kidneys would be less than the uptake by warm pig kidneys. However, the uptake of MitoQ in the cold declined deceased human kidneys was comparable to the uptake in the warm controlled DCD pig kidneys.

The above data indicate that uptake of MitoQ occurs primarily during the initial flushing of the organ and is then stable, greatly facilitating the administration of MitoQ to the organ prior to CSS. This stable, single dose remained within the range known to be safe and protective in other situations of IRI.
As there are two methods of cold preservation of kidneys in clinical practice; cold static storage (CSS) and hypothermic machine perfusion (HMP), I also assessed the uptake of MitoQ into the pig tissue using an HMP device. This showed that there was initial uptake of MitoQ upon flushing and that over time the levels of MitoQ increased. This is presumably due to uptake from the continuous circulation of the preservation solution in the HMP device, or perhaps due to the ability of the HMP to overcome the vascular spasm and open up new capillary networks, which are occluded during CSS; or a combination of both.

The uptake of MitoQ into the human kidneys has not been compared between the two methods of organ preservation (HMP vs. CSS). Significant and ongoing uptake of MitoQ into the human kidneys during HMP may result in higher tissue concentrations at the onset of reperfusion, which makes it difficult to maintain consistent, safe, and effective tissue concentrations during cold preservation. This can be overcome by limiting the delivery of MitoQ to the initial flushing of the kidney, before placing the kidney on the HMP device (that is, not in the HMP storage solution) or by delivering the MitoQ to the kidney once it is removed from the HMP device prior to reperfusion. However, MitoQ uptake in the controlled DCD pig model was completed after the first 6 h post perfusion and remained static thereafter using the HMP device. In addition, HMP increased MitoQ uptake by only 2-fold compared to CSS. Taken this together suggests MitoQ is most likely to remain within the therapeutic window using HMP during cold storage.

In conclusion, the data presented in this section indicates:

1. MitoQ is taken up efficiently by warm and cold kidneys
2. MitoQ uptake by warm kidneys (early delivery of MitoQ) is 2-fold higher than the uptake by cold kidneys (late delivery of MitoQ)
3. HMP increases MitoQ uptake by 2-fold compared to CSS in the controlled DCD pig model
4. Most of the MitoQ uptake occurs rapidly upon flushing the organ with MitoQ

5. MitoQ tissue concentrations are stable over time (certainly beyond 6 h using HMP)

Taken together, the above controlled DCD pig model data suggests the largest range in MitoQ tissue concentrations is likely to be about 4-fold: lowest in cold kidneys preserved in CSS and highest in warm kidneys preserved in HMP device. In this context, further experiments are required to test this hypothesis in human kidneys and to confirm that this range of tissue concentration is safe.

7.3 Therapeutic window and efficacy of MitoQ

As outlined in chapter 5, I was able to successfully characterise the MitoQ therapeutic window and assess MitoQ efficacy in ameliorating renal IRI using the controlled DCD pig model. MitoQ concentrations of 500 nM or 5 µM had no effect on renal blood flow, renal function or protein carbonyl formation. However, the renal blood flow showed a significant increase in the 50 µM of MitoQ group. In addition, total urine output increased significantly in the 50 µM MitoQ group compared to the control group. Creatinine clearance was numerically higher in the 50 µM MitoQ group but the difference did not reach statistical significance. Of note, there was no effect on fractional excretion of sodium or oxidative damage markers (protein carbonyl formation and isoprostanes). The simple TPP compound TPMP had no effect on renal blood flow, total urine output, fractional excretion of sodium or creatinine clearance, suggesting the MitoQ antioxidant moiety (ubiquinone) was responsible for protection and not the TPP targeting cation.

The use of 250 µM MitoQ in my controlled DCD pig model demonstrated a toxic effect, with the MitoQ kidney developing large areas of necrosis. As discussed in chapter 5, MitoQ is largely adsorbed to the mitochondrial inner membrane and the linker chain (10-carbon alkyl) enables the active antioxidant component (ubiquinol) to penetrate into the membrane core. The accumulation of high concentrations of MitoQ within the inner mitochondria membrane is likely to interfere with the membrane structure and the ability to carry out oxidative phosphorylation and ATP synthesis. This might lead to the induction of the mitochondrial permeability transition pore (MPTP) and cell death (necrosis/apoptosis). Further investigations are required to:

1. Examine the mechanism of apparent nephrotoxicity by high concentrations of MitoQ
2. Explore whether the TPP compound or the antioxidant moiety was responsible for the toxicity observed using 250 µM of MitoQ

The above data indicates that MitoQ was protective against some functional deficits, but not all in pig kidneys. This led me to investigate whether this protection could be extended to the declined deceased human kidneys. In clinical practice, 11% of the retrieved kidneys from deceased donors are subsequently declined for transplantation (3). The majority of declined kidneys are turned down due to poor perfusion, significant donor vascular disease, malignancy or poor pre-implantation kidney score.

The main reason for declining those kidneys by surgeons is based on the concerns about the impact of those unfavourable characteristics on long-term outcomes (91). Although those kidneys were declined for transplantation, they were suitable to investigate the MitoQ safety and efficacy on the EVNP circuit during the relative short duration of reperfusion (6 h). In addition, there is evidence that some kidneys may be discarded unnecessarily (92). In support, a previous study demonstrated that the majority of the kidneys declined due to poor perfusion are suitable for transplantation (57). In addition, our group has reported recently the successful transplantation of a pair of human kidneys declined due to poor perfusion and subsequently transplanted after perfusion and assessment using EVNP, both kidneys had initial graft function and good kidney function 3 months post transplantation (58).
The quality of human kidneys from deceased donors that were declined for transplantation are expected to be far more variable than pig kidneys, as those kidneys were declined for different reasons, with additional differences in donor characteristics, length and types of ischaemia. To overcome this variability, I have decided to assess MitoQ efficacy using pairs of declined human kidneys. This enabled one kidney to act as a control while the other kidney from the same donor was treated with MitoQ and both kidneys were assessed in parallel on two EVNP circuits.

Addition of 5 μM of MitoQ to the flush and the preservation solution had no effect on renal blood flow, renal function, or protein carbonyl formation. Total urine output, creatinine clearance and percentage fall of serum creatinine were numerically higher in the 50 μM MitoQ group compared to the control group, although the differences did not reach statistical significance during 3 h of EVNP. Despite the use of pairs of declined human kidneys, the results of declined deceased human kidneys were more variable than the controlled DCD pig kidneys. In support of this, the MitoQ protective effect on renal function was more significant in the 7 pairs of declined deceased human kidneys placed on the EVNP circuit for 3 h compared to the results of the 4 pairs of declined deceased human kidneys placed on the EVNP circuit for 6 h, raising the possibility of a type II statistical error (i.e. a false negative). Of note, MitoQ had no effect on fractional excretion of sodium or protein carbonyl formation during 3 h or 6 h of EVNP similar to the controlled DCD pig model results.

Administration of 100 μM of MitoQ during CSS preservation had an unexpected adverse effect on renal blood flow and fractional excretion of sodium unlike the protective effect observed in the controlled DCD pig model. In addition, 100 μM of MitoQ had no effect on urine production, creatinine clearance or protein carbonyl formation in the declined deceased human kidneys. Differences in mitochondria membrane potential, mitochondrial content, oxidative phosphorylation and mitochondrial ROS production between species may result in different uptake and therapeutic windows of MitoQ. In vivo experiments demonstrated that MitoQ can be delivered safely intravenously in mice (~ 20 mg MitoQ/kg), with toxicity only observed at ~ 27 mg MitoQ/kg (41). MitoQ was effective in ameliorating renal IRI in a mouse model at a dose of 4.4 mg MitoQ/kg (40). Together these data suggests that MitoQ has a wider therapeutic window in mouse kidneys compared to pig and human kidneys. However, the

limitation here is we are comparing in vivo efficacy and toxicity in mouse kidneys with ex vivo efficacy and toxicity in isolated organs (pig and human kidneys). To address this limitation, further experiments are required to assess MitoQ efficacy and toxicity in pig and human kidneys in vivo (pig transplants in the first instance). In addition, MitoQ concentrations in the controlled DCD pig kidney and the cold declined deceased human kidney tissues post-perfusion with 5 µM of MitoQ were at the range known to be safe and protective to ameliorate renal IRI. The absence of a protective effect in the 5 µM of MitoQ group during 6 h of EVNP in the controlled DCD pig model and the declined deceased human kidneys does not rule out a protective role that can be demonstrated at a later time point or in vivo. Of note, only one out of the 4 pairs of declined deceased human kidneys used to assess the efficacy of 5 µM MitoQ to ameliorate renal IRI during 6 h of EVNP was from a DBD donor. There may be a difference in MitoQ effect between DCD and DBD kidneys that was not demonstrated due to the limited sample size. In this context, further experiments are required to:

1. Investigate the therapeutic efficacy of MitoQ to ameliorate renal IRI using lower concentrations of MitoQ such as 5 µM in a pig transplantation model
2. Confirm the therapeutic effect of 50 µM of MitoQ using larger number of declined deceased human kidneys
3. Confirm or rule out the suspected drug toxicity observed in the kidneys treated with 100 µM of MitoQ in the declined deceased human kidneys
4. Investigate the therapeutic efficacy of MitoQ between different donors types (DCD vs. DBD).

The ability to demonstrate a therapeutic efficacy of MitoQ at low concentrations will eliminate the potential toxicity risks associated with a narrow therapeutic window. On the other hand, if the therapeutic window is indeed narrow in the deceased declined human kidneys, further investigations are required, for example to examine the impact of different ischaemia times, time point of administration and storage conditions in order to ensure maintenance of consistent, safe and effective MitoQ tissue concentrations during cold preservation. This might be difficult taking into consideration the hypothesized large range of MitoQ tissue concentration (4-fold; lowest in cold kidneys preserved in CSS, highest in warm kidneys preserved in HMP device). This can be overcome by limiting the delivery of MitoQ to the end of cold preservation prior to reperfusion, which may allow for lower and more controlled MitoQ tissue concentrations to be achieved.

The MitoQ dose-response information presented in this section is of clinical importance and will help us to decide on the appropriate starting dose, dose-titration steps, and maximum recommended dose in a future clinical trial.

7.4 Experimental end points

To assess the effect of MitoQ on function and damage to pig and declined deceased human kidneys, pairs of kidneys were placed on the EVNP circuit and a series of renal function, injury and oxidative damage markers were assessed over time. Experimental end points included assays of:

- Renal function: urine output, serum creatinine and creatinine clearance
- Renal injury markers: fractional excretion of sodium
- Perfusion parameters: renal blood flow (RBF)
- Oxidative damage markers: protein carbonyl and lipid peroxidation (isoprostane)

The experimental endpoints for measuring renal injury and oxidative damage require further validation.

7.4.1 Renal injury markers

Fractional excretion of sodium was a sensitive marker of renal injury when the relative impact of WIT and CIT were assessed using the DCD controlled pig model. However, MitoQ had no beneficial impact on the fractional excretion of sodium in the pig and deceased declined human kidneys models.

Fractional excretion of sodium represents the percentage of sodium filtered by the kidney that is excreted in the urine. The majority of sodium (65%) is reabsorbed in the proximal tubule by passive transport from lumen into tubular cells. In contrast, creatinine is freely filtered by glomeruli and only 15% of excreted urine creatinine is derived from proximal tubular secretion. All segments of the nephron (glomeruli, proximal convoluted tubule, loop of Henle and distal convoluted tubule) can be affected during ischaemia. However, the proximal tubular cells are more susceptible to ischaemic insult (93, 94). This can be partially explained by the fact that proximal tubule has relatively little or no glycolytic capacity under ischaemic conditions. This leads to rapid depletion of intracellular ATP in the proximal tubule following the onset of ischaemia resulting in structural changes and impaired sodium reabsorption. In addition, depletion of ATP also results in cell death by apoptosis or necrosis predominantly in the region of the proximal tubules (94). The proximal tubule has also a complex vascular supply and there is a marked microvascular hypoperfusion and congestion in this region following reperfusion, leading to ongoing local ischaemia even when cortical blood flow is restored (95). The increased susceptibility of the proximal tubule to ischaemia, on-going hypoxia and reduced renal flow during reperfusion subsequently extend the initial IRI tubular injury. This may explain the absence of a protective effect of MitoQ on fractional excretion of sodium during the limited duration of EVNP (6 h). In support of this possibility, erythropoietin (EPO) has been shown to have an anti-apoptotic action and a protective effect on proximal renal tubular epithelial cells in a rat model of renal IRI (96). However, EPO has not shown any protective effect on fractional excretion of sodium during the limited duration of EVNP (2 h) in a pig model of renal IRI (62). In contrast, nitric oxide and carbon monoxide

have both demonstrated a protective effect on fractional excretion of sodium during 3 h of EVNP in a pig model of renal IRI (97) . This can be explained by the vasodilatory effect of nitric oxide and carbon monoxide, which may prevent the local tubular ischaemia and ongoing-hypoxia during the initial phase of IRI.

Fractional excretion of sodium has been shown to be a sensitive marker for nephrotoxicity (98). In this context, the adverse effect of high concentrations of MitoQ on fractional excretion of sodium in the controlled DCD pig model and the declined deceased human kidneys suggests that such concentrations may have reached or surpassed the upper limit of the MitoQ therapeutic window. High concentrations of MitoQ may lead to necrosis and apoptosis of tubular cells through interfering with the structural integrity of the mitochondrial inner membrane and functions dependent on its integrity, due to it's tendency to adsorb onto and insert into the mitochondrial inner membrane.

Further experiments are required to explore the effect of MitoQ on other alternative markers of renal injury. Neutrophil gelatinase-associated lipocalin (NGAL) is an iron-transporting protein that rapidly accumulates in the kidney tubules and urine after nephrotoxic and ischaemic insults. Urinary NGAL has been established as an early, sensitive, non-invasive biomarker for acute kidney injury following transplantation (99, 100). In addition, urinary NGAL has been successfully used to determine the severity of acute kidney injury in a pig model of renal IRI (101). In my controlled DCD pig model and declined deceased human kidney model urine samples were collected hourly during EVNP to measure creatinine clearance and fractional excretion of sodium, 2 mL of each collected urine sample was snap-frozen in liquid nitrogen and stored at -80 °C for future analysis. In light of the fractional excretion of sodium results, future experiments are required to examine the effect of MitoQ on urinary NGAL during EVNP.

7.4.2 Oxidative damage markers

Protein carbonyl formation and lipid peroxidation have been established as oxidative injury biomarkers in IRI (64, 68). However, treating pig and deceased declined human kidneys with MitoQ during cold storage and prior to ischaemia did not result in a significant reduction of the protein carbonyl content or isoprostane formation in renal tissues during 6 h of EVNP, compared to the control group. This may be partially explained, as discussed earlier, by the relatively short duration of reperfusion on the EVNP circuit (6 h). This may reduce the likelihood of detecting a beneficial effect of MitoQ that may become apparent beyond the limited duration of EVNP. In support of this possibility, there were no significant differences in oxidative damage markers for samples taken 60 min post reperfusion using a small animal model of renal IRI (11). The differences in oxidative damage markers were only significant at 24 h post renal IRI (40). In addition, MitoQ demonstrated a significant protective effect on oxidative damage markers for samples taken 24 h post reperfusion using a small animal model of cardiac IRI (50). In this

model, the MitoQ effect on oxidative damage markers was not investigated at an earlier time point. However, there were no significant differences in mitochondria ROS levels between the grafts exposed to a short period of ischaemia (30 min CIT) and prolonged ischaemia (4 h CIT) at the early phases of reperfusion (0 – 2 h). The differences were only significant in ROS levels between the two groups (short ischaemia vs. prolonged ischaemia) after 24 h of reperfusion. In my controlled DCD pig model and deceased human kidneys model, oxidative damage markers increased (albeit not statistically significant) at the end of 6 h of EVNP compared to levels at the end of cold preservation. Taken together these data suggest mitochondria oxidative damage is a slow progressive process occurring over a long period following reperfusion and MitoQ may demonstrate a therapeutic effect at a later time point (e.g 24 h post reperfusion).

In this context, further investigations are required to:

1. Investigate the effect of MitoQ on other oxidative injury markers (e.g. mitochondrial DNA damage)
2. Further characterize renal injury and oxidative damage beyond 6 h of EVNP; ideally up to 7 days which would only be possible in a full transplant model

Mitochondrial DNA (mtDNA) damage has been established as a marker of IRI (40, 79). MitoQ significantly reduced oxidative injury to mtDNA in two small animal models of IRI. mtDNA damage is measured by quantifying the decrease in amplification of DNA extracted from kidney tissues, based on the principle that DNA damage blocks the progression of polymerase during PCR, resulting in a reduction of the amplification (102, 103).

Damage to mtDNA can be assessed using a quantitative PCR method. Some types of oxidative damage to DNA, such as strand breaks, apurinic (AP) sites, and some oxidised bases, can block the progression of the polymerase during PCR. For a given target sequence, any damage of this kind results in a reduction in amplification. By controlling the number of cycles in the PCR to ensure that the reaction remains within the linear phase, the amount of product at the end of the reaction is proportional to the starting template amount. This allows for comparison of DNA damage between different samples. In this context, the pig and human mtDNA primers and PCR condition parameters should be optimised first to provide a reproducible assay to measure mtDNA oxidative damage. This is currently being investigated by a PhD student in the MRC Mitochondrial Biology Unit (Anja Gruszczyk). To measure oxidative damage assays (protein carbonyl formation and lipid peroxidation) tissue samples were taken from pig and declined deceased human kidneys at different times depending on the model used, ~50 mg of each collected tissue sample was snap-frozen in liquid nitrogen and stored at -80 °C for future analysis of mtDNA oxidative damage.

7.4.3 Mitochondrial reactive oxygen species

As discussed in chapter 1, there are several potential sources of ROS during IRI (e.g. mitochondria, NOXs, xanthine oxidases). The exact role of mitochondrial ROS in renal IRI is not fully understood due in part to the difficulties in studying mitochondrial ROS in vivo. In this context, a novel mitochondria targeted ratiometric probe MitoB/MitoP has been developed by our laboratory at the MRC Mitochondrial Biology Unit (104). The conversion of MitoB to MitoP is formed by the reaction with mitochondrial hydrogen peroxide (H_2O_2) (and to some extent by peroxynitrite) and the concentrations in the tissues were determined by LC-MS/MS to indicate relative changes in the levels of H_2O_2.

The MitoB probe was successfully used in a small animal model of cardiac IRI (50). In this model, there was a significant increase in the MitoB/MitoP ratio in transplanted heart grafts in samples taken at the end of 24 h of reperfusion, compared with samples taken at 120 min reperfusion. In addition, increasing the CIT (from 30 min to 4 h CIT) in the transplanted heart grafts showed a significant rise in the MitoP/MitoB ratio at 24 h reperfusion, but not at 120 min reperfusion. Taken together these data suggest that mitochondrial ROS production is a continuous and slowly progressive process. In this context, it is unlikely that MitoQ could demonstrate a therapeutic effect on mitochondrial ROS production during the limited duration of EVNP. However, before this can be concluded further experiments are required to:

1. Optimise the dose, time point and mode of delivery of the MitoB probe
2. Characterise the relative impact of warm ischaemia and cold ischaemia on mitochondrial ROS production during EVNP
3. Characterise the relative impact of mitochondria ROS production on oxidative damage markers during EVNP at different time points
4. Check the impact of the MitoB probe on the therapeutic window of MitoQ
5. Investigate the effect of MitoQ on mitochondrial ROS production during EVNP

The mitochondrial MitoB probe may be beneficial to investigate the therapeutic efficacy of MitoQ and the impact on oxidative damage markers beyond the limited duration of EVNP in a full pig transplant model. However, the dose, time point and mode of delivery of MitoB will have to be optimised first.

7.4.4 Histopathology

There were no significant differences between the control group and the leukocyte-depleted group in the histopathology injury score for the pig kidney biopsies during the limited duration of EVNP (6 h). As discussed earlier, this is not surprising as the recovery from ATN may continue for several days or weeks. However, the histological assessment of kidneys biopsies may be beneficial to confirm or rule out the suspected drug toxicity observed in the kidneys treated with 100 µM MitoQ in the declined deceased

human kidneys group. In addition, it may help us to understand the nephrotoxic mechanism of MitoQ using renal biopsies from the kidneys treated with 250 µM MitoQ in the controlled DCD pig model. As showed in chapter 2, a wedge biopsy sample (~120 mg tissue wet weight) was taken from the pig kidneys at different times depending on the model used, but all within 24 h of retrieving the kidneys. About 20 mg of each collected biopsy was fixed, sectioned, stained with haematoxylin and eosin, and stored in the Department of Surgery for future analysis by a histopathologist.

In addition, the histological assessment of renal kidneys biopsies at a later time point (e.g. 7 days) in a full pig transplant model may be beneficial to investigate the therapeutic efficacy of MitoQ in ameliorating renal IRI.

7.5 Long-term effects of MitoQ

The EVNP circuit provided an ideal platform to examine the safety and the efficacy of MitoQ in ameliorating renal IRI. However, EVNP was limited by the relatively short duration of reperfusion. The use of 6 h of EVNP provided insufficient short-term information on functional and oxidative injury markers of renal IRI, and may miss any therapeutic efficacy of MitoQ that could happen beyond this early reperfusion phase. As discussed in chapter 5, it is technically difficult to extend the reperfusion period beyond 6 h in the EVNP circuit due to increased risk of blood haemolysis which may bias the experiments chemical results (higher estimation of potassium and creatinine). In addition, it is difficult to maintain measurable creatinine levels, as there is no external metabolic source of creatinine in the isolated perfusion circuit. Creatinine infusion at a constant rate may be a better alternative than spiking the EVNP circuit with a loading dose of creatinine. However, future experiments (outlined below) are required to explore the possibility of extending the current duration of EVNP beyond 6 h.

1. Characterise the rate and the concentration of the creatinine infusion
2. Assess the potential risk of blood haemolysis beyond 6 h of EVNP

In the controlled DCD pig model, kidneys were reperfused with autologous blood. However, declined deceased human kidneys were reperfused with ABO-compatible donated human packed red blood. Leukocytes play a key role in IRI through the activation of inflammatory systemic response which may lead to cellular injury and death (105). In addition, as discussed in chapter 1, leukocytes are able to produce ROS during reperfusion, however, the exact contribution of leukocytes to ROS production is not fully understood. The use of leukocyte-depleted blood has been shown to reduce IRI and improve kidney function in pig and human kidney models (33, 106). Therefore, *ex vivo* perfusion with leukocyte depleted blood has its limitations and provides no information on the role of MitoQ on systematic inflammation and injury produced by leucocytes upon reperfusion. In this context, further experiments are required using declined deceased human kidneys to:

1. Investigate the relative effect of leukocyte depleted blood during EVNP on kidney function and oxidative damage
2. Evaluate the role of MitoQ in ameliorating IRI using ABO-compatible donated human whole blood

In addition, pig kidneys on the EVNP were not exposed to systemic neuro-hormonal and immunological factors that influence the severity of renal IRI in clinical practice. A full renal transplantation pig model would overcome these limitations and enable the assessment of the long-term effects of MitoQ (ideally for 7 days or longer). However, this is a very costly and technically complex model. The collected urine and venous blood samples could be used to investigate:

1. Renal function (e.g. serum creatinine, creatinine clearance)
2. Renal injury markers (e.g. fractional excretion of sodium, NGAL)

Pigs can be killed at different time points (e.g. 24 h, 7 days) to assess for:

1. Oxidative damage markers (e.g. protein carbonyl formation, mtDNA damage, lipid peroxidation)
2. Mitochondrial ROS
3. Histology

To facilitate the establishment of a successful reproducible full renal transplantation pig model, further experiments are required to:

1. Characterise the best pig model (allotransplant vs. autotransplant)
2. Optimise the pre and post operative surgical care
3. Optimise kidney graft retrieval and implantation protocol

7.6 Translation into clinical practice

The main aim of this thesis was to investigate whether the promising therapeutic effects of MitoQ demonstrated in the small animal IRI models could be translated into clinical practice.
The translation of the promising therapeutic results of MitoQ from the mouse to the pig and subsequently to the human kidney models was challenging, demanding and time consuming. Improving my efficiency, organization and experimental design techniques (where each experiment answered a specific question) allowed me to successfully achieve my main goal within a relatively short period of time (3 years). In support of this assertion, to test the safety and the efficacy of MitoQ as a therapeutic candidate for amelioration of IRI in clinical transplantation I have used 150 pig kidneys and 80 declined deceased human kidneys. In addition, the collaboration between basic science researchers (MRC Mitochondrial Biology Unit) and academic surgeons (Addenbrooke's Hospital) was rewarding. This has allowed my scientific biomedical research to address important clinical questions and facilitate successful application into clinical practice.

The lesson learned from this thesis is that translational biomedical research projects will greatly benefit from a multidisciplinary approach and collaborations. This will allow the use of a wider range of resources and different areas of expertise. I am hoping that the work presented in my thesis will encourage researchers and future PhD students to consider a multidisciplinary approach for their future research to have a better chance of success. The work presented in my thesis will hopefully pave the way to initiate a randomised type II clinical trial to assess the efficacy of MitoQ in ameliorating renal IRI. Finally, the successful translation of MitoQ therapy into clinical practice has the potential to improve graft and patient survival post kidney transplantation. MitoQ has the potential to decrease the high risk of DGF and PNF associated with the use of declined marginal organs and thus, expand the pool of organs suitable for transplantation.

References

1. Thornton SR, Hamilton N, Evans D, Fleming T, Clarke E, Morgan J, et al. Outcome of kidney transplantation from elderly donors after cardiac death. Transplantation proceedings. 2011;43(10):3686-9.

2. Yildirim A. The importance of patient satisfaction and health-related quality of life after renal transplantation. Transplantation proceedings. 2006;38(9):2831-4.

3. NHS Blood and Transplant, Organ donation and activity report 2014–2015. [Internet]. [cited 2016 Aug 10]. Available from: http://www.odt.nhs.uk/uk-transplant-registry/annual-activity-report/

4. Mallon DH, Summers DM, Bradley JA, Pettigrew GJ. Defining delayed graft function after renal transplantation: simplest is best. Transplantation. 2013;96(10):885-9.

5. Groen H, Moers C, Smits JM, Treckmann J, Monbaliu D, Rahmel A, et al. Cost-effectiveness of hypothermic machine preservation versus static cold storage in renal transplantation. Am J Transplant. 2012;12(7):1824-30.

6. Hamed MO, Chen Y, Pasea L, Watson CJ, Torpey N, Bradley JA, et al. Early graft loss after kidney transplantation: risk factors and consequences. American journal of transplantation : official journal of the American Society of Transplantation and the American Society of Transplant Surgeons. 2015;15(6):1632-43.

7. Summers DM, Johnson RJ, Allen J, Fuggle SV, Collett D, Watson CJ, et al. Analysis of factors that affect outcome after transplantation of kidneys donated after cardiac death in the UK: a cohort study. Lancet. 2010;376(9749):1303-11.

8. Port FK, Bragg-Gresham JL, Metzger RA, Dykstra DM, Gillespie BW, Young EW, et al. Donor characteristics associated with reduced graft survival: an approach to expanding the pool of kidney donors. Transplantation. 2002;74(9):1281-6.

9. Honda HM, Korge P, Weiss JN. Mitochondria and ischemia/reperfusion injury. Annals of the New York Academy of Sciences. 2005;1047:248-58.

10. Smith RA, Murphy MP. Animal and human studies with the mitochondria-targeted antioxidant MitoQ. Annals of the New York Academy of Sciences. 2010;1201:96-103.

11. Matas AJ, Payne WD, Sutherland DE, Humar A, Gruessner RW, Kandaswamy R, et al. 2,500 living donor kidney transplants: a single-center experience. Annals of surgery. 2001;234(2):149-64.

12. O'Brien MD. Criteria for diagnosing brain stem death. BMJ (Clinical research ed). 1990;301(6743):108-9.

13. Barklin A. Systemic inflammation in the brain-dead organ donor. Acta anaesthesiologica Scandinavica. 2009;53(4):425-35.

14. Bos EM, Leuvenink HGD, van Goor H, Ploeg RJ. Kidney grafts from brain dead donors: Inferior quality or opportunity for improvement? Kidney Int. 2007;72(7):797-805.

15. Reid AW, Harper S, Jackson CH, Wells AC, Summers DM, Gjorgjimajkoska O, et al. Expansion of the kidney donor pool by using cardiac death donors with prolonged time to cardiorespiratory arrest. American journal of transplantation : official journal of the American Society of Transplantation and the American Society of Transplant Surgeons. 2011;11(5):995-1005.
16. Jani A, Zimmerman M, Martin J, Lu L, Turkmen K, Ravichandran K, et al. Perfusion storage reduces apoptosis in a porcine kidney model of donation after cardiac death. Transplantation. 2011;91(2):169-75.
17. Deng R, Gu G, Wang D, Tai Q, Wu L, Ju W, et al. Machine perfusion versus cold storage of kidneys derived from donation after cardiac death: a meta-analysis. PloS one. 2013;8(3):e56368.
18. Eltzschig HK, Eckle T. Ischemia and reperfusion[mdash]from mechanism to translation. Nat Med. 2011;17(11):1391-401.
19. Azuma H, Nadeau K, Takada M, Mackenzie HS, Tilney NL. Cellular and molecular predictors of chronic renal dysfunction after initial ischemia/reperfusion injury of a single kidney. Transplantation. 1997;64(2):190-7.
20. Friedman JR, Nunnari J. Mitochondrial form and function. Nature. 2014;505(7483):335-43.
21. Devarajan P. Cellular and molecular derangements in acute tubular necrosis. Current opinion in pediatrics. 2005;17(2):193-9.
22. Molitoris BA. Actin cytoskeleton in ischemic acute renal failure. Kidney international. 2004;66(2):871-83.
23. Ambrosio G, Flaherty JT, Duilio C, Tritto I, Santoro G, Elia PP, et al. Oxygen radicals generated at reflow induce peroxidation of membrane lipids in reperfused hearts. The Journal of clinical investigation. 1991;87(6):2056-66.
24. Ambrosio G, Zweier JL, Duilio C, Kuppusamy P, Santoro G, Elia PP, et al. Evidence that mitochondrial respiration is a source of potentially toxic oxygen free radicals in intact rabbit hearts subjected to ischemia and reflow. The Journal of biological chemistry. 1993;268(25):18532-41.
25. Turrens JF, Beconi M, Barilla J, Chavez UB, McCord JM. Mitochondrial generation of oxygen radicals during reoxygenation of ischemic tissues. Free radical research communications. 1991;12-13 Pt 2:681-9.
26. Bulteau AL, Lundberg KC, Humphries KM, Sadek HA, Szweda PA, Friguet B, et al. Oxidative modification and inactivation of the proteasome during coronary occlusion/reperfusion. The Journal of biological chemistry. 2001;276(32):30057-63.
27. Di Lisa F, Bernardi P. Mitochondria and ischemia-reperfusion injury of the heart: fixing a hole. Cardiovascular research. 2006;70(2):191-9.
28. Lesnefsky EJ, Moghaddas S, Tandler B, Kerner J, Hoppel CL. Mitochondrial dysfunction in cardiac disease: ischemia--reperfusion, aging, and heart failure. Journal of molecular and cellular cardiology. 2001;33(6):1065-89.

29. Sena LA, Chandel NS. Physiological roles of mitochondrial reactive oxygen species. Molecular cell. 2012;48(2):158-67.

30. D'Autreaux B, Toledano MB. ROS as signalling molecules: mechanisms that generate specificity in ROS homeostasis. Nature reviews Molecular cell biology. 2007;8(10):813-24.

31. Murphy MP. How mitochondria produce reactive oxygen species. The Biochemical journal. 2009;417(1):1-13.

32. Bedard K, Krause KH. The NOX family of ROS-generating NADPH oxidases: physiology and pathophysiology. Physiological reviews. 2007;87(1):245-313.

33. Harper S, Hosgood S, Kay M, Nicholson M. Leucocyte depletion improves renal function during reperfusion using an experimental isolated haemoperfused organ preservation system. The British journal of surgery. 2006;93(5):623-9.

34. Hosgood SA, Patel M, Nicholson ML. The conditioning effect of ex vivo normothermic perfusion in an experimental kidney model. The Journal of surgical research. 2013;182(1):153-60.

35. O'Callaghan JM, Knight SR, Morgan RD, Morris PJ. Preservation solutions for static cold storage of kidney allografts: a systematic review and meta-analysis. American journal of transplantation : official journal of the American Society of Transplantation and the American Society of Transplant Surgeons. 2012;12(4):896-906.

36. Murphy MP, Smith RA. Targeting antioxidants to mitochondria by conjugation to lipophilic cations. Annual review of pharmacology and toxicology. 2007;47:629-56.

37. Smith RA, Murphy MP. Mitochondria-targeted antioxidants as therapies. Discovery medicine. 2011;11(57):106-14.

38. Kelso GF, Porteous CM, Coulter CV, Hughes G, Porteous WK, Ledgerwood EC, et al. Selective targeting of a redox-active ubiquinone to mitochondria within cells: antioxidant and antiapoptotic properties. The Journal of biological chemistry. 2001;276(7):4588-96.

39. James AM, Cocheme HM, Smith RA, Murphy MP. Interactions of mitochondria-targeted and untargeted ubiquinones with the mitochondrial respiratory chain and reactive oxygen species. Implications for the use of exogenous ubiquinones as therapies and experimental tools. The Journal of biological chemistry. 2005;280(22):21295-312.

40. Dare AJ, Bolton EA, Pettigrew GJ, Bradley JA, Saeb-Parsy K, Murphy MP. Protection against renal ischemia–reperfusion injury in vivo by the mitochondria targeted antioxidant MitoQ. Redox Biology. 2015;5:163-8.

41. Smith RA, Porteous CM, Gane AM, Murphy MP. Delivery of bioactive molecules to mitochondria in vivo. Proceedings of the National Academy of Sciences of the United States of America. 2003;100(9):5407-12.

42. Rodriguez-Cuenca S, Cocheme HM, Logan A, Abakumova I, Prime TA, Rose C, et al. Consequences of long-term oral administration of the mitochondria-targeted antioxidant MitoQ to wild-type mice. Free radical biology & medicine. 2010;48(1):161-72.

43. Porteous CM, Logan A, Evans C, Ledgerwood EC, Menon DK, Aigbirhio F, et al. Rapid uptake of lipophilic triphenylphosphonium cations by mitochondria in vivo following intravenous injection: implications for mitochondria-specific therapies and probes. Biochimica et biophysica acta. 2010;1800(9):1009-17.

44. Adlam VJ, Harrison JC, Porteous CM, James AM, Smith RA, Murphy MP, et al. Targeting an antioxidant to mitochondria decreases cardiac ischemia-reperfusion injury. FASEB journal : official publication of the Federation of American Societies for Experimental Biology. 2005;19(9):1088-95.

45. Graham D, Huynh NN, Hamilton CA, Beattie E, Smith RA, Cocheme HM, et al. Mitochondria-targeted antioxidant MitoQ10 improves endothelial function and attenuates cardiac hypertrophy. Hypertension. 2009;54(2):322-8.

46. Gane EJ, Weilert F, Orr DW, Keogh GF, Gibson M, Lockhart MM, et al. The mitochondria-targeted anti-oxidant mitoquinone decreases liver damage in a phase II study of hepatitis C patients. Liver international : official journal of the International Association for the Study of the Liver. 2010;30(7):1019-26.

47. Snow BJ, Rolfe FL, Lockhart MM, Frampton CM, O'Sullivan JD, Fung V, et al. A double-blind, placebo-controlled study to assess the mitochondria-targeted antioxidant MitoQ as a disease-modifying therapy in Parkinson's disease. Movement disorders : official journal of the Movement Disorder Society. 2010;25(11):1670-4.

48. Li Y, Zhang H, Fawcett JP, Tucker IG. Quantitation and metabolism of mitoquinone, a mitochondria-targeted antioxidant, in rat by liquid chromatography/tandem mass spectrometry. Rapid communications in mass spectrometry : RCM. 2007;21(13):1958-64.

49. Neuzil J, Widen C, Gellert N, Swettenham E, Zobalova R, Dong LF, et al. Mitochondria transmit apoptosis signalling in cardiomyocyte-like cells and isolated hearts exposed to experimental ischemia-reperfusion injury. Redox report : communications in free radical research. 2007;12(3):148-62.

50. Dare AJ, Logan A, Prime TA, Rogatti S, Goddard M, Bolton EM, et al. The mitochondria-targeted anti-oxidant MitoQ decreases ischemia-reperfusion injury in a murine syngeneic heart transplant model. The Journal of Heart and Lung Transplantation. 2015; 34(11):1471-80.

51. Hosgood S, Harper S, Kay M, Bagul A, Waller H, Nicholson ML. Effects of arterial pressure in an experimental isolated haemoperfused porcine kidney preservation system. The British journal of surgery. 2006;93(7):879-84.

52. Lee G, Hosgood SA, Patel MS, Nicholson ML. Hydrogen sulphide as a novel therapy to ameliorate cyclosporine nephrotoxicity. The Journal of surgical research. 2015;197(2):419-26.

53. Hosgood SA, Randle LV, Patel M, Watson CJ, Bradley JA, Nicholson ML. Sildenafil citrate in a donation after circulatory death experimental model of renal ischemia-reperfusion injury. Transplantation. 2014;98(6):612-7.
54. Nicholson ML, Hosgood SA. Renal transplantation after ex vivo normothermic perfusion: the first clinical study. American journal of transplantation : official journal of the American Society of Transplantation and the American Society of Transplant Surgeons. 2013;13(5):1246-52.
55. Hosgood SA, Nicholson ML. First in man renal transplantation after ex vivo normothermic perfusion. Transplantation. 2011;92(7):735-8.
56. Hosgood SA, Barlow AD, Hunter JP, Nicholson ML. Ex vivo normothermic perfusion for quality assessment of marginal donor kidney transplants. The British journal of surgery. 2015;102(11):1433-40.
57. Hosgood SA, Barlow AD, Dormer J, Nicholson ML. The use of ex-vivo normothermic perfusion for the resuscitation and assessment of human kidneys discarded because of inadequate in situ perfusion. J Transl Med. 2015;13:329.
58. Hosgood SA, Saeb-Parsy K, Hamed MO, Nicholson ML. Successful Transplantation of Human Kidneys Deemed Untransplantable but Resuscitated by Ex Vivo Normothermic Machine Perfusion. American journal of transplantation : official journal of the American Society of Transplantation and the American Society of Transplant Surgeons. 2016.
59. Ross MF, Prime TA, Abakumova I, James AM, Porteous CM, Smith RA, et al. Rapid and extensive uptake and activation of hydrophobic triphenylphosphonium cations within cells. The Biochemical journal. 2008;411(3):633-45.
60. St Peter SD, Imber CJ, De Cenarruzabeitia IL, McGuire J, James T, Taylor R, et al. Beta-galactosidase as a marker of ischemic injury and a mechanism for viability assessment in porcine liver transplantation. Liver transplantation : official publication of the American Association for the Study of Liver Diseases and the International Liver Transplantation Society. 2002;8(1):21-6.
61. Jung K. [The determination of creatinine--the Jaffe reaction 100 years later. On the occasion of the 75th anniversary of the death of Max Jaffe, discoverer of the picric acid reaction of creatinine]. Zeitschrift fur Urologie und Nephrologie. 1987;80(2):65-8.
62. Bagul A, Hosgood SA, Kaushik M, Nicholson ML. Effects of erythropoietin on ischaemia/reperfusion injury in a controlled nonheart beating donor kidney model. Transplant international : official journal of the European Society for Organ Transplantation. 2008;21(5):495-501.
63. Coca SG, Parikh CR. Urinary biomarkers for acute kidney injury: perspectives on translation. Clinical journal of the American Society of Nephrology : CJASN. 2008;3(2):481-90.
64. Dalle-Donne I, Rossi R, Giustarini D, Milzani A, Colombo R. Protein carbonyl groups as biomarkers of oxidative stress. Clinica chimica acta; international journal of clinical chemistry. 2003;329(1-2):23-38.

65. Smith PK, Krohn RI, Hermanson GT, Mallia AK, Gartner FH, Provenzano MD, et al. Measurement of protein using bicinchoninic acid. Analytical biochemistry. 1985;150(1):76-85.

66. BioCell Protein Carbonyl Assay Kit [11 August 2016]. Available from: http://biocellcorp.co.nz/diagnostics/

67. Milne GL, Gao B, Terry ES, Zackert WE, Sanchez SC. Measurement of F2- isoprostanes and isofurans using gas chromatography-mass spectrometry. Free radical biology & medicine. 2013;59:36-44.

68. de Vries DK, Kortekaas KA, Tsikas D, Wijermars LG, van Noorden CJ, Suchy MT, et al. Oxidative damage in clinical ischemia/reperfusion injury: a reappraisal. Antioxidants & redox signaling. 2013;19(6):535-45.

69. Medina S, Dominguez-Perles R, Gil JI, Ferreres F, Garcia-Viguera C, Martinez-Sanz JM, et al. A ultra-pressure liquid chromatography/triple quadrupole tandem mass spectrometry method for the analysis of 13 eicosanoids in human urine and quantitative 24 hour values in healthy volunteers in a controlled constant diet. Rapid communications in mass spectrometry : RCM. 2012;26(10):1249-57.

70. Medina S, Dominguez-Perles R, Cejuela-Anta R, Villano D, Martinez-Sanz JM, Gil P, et al. Assessment of oxidative stress markers and prostaglandins after chronic training of triathletes. Prostaglandins & other lipid mediators. 2012;99(3-4):79-86.

71. Moita E, Gil-Izquierdo A, Sousa C, Ferreres F, Silva LR, Valentao P, et al. Integrated analysis of COX-2 and iNOS derived inflammatory mediators in LPS-stimulated RAW macrophages pre-exposed to Echium plantagineum L. bee pollen extract. PloS one. 2013;8(3):e59131.

72. Belzer F, Ashby BS, Dunphy JE. 24-HOUR AND 72-HOUR PRESERVATION OF CANINE KIDNEYS. The Lancet. 1967;290(7515):536-9.

73. Collins G. Kidney preservation. In: Collins GM, Dubernard JM, Land W, Persijn GG, editors. Procurement, Preservation and Allocation of Vascularized Organs: Springer Netherlands; 1997. p. 153-7.

74. Perico N, Ruggenenti P, Scalamogna M, Remuzzi G. Tackling the shortage of donor kidneys: how to use the best that we have. American journal of nephrology. 2003;23(4):245-59.

75. Bathini V, McGregor T, McAlister VC, Luke PPW, Sener A. Renal Perfusion Pump Vs Cold Storage for Donation After Cardiac Death Kidneys: A Systematic Review. The Journal of Urology. 2013;189(6):2214-20.

76. Moustafellos P, Hadjianastassiou V, Roy D, Muktadir A, Contractor H, Vaidya A, et al. The Influence of Pulsatile Preservation in Kidney Transplantation From Non–Heart-Beating Donors. Transplantation proceedings. 2007;39(5):1323-5.

77. Watson CJ, Wells AC, Roberts RJ, Akoh JA, Friend PJ, Akyol M, et al. Cold machine perfusion versus static cold storage of kidneys donated after cardiac death: a UK multicenter randomized controlled trial. American journal of transplantation : official journal of the American Society of Transplantation and the American Society of Transplant Surgeons. 2010;10(9):1991-9.

78. Adlam VJ, Harrison JC, Porteous CM, James AM, Smith RAJ, Murphy MP, et al. Targeting an antioxidant to mitochondria decreases cardiac ischemia-reperfusion injury. The FASEB Journal. 2005;19(9):1088-95.

79. Dare AJ, Logan A, Prime TA, Rogatti S, Goddard M, Bolton EM, et al. The mitochondria-targeted anti-oxidant MitoQ decreases ischemia-reperfusion injury in a murine syngeneic heart transplant model. The Journal of heart and lung transplantation : the official publication of the International Society for Heart Transplantation. 2015;34(11):1471-80.

80. Patel SK, Pankewycz OG, Nader ND, Zachariah M, Kohli R, Laftavi MR. Prognostic Utility of Hypothermic Machine Perfusion in Deceased Donor Renal Transplantation. Transplantation proceedings. 2012;44(7):2207-12.

81. Giraud S, Favreau F, Chatauret N, Thuillier R, Maiga S, Hauet T. Contribution of large pig for renal ischemia-reperfusion and transplantation studies: the preclinical model. Journal of biomedicine & biotechnology. 2011;2011:532127.

82. Pereira-Sampaio MA, Favorito LA, Sampaio FJ. Pig kidney: anatomical relationships between the intrarenal arteries and the kidney collecting system. Applied study for urological research and surgical training. J Urol. 2004;172(5 Pt 1):2077-81.

83. Hosgood SA, Bagul A, Yang B, Nicholson ML. The Relative Effects of Warm and Cold Ischemic Injury in an Experimental Model of Nonheartbeating Donor Kidneys. Transplantation. 2008;85(1):88-92 10.1097/01.tp.0000296055.76452.1b.

84. Bellingham JM, Santhanakrishnan C, Neidlinger N, Wai P, Kim J, Niederhaus S, et al. Donation after cardiac death: a 29-year experience. Surgery. 2011;150(4):692-702.

85. Waller HL, Harper SJF, Hosgood SA, Bagul A, Kay MD, Kaushik M, et al. Differential expression of cytoprotective and apoptotic genes in an ischaemia-reperfusion isolated organ perfusion model of the transplanted kidney. Transplant International. 2007;20(7):625-31.

86. Halazun KJ, Al-Mukhtar A, Aldouri A, Willis S, Ahmad N. Warm ischemia in transplantation: search for a consensus definition. Transplantation proceedings. 2007;39(5):1329-31.

87. Gioscia-Ryan RA, LaRocca TJ, Sindler AL, Zigler MC, Murphy MP, Seals DR. Mitochondria-targeted antioxidant (MitoQ) ameliorates age-related arterial endothelial dysfunction in mice. The Journal of physiology. 2014;592(12):2549-61.

88. Hansbro SD, Sharpe DA, Catchpole R, Welsh KR, Munsch CM, McGoldrick JP, et al. Haemolysis during cardiopulmonary bypass: an in vivo comparison of standard roller pumps, nonocclusive roller pumps and centrifugal pumps. Perfusion. 1999;14(1):3-10.

89. Samra M, Abcar AC. False estimates of elevated creatinine. The Permanente journal. 2012;16(2):51-2.

90. Remuzzi G, Cravedi P, Perna A, Dimitrov BD, Turturro M, Locatelli G, et al. Long-term outcome of renal transplantation from older donors. N Engl J Med. 2006;354(4):343-52.

91. Rao PS, Ojo A. The alphabet soup of kidney transplantation: SCD, DCD, ECD--fundamentals for the practicing nephrologist. Clinical journal of the American Society of Nephrology : CJASN. 2009;4(11):1827-31.

92. Callaghan CJ, Harper SJ, Saeb-Parsy K, Hudson A, Gibbs P, Watson CJ, et al. The discard of deceased donor kidneys in the UK. Clinical transplantation. 2014;28(3):345-53.

93. Ruegg CE, Mandel LJ. Bulk isolation of renal PCT and PST. I. Glucose-dependent metabolic differences. The American journal of physiology. 1990;259(1 Pt 2):F164-75.

94. Sharfuddin AA, Molitoris BA. Pathophysiology of ischemic acute kidney injury. Nature reviews Nephrology. 2011;7(4):189-200.

95. Molitoris BA, Sutton TA. Endothelial injury and dysfunction: role in the extension phase of acute renal failure. Kidney Int. 2004;66(2):496-9.

96. Sharples EJ, Patel N, Brown P, Stewart K, Mota-Philipe H, Sheaff M, et al. Erythropoietin protects the kidney against the injury and dysfunction caused by ischemia-reperfusion. Journal of the American Society of Nephrology : JASN. 2004;15(8):2115-24.

97. Hosgood SA, Bagul A, Kaushik M, Rimoldi J, Gadepalli RS, Nicholson ML. Application of nitric oxide and carbon monoxide in a model of renal preservation. The British journal of surgery. 2008;95(8):1060-7.

98. Cirami C, Bianchi AM, Galigani P, Gadducci A, Colombi L, Facchini V, et al. [Cisplatin nephrotoxicity: effects on fractional excretion of sodium and enzymuria]. Minerva medica. 1990;81(1-2):79-86.

99. Malyszko J, Malyszko JS, Mysliwiec M. Serum neutrophil gelatinase-associated lipocalin correlates with kidney function in renal allograft recipients. Clinical transplantation. 2009;23(5):681-6.

100. Mishra J, Ma Q, Kelly C, Mitsnefes M, Mori K, Barasch J, et al. Kidney NGAL is a novel early marker of acute injury following transplantation. Pediatric nephrology (Berlin, Germany). 2006;21(6):856-63.

101. Hosgood SA, Hunter JP, Nicholson ML. Early urinary biomarkers of warm and cold ischemic injury in an experimental kidney model. The Journal of surgical research. 2012;174(2):e85-90.

102. Hunter SE, Jung D, Di Giulio RT, Meyer JN. The QPCR assay for analysis of mitochondrial DNA damage, repair, and relative copy number. Methods (San Diego, Calif). 2010;51(4):444-51.

103. Barja G, Herrero A. Oxidative damage to mitochondrial DNA is inversely related to maximum life span in the heart and brain of mammals. FASEB journal : official publication of the Federation of American Societies for Experimental Biology. 2000;14(2):312-8.

104. Cocheme HM, Logan A, Prime TA, Abakumova I, Quin C, McQuaker SJ, et al. Using the mitochondria-targeted ratiometric mass spectrometry probe MitoB to measure H2O2 in living Drosophila. Nature protocols. 2012;7(5):946-58.

105. Francischetti I, Moreno JB, Scholz M, Yoshida WB. Leukocytes and the inflammatory response in ischemia-reperfusion injury. Revista brasileira de cirurgia cardiovascular : orgao oficial da Sociedade Brasileira de Cirurgia Cardiovascular. 2010;25(4):575-84.
106. Hosgood SA, Patel M, Nicholson ML. The conditioning effect of ex vivo normothermic perfusion in an experimental kidney model. The Journal of surgical research. 2013;182.
107. Chouchani ET, Pell VR, Gaude E, Aksentijevic D, Sundier SY, Robb EL, et al. Ischaemic accumulation of succinate controls reperfusion injury through mitochondrial ROS. Nature. 2014;515(7527):431-5.

Appendices

Succinate as a marker and driver of IRI

Succinate is an important intermediate in the citric acid cycle, and acts as a reducing agent, donating two electrons used for oxidative phosphorylation in the electron transport chain. The accumulation of succinate during ischaemia has recently been shown to be a metabolic marker of ischaemic injury, and correlates with the extent of reactive oxygen species production and oxidative damage during reperfusion (107).

Understanding the trend of succinate levels during ischaemia (WIT and CIT) may help to determine the length of WIT and CIT that organs are able to tolerate before the damage becomes too severe and irrecoverable. In this context, I have initiated preliminary experiments to explore the trend of succinate accumulation during ischaemia using the controlled DCD pig model and the declined deceased human kidneys.

In the controlled DCD pig model, the baseline levels of succinate during normoxaemia were determined by taking an *in situ* biopsy from kidneys (n = 4) in anaesthetised and ventilated pigs. The kidneys were subsequently removed and exposed to 10 min of WIT followed by 18 h of CIT at 4 °C using CSS. Almost all of the increase in the succinate concentration was observed during the initial WIT, with only a marginal additional increase during the 18 h of CIT. The same kidneys were then perfused with oxygenated autologous blood using an EVNP circuit. Succinate levels returned towards baseline levels after 30 min of reperfusion with oxygenated autologous blood (Figure 7.1).

The ideal experiment to investigate the trend of succinate accumulation during ischaemia in human kidneys is to do a similar model as the pig DCD model described above. However, this is not possible at present because the declined deceased human kidneys are received after a variable period of CIT. Consequently, I did not have any samples from normoxaemic human kidneys before they were retrieved for transplantation in DBD donors, or at the end of WIT for DCD donors. In order to have an approximation of succinate levels during normoxaemia, I decided to reperfuse human kidneys on the EVNP circuit and measure succinate levels while oxygenated on the EVNP circuit, notwithstanding the caveat that these kidneys are likely to be undergoing IRI which may prevent succinate levels from returning back to physiological normoxaemia levels. Starting from this (albeit suboptimal) point, I exposed the kidneys to CIT and took biopsies to see how succinate levels alter during ischaemia.

In this context, a kidney biopsy after 1 h of EVNP was used to determine the baseline succinate levels during normoxaemia. The deceased declined human kidneys (n = 3) were then subjected to 6 h of CIT at 4 °C using CSS. Succinate levels increased several fold during 6 h of CIT but subsequently returned back to baseline levels after 10 min reperfusion with oxygenated blood on the EVNP circuit (Figure 7.2).

Further investigations are required to:

1. Investigate whether the mode of kidney preservation (CSS vs. HMP) has a different impact on succinate levels during cold preservation
2. Investigate the trend of succinate accumulation during cold preservation in a controlled DBD pig model (no WI) to characterise the relative impact of WIT and CIT on succinate levels during cold storage
3. Investigate if the type of kidney donor (DCD vs. DBD) has a different impact on succinate levels during cold storage, this can give some insight into the relative effect of WIT on succinate levels in human kidneys

Characterising the changes in succinate concentration during ischaemia will allow us to understand how prolonged WIT and CIT may lead to DGF and PNF post kidney transplantation. In this context, succinate could be a potential therapeutic target to ameliorate renal IRI. This is the subject of another PhD student (Tim Beach) and his project will commence in October 2016.

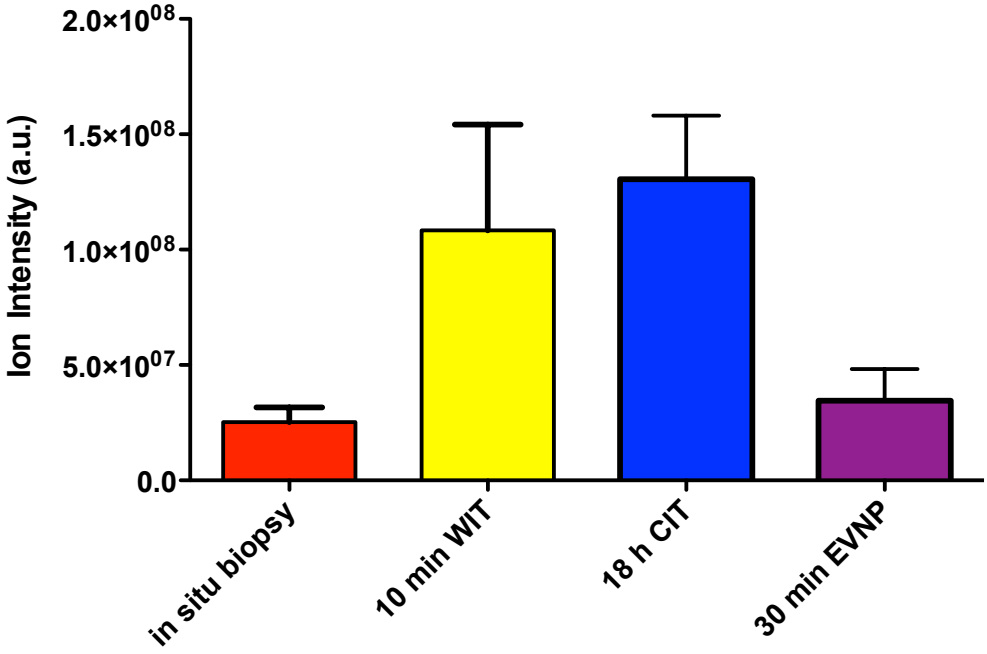

Figure 8.1. Succinate levels in the controlled DCD pig kidneys. The kidneys (n = 4) were exposed to 10 min of WIT followed by 18 h of CIT using CSS and then placed on the EVNP circuit. Wedge biopsies were obtained at the indicated times. Succinate levels were increased significantly at the end of 10 min of WIT compared to the *in situ* levels (10 min WIT 1.1 ± 0.4 vs. *in situ* 0.3 ± 0.1; $x10^{08}$ arbitrary units; p = 0.039; paired t-test). Of note, there were no significant changes in succinate levels at the end of 18 h of CIT compared to the succinate levels at the end of 10 min of WIT (18 h CIT 1.3 ± 0.3 vs. 10 min WIT 1.1 ± 0.4; $x10^{08}$ arbitrary units; p = 0.0.299; paired t-test). Succinate levels were decreased significantly after 30 min of reperfusion compared to the succinate levels at the end of 18 h of CIT and returned towards background levels (30 min EVNP 0.3 ± 0.1 vs. 10 18 h CIT 1.3 ± 0.3; $x10^{08}$ arbitrary units; p = 0.012; paired t-test). Data are mean ± SD.

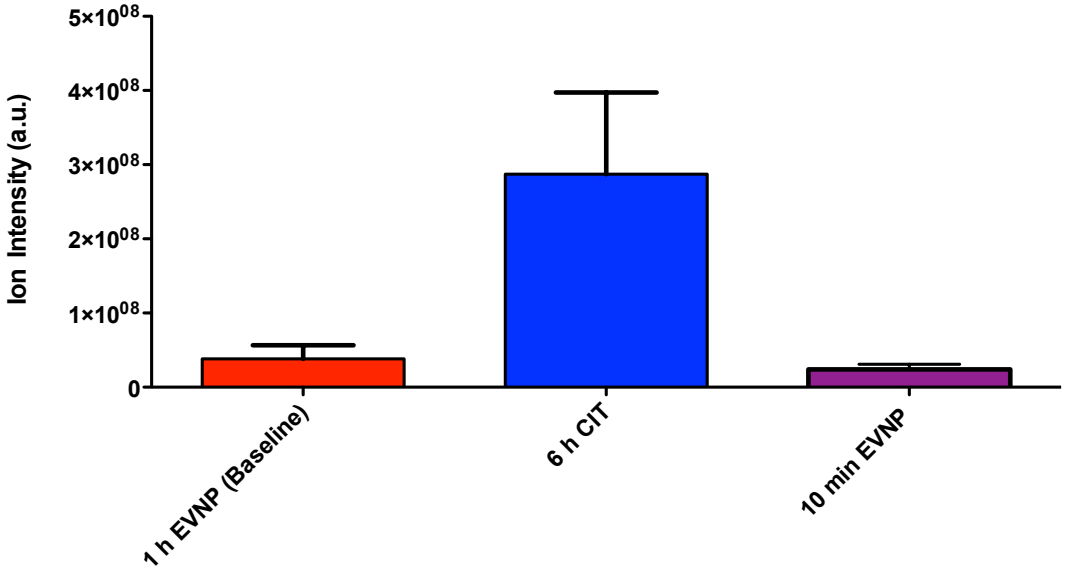

Figure 8.2. Succinate levels in the deceased declined human kidneys. The kidneys (n = 3) were placed on the EVNP circuit for 1 h to determine the baseline succinate levels during normoxaemia. The kidneys were then exposed to 6 h of CIT using CSS and then placed on the EVNP circuit again. Wedge biopsies were obtained at the indicated times. Succinate levels were numerically higher at the end of 6 h of CIT compared to the base line levels (at the end of 1 h of EVNP), but the differences did not reach statistical significance (6 h CIT 2.9 ± 1.1 vs. baseline 0.4 ± 0.2; x 10^{08} arbitrary units; p = 0.078; paired t-test). Of note, succinate levels were decreased (albeit not statistically significant) after 10 min of reperfusion compared to the succinate levels at the end of 6 h of CIT and returned towards base levels (10 min WIT 0.2 ± 0.1 vs. 6 h CIT 2.9 ± 1.1; x 10^{08} arbitrary units; p = 0.055; paired t-test). Data are mean ± SD.

Other projects

In addition to examining kidney IRI, we had a number clinical and lab projects in the department, which used EVNP to investigate IRI in pancreata (pigs and human), small bowel (pigs), and liver (human). These projects were lead by Dr. Kourosh Saeb-Parsy, Prof Mike Nicholson, Prof Watson and Dr. Adam Barlow (Department of Surgery, Addenbrooke's Hospital, Cambridge), but I was actively involved and contributed to those projects.

Publications arising from this thesis

1. Successful transplantation of human kidneys deemed untransplantable but resuscitated by ex-vivo normothermic machine perfusion. SA Hosgood, K Saeb-Parsy, MO Hamed and ML Nicholson. Am J Transplant. 2016 Jun 7. doi: 10.1111/ajt.13906.

2. Use of *ex vivo* normothermic perfusion for quality assessment of discarded human donor pancreases. Barlow AD, Hamed MO, Mallon DH, Brais RJ, Gribble FM, Scott MA, Howat WJ Bradley JA, Bolton EM, Pettigrew GJ, Hosgood SA, Nicholson ML, Saeb-Parsy K. Am J Transplant. 2015 Sep;15(9):2475-82. doi: 10.1111/ajt.13303

3. Early Graft Loss After Kidney Transplantation: Risk Factors and Consequences. Mazin O Hamed, Yining Chen, Laura Pasea, Christopher J Watson, Nicholas Torpey, J Andrew Bradley, Gavin Pettigrew, Kourosh Saeb-Parsy. Am J Transplant. 2015 Jun;15(6):1632-43. doi: 10.1111/ajt.13162

Prizes arising from this thesis

1. Future Projects Prize (1st Prize): Evaluation of a Novel Mitochondria-targeted Anti-oxidant Therapy for Ischaemia Reperfusion Injury in a Model of Kidney Transplantation. SARS Conference – London, 6 & 7 January 2016. M Hamed, S Hosgood, A Logan, A Dare, A Barlow, J Martin, N Georgakopoulos, G Pettigrew, E Bolton, J A Bradley, M Nicholson, M Murphy, K Saeb-Parsy

2. Shortlisted for Patey Prize: Ex-vivo normothermic perfusion with the noble gas argon in an experimental model of kidney transplantation. SARS Conference – London, 6 & 7 January 2016. M Hamed, SA Hosgood, K Saeb-Parsy, ML Nicholson

3. Poster of Distinction Presentation: Early Graft Lost After Kidney Transplantation: Risk Factors and Consequences. SARS Conference – Cambridge, 8 & 9 January 2014. Mazin Hamed, Laura Pasea, J Andrew Bradley, Gavin Pettigrew, Kourosh Saeb- Parsy

4. Best Oral Presentation: Early Graft Loss Post Kidney Transplantation is Important Risk Factor For Patient Mortality. ESOT conference – Vienna, 8th – 11th September 2013. Mazin Hamed, Laura Pasea, J Andrew Bradley, Gavin Pettigrew, Kourosh Saeb- Parsy